

Modelling of Temporary Wet Storage of Floating Offshore Wind Foundations

Thesis report

Dieuwer Keunen



Modelling of Temporary Wet Storage of Floating Offshore Wind Foundations

Thesis report

by

Dieuwer Keunen

to obtain the degrees of:

Master of Science Offshore & Dredging Engineering at the Delft University of Technology

Master of Science Wind Energy Technology at the Norwegian University of Science and Technology

to be defended publicly on Thursday October 3, 2024 at 12:45.

Project duration: September 5, 2023 – October 3, 2024
Student numbers: 4705718 (TU Delft) 122256 (NTNU)

Thesis committee

Chair:	Dr. ir. Oriol Colomés Gene	TU Delft
Committee members:	Prof. Dr. ir. Erin Bachynski-Polić	NTNU
	Prof. Dr. ir. Marilena Greco	NTNU
	ir. Karin Leijns	HES
	Dr. ir. Bart Ummels	TU Delft
	ir. Elisa Romero Pascual	HES
	Dr. ir. Øyvind Ygre Rogne	SINTEF

Cover: Windfloat Atlantic under Wikimedia Commons

An electronic version of this thesis is available at <http://repository.tudelft.nl/>.

Preface

This thesis is the culmination of my studies in the European Wind Energy Masters at the Norwegian University of Science and Technology (NTNU) and Delft University of Technology (TU Delft). Conducted in collaboration with Heerema Engineering Solutions (HES), this research explores solutions in the field of floating offshore wind energy, specifically focusing on mooring systems for wet storage. I would like to extend my deepest gratitude to my committee members for their guidance and support throughout this journey.

I am grateful to Oriol Colomé Gene for his sharp feedback and positive problem-solving attitude. His contributions significantly improved the quality of my argumentation and strengthened the clarity of my research.

To Erin Bachynski-Polić from NTNU, I am thankful for her openness and approachability. Erin's insightful explanations and willingness to engage in discussions allowed me to better grasp complex concepts. Although Erin's leave began just a week before my graduation, her support throughout the project was invaluable.

I would also like to acknowledge Marilena Greco, who kindly stepped in as a replacement committee member in Erin's absence, ensuring continuity in the assessment process.

My heartfelt thanks to Karin Leijs from Heerema Engineering Solutions for her daily support and willingness to help me navigate challenging aspects of this study. Her consistent dedication and technical insights were vital to overcoming many obstacles.

I am equally grateful to Bart Ummels from TU Delft for his guidance. Bart's patient approach in addressing my doubts, even the ones I was hesitant to ask, greatly enhanced the depth and quality of my work.

A special mention goes to Elisa Romero Pascual from Heerema Engineering Solutions for her pragmatic advice and realistic perspective on the potential applications of this research. Her encouragement to clearly define the research scope was a great motivator and helped me maintain focus during the project.

Lastly, I would like to thank Øyvind Ygre Rogne, who joined the committee as an external examiner. His insights and feedback during the final stages will help shape the assessment of this work on my graduation day.

As I conclude this thesis, I reflect on an incredibly enriching academic journey. I am eager to continue to contribute to the energy transition and to explore the practical applications of this research.

*Dieuwer Keunen
Amsterdam, September 2024*

Summary

Offshore wind energy has become an important contributor to global renewable energy efforts, particularly as the industry seeks to expand into deeper waters where traditional fixed-bottom turbines are no longer feasible. In these deeper waters, floating offshore wind turbines (FOWTs) offer a promising solution, allowing for the generation of renewable energy in locations with stronger, more consistent winds. However, with the increasing use of FOWTs comes a set of logistical challenges that need to be addressed to ensure their commercial viability and large-scale deployment. One of these challenges is the large-scale production of floating foundations.

One significant challenge to the commercial success of FOWTs is the slow fabrication rate of semi-submersible floaters, which require extensive welding and assembly. In contrast to faster monopile fabrication, these floaters are more complex and take longer to produce. Since installation campaigns are typically limited to favorable weather periods, especially in the summer months, many floaters need to be ready in advance, placing strain on fabrication yards and causing space constraints. Wet storage provides a viable solution by allowing temporary storage of floaters in coastal areas, freeing up space in fabrication yards for continuous production. This research explores the existing literature on wet storage mooring systems and identifies key design criteria, environmental considerations, and components such as mooring lines, anchors, and auxiliary equipment.

To evaluate mooring system designs, a Multi-Criteria Decision Analysis (MCDA) framework was developed, facilitating structured comparisons and trade-offs between various design objectives. Although the MCDA enables informed decision making, dynamic analysis is essential to obtain deeper insights into system performance. In this study, frequency domain (FD) analysis was employed for rapid evaluations of the behavior of the mooring system. FD analysis proved sufficient for preliminary studies and is an ideal tool for exploring design variations. It efficiently captures first-order loading effects, which are typically dominant in expected wet storage conditions. However, for detailed design stages, to account for nonlinear behaviors such as slow drift and mooring line stiffness, time domain (TD) analysis is recommended to validate final configurations and ensure compliance with design codes.

Dynamic analysis of the mooring systems compared catenary and taut configurations under various environmental conditions. Concept-specific constraints such as maximum fairlead tension, uplift allowance, mooring line angles, and minimum anchor distances were incorporated into each mooring concept. Furthermore, diffraction analyses were conducted with varying water depths and floater drafts to accurately define floater behavior under different conditions, and a mesh validation was performed to ensure that the mesh was fine enough for this study. Further validation of the full model was done by comparing the calculated Load Response Amplitude Operators (RAOs) and natural frequencies with the reference turbine to ensure model accuracy. Tidal ranges and line diameters significantly influenced mooring performance, impacting tensions, loads, and floater displacements. The results indicated that the catenary system consistently met these constraints and demonstrated resilience across the full tidal range, where a clear trade-off between tensions and displacements can be observed. However, the taut system experienced tension overloads, particularly at high tide, where it often exceeded line breaking strength, with only a single taut configuration yielding valid results. Despite being more spatially efficient, the taut system's reliability was compromised compared to the catenary system.

Several recommendations for future research are identified to further the understanding of mooring systems in wet storage applications. These include conducting TD analyses to capture non-linear behaviors, exploring alternative mooring configurations such as Honeymooring or pile fields, refining design standards, and evaluating the economic and logistical feasibility of wet storage solutions. Additionally, investigating different storage locations is essential, as this study focused on a single location, and variations in environmental conditions could significantly influence mooring performance.

Contents

Preface	i
Summary	ii
Nomenclature	viii
1 Introduction	1
1.1 Background	1
1.1.1 Growth of offshore wind	1
1.1.2 Types of offshore wind turbines	2
1.1.3 Installation procedure of semi-submersibles	2
1.1.4 Wet storage of floating offshore wind foundations	3
1.2 Knowledge gap	4
1.3 Problem statement	5
1.4 Research objectives and questions	5
1.5 Approach and methodology	5
1.6 Demarcation and scope	6
1.7 Report structure	7
2 Theoretical background	8
2.1 Mooring systems	8
2.1.1 Mooring profiles	8
2.1.2 Mooring components	12
2.1.3 Mooring lines	12
2.1.4 Auxiliary equipment	16
2.1.5 Anchors	16
2.2 Modelling of floating offshore wind foundations	19
2.2.1 Hydrodynamics	19
2.2.2 Differences between offshore and nearshore locations	24
2.2.3 Equations of motion	26
2.2.4 Frequency domain analysis	26
3 Framework development	30
3.1 Multi-Criteria Decision Analysis	30
3.1.1 Criteria	30
3.1.2 Dependencies	31
3.1.3 Weights	32
3.2 Design basis	32
4 Model development and validation	34
4.1 Environmental conditions	34
4.1.1 Case study location	35
4.2 Floater definition	39
4.2.1 Diffraction analysis	40
4.3 Mooring system definition	42
4.3.1 Governing parameters	42
4.3.2 Anchor distance and line length algorithm	44
4.3.3 General constraints for mooring systems	45
4.3.4 Catenary mooring system	45
4.3.5 Taut mooring system	45
4.4 Model validation	46

4.4.1	Load Response Amplitude Operators (RAOs)	46
4.4.2	Natural frequencies	51
5	Results	56
5.1	Dynamic behavior	56
5.1.1	Catenary mooring systems	56
5.1.2	Taut mooring systems	65
5.1.3	Comparison of catenary and taut concepts	71
5.2	Other criteria	71
5.2.1	Spatial utilization	71
5.2.2	Accessibility	71
5.2.3	Hook-up efficiency	72
5.2.4	Cost	72
5.3	Multi-Criteria Decision Analysis	72
5.3.1	Scoring of mooring systems	72
5.3.2	Weighed scores	73
5.3.3	Sensitivity analysis	74
5.3.4	Discussion	75
6	Conclusions	76
6.1	Design objectives and criteria	76
6.2	Environmental conditions	76
6.3	Viable mooring concepts	77
6.4	Modeling approach	78
6.5	Quantitative comparison of mooring system designs	78
6.6	Applicability to other foundation types	79
6.7	Designing mooring systems for wet storage	79
7	Recommendations	80
7.1	Expanding the problem definition	80
7.2	Modeling improvements	80
	References	82
A	Anchor distance and line lengths algorithm	89
A.1	File creation	89
A.1.1	Constraint handling	89
A.1.2	Expanding to multiple floaters	90
A.2	Post-processing	90
B	Load RAOs	91
B.1	Comparison with available literature	91
B.2	Effect of draft	93
B.3	Effect of moored draft	94
B.4	Comparison of water depths	96
B.5	Effect of tidal range	97
C	Free-decay plots	99
D	Added mass over frequency for all DOFs	103

List of Figures

1.1	Growth of wind capacity in Europe [102]	1
1.2	Types of offshore wind foundations [56]	2
1.3	Final assembly and tow-out of FOWTs [50]	3
1.4	Final assembly of the primary structure of a steel semi-submersible [83]	3
1.5	Load-out process of a semi-submersible foundation [3]	4
1.6	Research approach and methodology	6
2.1	Schematic of three mooring systems: (A) Catenary, (B) TLP, (C) Taut [107]	9
2.2	Characteristic points of a catenary line [11]	9
2.3	Influence of water depth on horizontal mooring stiffness for a specific case study [106]	10
2.4	Top angles of catenary lines in shallow waters [106]	11
2.5	Clump weights added in taut mooring lines [59]	12
2.6	Mooring line types according to construction material [20]	13
2.7	Variable stiffness characteristics of polyester mooring lines according to the Falkenburg SYrope model [36]	15
2.8	Overview of six different anchor types [98]	16
2.9	Comparison of drag embedment and vertical load anchors [74]	17
2.10	Potential wind farm configurations using multiline anchors [40]	18
2.11	V-shape four-line mooring system for 14 turbines [104]	19
2.12	Applicability of wave theories [16]	20
2.13	Discretized line model in OrcaFlex [80]	24
2.14	Wave refraction when waves approach a coast line [47]	24
2.15	Conservation of mechanical energy flux between section <i>A</i> and <i>B</i> [32]	25
2.16	Squeezing of orbitals for shallower water and exponential decay of wave energy [69]	25
3.1	Interdependence of criteria	32
3.2	Design basis for a wet storage mooring system	33
4.1	Celtic Sea FLOW leasing zones [65]	35
4.2	Locations of Directional Waveriders [85]	36
4.3	Spectral density wave train	37
4.4	General configuration of VolturnUS-S floater designed for the IEA 15-MW reference turbine [4]	40
4.5	Overview of VolturnUS-S mesh [77]	41
4.6	Wavelength over wave period for various water depths	42
4.7	Tidal influence on mooring line	43
4.8	Influence of line diameter on mooring system	44
4.9	Node locations for an anchor distance of 85 m	44
4.10	Catenary mooring system layout	45
4.11	Taut mooring system layout	46
4.12	Comparison with NREL reference platform for the surge direction	47
4.13	Effect of draft on surge direction	48
4.14	Effect of draft on heave direction	48
4.15	Effect of draft on pitch direction	49
4.16	Effect of moored draft for the heave direction	49
4.17	Effect of water depth on surge direction	50
4.18	Effect of water depth on heave direction	50
4.19	Effect of tidal range on heave direction	51
4.20	Model constraint just before release for pitch DOF	52

4.21	Response and free decay for pitch DOF	53
4.22	Added mass as a function of frequency for surge-surge	55
5.1	Anchor distance and line length over line diameter	57
5.2	Schematic of a catenary mooring line [51]	58
5.3	Pretensions for the fairlead side of the mooring lines	59
5.4	Declinations on the fairlead side for an upwind line	59
5.5	Spectral density and RAO of effective tension of an upwind line	60
5.6	Fairlead tensions for various environmental conditions	62
5.7	Static tensions for the anchor side of an upwind mooring line	63
5.8	Static and MPM tensions for the anchor side of an upwind mooring line	63
5.9	Vertical force component (E_z) at the anchor	64
5.10	Y displacements	65
5.11	Declinations on the fairlead side for an upwind line	66
5.12	Static tensions for the fairlead side of the mooring lines (Polyester)	67
5.13	Pretensions for the fairlead side of the mooring lines (Nylon)	67
5.14	Static and MPM tensions for the fairlead side of the mooring lines (Nylon)	68
5.15	Horizontal (E_y) and vertical (E_z) forces at the anchor for Nylon mooring lines at WD45	69
5.16	Maximum Y-direction displacements of the floater for Nylon mooring lines	70
A.1	Node locations for an anchor distance of 85 m	90
B.1	Comparison of NREL and Orcina results for surge load RAO	91
B.2	Comparison of NREL and Orcina results for heave load RAO	92
B.3	Comparison of NREL and Orcina results for pitch load RAO	92
B.4	Effect of draft on surge load RAO	93
B.5	Effect of draft on heave load RAO	93
B.6	Effect of draft on pitch load RAO	94
B.7	Effect of mooring draft on surge load RAO	94
B.8	Effect of mooring draft on heave load RAO	95
B.9	Effect of mooring draft on pitch load RAO	95
B.10	Comparison of water depths on surge load RAO	96
B.11	Comparison of water depths on heave load RAO	96
B.12	Comparison of water depths on pitch load RAO	97
B.13	Effect of tidal range on surge load RAO	97
B.14	Effect of tidal range on heave load RAO	98
B.15	Effect of tidal range on pitch load RAO	98
C.1	Decay time history for surge	99
C.2	Decay time history for sway	100
C.3	Decay time history for heave	100
C.4	Decay time history for roll	101
C.5	Decay time history for pitch	101
C.6	Decay time history for yaw	102
D.1	Added mass as a function of frequency for surge-surge DOF	103
D.2	Added mass as a function of frequency for sway-sway DOF	103
D.3	Added mass as a function of frequency for heave-heave DOF	104
D.4	Added mass as a function of frequency for roll-roll DOF	104
D.5	Added mass as a function of frequency for pitch-pitch DOF	104
D.6	Added mass as a function of frequency for yaw-yaw DOF	104

List of Tables

2.1	Mooring line materials, adapted from the oil and gas industry [20]	14
2.2	Cost comparison between anchors and piles, in which plus means less expensive and minus means more expensive, adapted from [98]	17
3.1	Criteria to access	30
3.2	Weights	32
4.1	Storm analysis for the Minehead buoy [85]	36
4.2	Draft and water depth configurations for diffraction analysis	41
4.3	Initial displacements for free-decay simulations	52
4.4	Free decay of mooring system sensitive DOFs	52
4.5	Free decay of mooring system insensitive DOFs	53
4.6	Modal analysis of mooring system sensitive DOFs	54
4.7	Modal analysis of mooring system insensitive DOFs	54
5.1	Bollard pull data for selected ships [17]	60
5.2	Velocities in Y direction for different line diameters and water depths	65
5.3	Accelerations in Y direction for different line diameters and water depths	65
5.4	Line breaking strengths for Polyester and Nylon [78]	66
5.5	MPM velocities in Y direction for Nylon mooring lines	70
5.6	MPM accelerations in Y direction for Nylon mooring lines	70
5.7	Criteria and weights for MCDA	72
5.8	MCDA scores for catenary and taut mooring systems	72
5.9	Weighted MCDA scores for catenary and taut mooring systems	73
5.10	Adjusted criteria weights for scenario 1	74
5.11	Weighted MCDA scores for scenario 1	74
5.12	Adjusted criteria weights for scenario 2	74
5.13	Weighted MCDA Scores for Scenario 2	75

Nomenclature

Abbreviations

Abbreviation	Definition
BVP	Boundary Value Problem
COM	Center of Mass
DOF	Degree Of Freedom
ERA-5	Reanalysis Dataset for Climate and Weather
FD	Frequency Domain
FLOW	Floating Offshore Wind
FOW	Floating Offshore Wind
FOWT	Floating Offshore Wind Turbine
HES	Heerema Engineering Solutions
HTV	Heavy Transport Vessel
IG	Infragravity
LD	Line Diameter
MCDA	Multi-Criteria Decision Analysis
MF	Manufacturing and Fabrication
MPM	Most Probable Maximum
NTNU	Norwegian University of Science and Technology
OWT	Offshore Wind Turbine
PSD	Power Spectral Density
QTF	Quadratic Transfer Function
RAO	Response Amplitude Operator
S&I	Staging and Integration
SPM	Single Point Mooring
SPMT	Self-Propelled Modular Transporters
SWAN	Simulating Waves Nearshore
TD	Time Domain
TLP	Tension Leg Platform
WD	Water Depth
WTG	Wind Turbine Generator

Symbols

Symbol	Definition
A	Waterplane area of the structure
A_{∞}	Added mass at infinite frequency
\mathbf{A}	Added mass matrix
$A_{frontal,cyl}$	Frontal area of a column
$A_{frontal,tot}$	Total frontal area of the columns
A_{heave}	Heave area
A_{pitch}	Pitch area moment
A_{roll}	Roll area moment
A_{surge}	Surge area
A_{sway}	Sway area
A_{yaw}	Yaw area moment

Symbol	Definition
$b(\omega)$	Linear radiation damping matrix
\mathbf{B}	Radiation damping matrix
C	Damping matrix
C_d	Drag coefficient
C_{heave}	Heave drag coefficient
C_{pitch}	Pitch drag coefficient
C_{roll}	Roll drag coefficient
C_{surge}	Surge drag coefficient
C_{sway}	Sway drag coefficient
C_{yaw}	Yaw drag coefficient
D_f	Horizontal projection of the curve
D_v	Horizontal catenary length in static equilibrium
d	Water depth
d_c	Chain nominal diameter
E_y	Horizontal force component at the anchor
E_z	Vertical force component at the anchor
$F(t)$	External forces acting on the system
\mathbf{F}_{wave}	Total wave force
$\mathbf{F}_{\text{incident}}$	Incident wave force
$\mathbf{F}_{\text{diffraction}}$	Diffraction wave force
$\mathbf{F}_{\text{radiation}}$	Radiation wave force
$\mathbf{F}_{2\text{nd}}$	Second-order wave force
\mathbf{F}_{mean}	Mean drift force
$\mathbf{F}_{\text{difference}}$	Difference-frequency wave drift force
\mathbf{F}_{sum}	Sum-frequency wave force
F_x	Horizontal force
F_z	Vertical force
f_x, f_y, f_z	Drag forces in the x-, y-, and z-directions
g	Gravitational acceleration
H	Line height
H_s	Significant wave height
h	Water depth
k	Wave number
k_G	Horizontal, geometric, in-elastic stiffness of a catenary mooring line
l_s	Length of the suspended mooring line
L	Characteristic length of the structure
M	Mass matrix of the floater
m_x, m_y, m_z	Drag moments about the x-, y-, and z-directions
\mathbf{n}	Normal vector to a surface
Q	Line breaking load
$R(t)$	Retardation function
S	Line length
S_c	Characteristic line capacity
s	Horizontal span
s_{coef}	Minimum safety coefficient
T	Tension
T_H	Horizontal line tension
T_V	Vertical line tension
T_p	Peak wave period
T_z	Mean period of zero up-crossings
T_c	Mean period of crests
$T_{c,\text{dyn}}$	Dynamic contribution to tension
$T_{c,\text{mean}}$	Mean line tension
u, v, w	Directional components of the fluid velocity vector

Symbol	Definition
V	Velocity
\mathbf{V}	Fluid velocity vector
\mathbf{v}	Relative velocity of sea or air past the vessel
X_i	Dimensional excitation force or moment
\tilde{X}_i	Non-dimensional excitation force or moment from WAMIT
\mathbf{X}	Floating body motion
$\ddot{\mathbf{X}}_g$	Acceleration of the center of gravity
x	Horizontal offset
Y	Y-axis (displacements, velocities, accelerations in Y-direction)
α	Top angle of the catenary line
β	Top angle of the catenary line in shallow water
Δx_{adm}	Allowable platform offset
\dot{q}	Velocity vector of the platform
\ddot{q}	Acceleration vector of the platform
ϵ	Spectral bandwidth
γ_{dyn}	Load factor for dynamic contribution
γ_{mean}	Load factor for mean line tension
λ	Wavelength
ϕ	Velocity potential
$\phi^{incident}$	Incident wave potential
$\phi^{diffraction}$	Diffraction potential
$\phi^{(1)}$	First-order velocity potential
$\phi^{(2)}$	Second-order velocity potential
ρ	Density (water or air)
ω	Angular frequency
ω_r	Line unit weight in water
$\boldsymbol{\omega}$	Vorticity vector
$\xi_r^{(1)}$	First-order relative wave elevation

Introduction

1.1. Background

The shift from fossil fuels to renewable energy sources is essential in mitigating climate change, with offshore wind energy playing a key role. Offshore wind turbines (OWTs) have benefits that include access to robust and consistent wind resources, as well as reduced onshore noise and visual impact. Floating offshore wind turbines (FOWTs) augment these advantages by enabling deployment in deeper waters, thereby harnessing greater wind resources where bottom-fixed structures are not practical.

1.1.1. Growth of offshore wind

The offshore wind market is growing rapidly. Europe, driven by favorable conditions and the growing need to harness offshore wind resources, has seen significant expansion. In 2023, wind power accounted for 19% of Europe's electricity consumption, with contributions from both offshore and onshore installations [102]. Asia, especially China, has shown rapid growth, adding 6.3 GW of offshore wind energy in 2023 [44]. Advances in wind turbine technology have led to larger and more powerful turbines. The largest operational prototype currently is capable of generating 18 MW, and reference turbines of 22 MW have been proposed [108].

The growth of offshore wind capacity has been rapid, as illustrated in Figure 1.1, which shows the increasing cumulative and annual installations of offshore wind turbines in Europe over the past decade.

FIGURE B. 2024-30 annual onshore and offshore wind power installations in the EU - WindEurope's Outlook

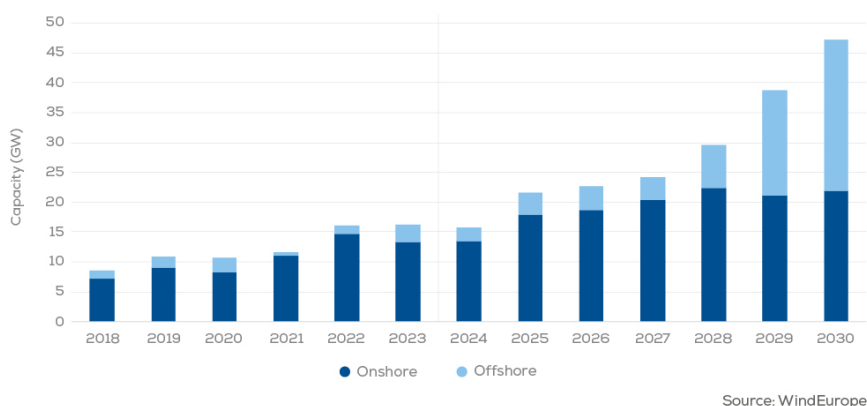


Figure 1.1: Growth of wind capacity in Europe [102]

1.1.2. Types of offshore wind turbines

Offshore wind turbines are classified into two main categories: bottom-fixed and floating, each with unique characteristics, technological readiness, advantages, and feasible water depths. Figure 1.2 illustrates various wind turbine foundations, highlighting the most prevalent ones within these categories.

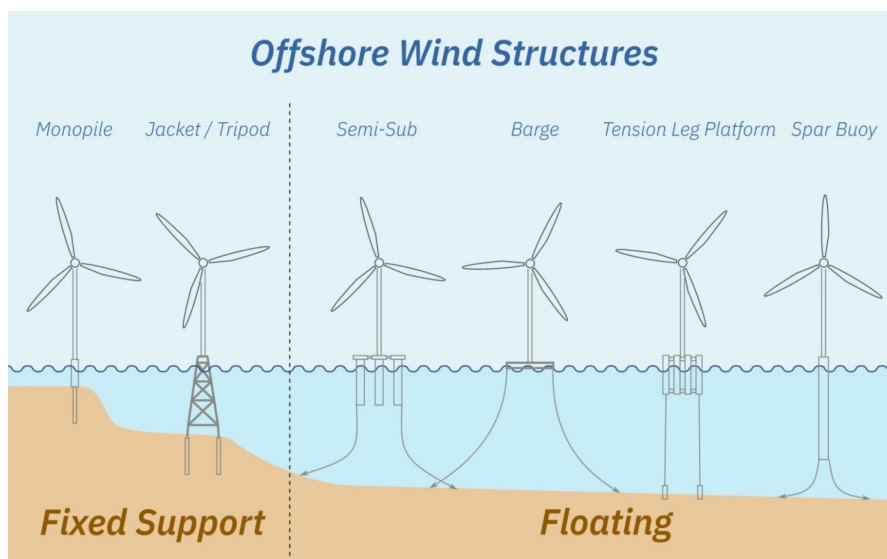


Figure 1.2: Types of offshore wind foundations [56]

Bottom-fixed turbines are suitable for shallow waters and can be installed at rates that are steadily increasing as the industry scales up. Fabrication yards are aiming to handle tens to hundreds of turbines per year to meet rising demand, which enhances the scalability and commercial viability of bottom-fixed turbines [55, 71]. These turbines are installed in the seabed using structures like monopiles, jackets, or tripods, making them stable and easier to install in depths of up to 50-65 meters [19].

In contrast, FOWTs are potentially more cost-effective in deeper waters where bottom-fixed turbines become excessively expensive [106, 9, 63]. FOWTs are deployable in depths greater than 65 meters and offer site flexibility and access to stronger winds. However, they face distinct installation and mooring challenges due to their complex substructures, such as semi-submersibles, spar-buoys, and tension-leg platforms (TLPs).

Currently, there are only a few operational FOWT projects worldwide, highlighting the pre-commercial stage of this technology [54]. Pioneering projects like Hywind Tampen [35] and WindFloat Atlantic [103] have demonstrated the potential of FOWTs. To achieve commercial viability, it is crucial to address supply chain issues. Wet storage can mitigate risks, enhance asset utilization, and aid in managing installation schedules [22].

1.1.3. Installation procedure of semi-submersibles

However, the fabrication rate for FOWTs is slower as a result of larger and more complex foundations. Foundations such as semi-submersible platforms require large amounts of steel and have larger dimensions than bottom-fixed structures. In addition, semi-submersibles require a number of different subcomponents and a considerable amount of welding to assemble [66]. This leads to reduced fabrication rates and increased strain on supply chains. This challenge needs to be addressed for commercialization.

Due to the immaturity of floating offshore wind, the industry has not yet consolidated towards a single installation procedure [54, 60]. Figure 1.3 shows one of the expected installation procedures for semi-submersible FOWTs [50]. In the fabrication harbour, the semi-submersibles are assembled through a process that involves welding subcomponents into the full floater, as illustrated in Figure 1.4. Once the subcomponents are welded together to form the complete floater, the structure undergoes a load-out or float-out procedure. This involves transferring the floater from the assembly platform to the water,

as depicted in Figure 1.5. This can be done using a Self-Propelled Modular Transporter (SPMT) onto a Heavy Transport Vessel (HTV) or a submersible barge [22]. The HTV then transports the substructure to the fit-out quay where it submerges and the semi-submersible is floated off. After the float-out process, the turbine is integrated by a quay-side crane. Finally, the entire structure, including the turbine, is towed to the offshore location for mating with the pre-laid mooring system.

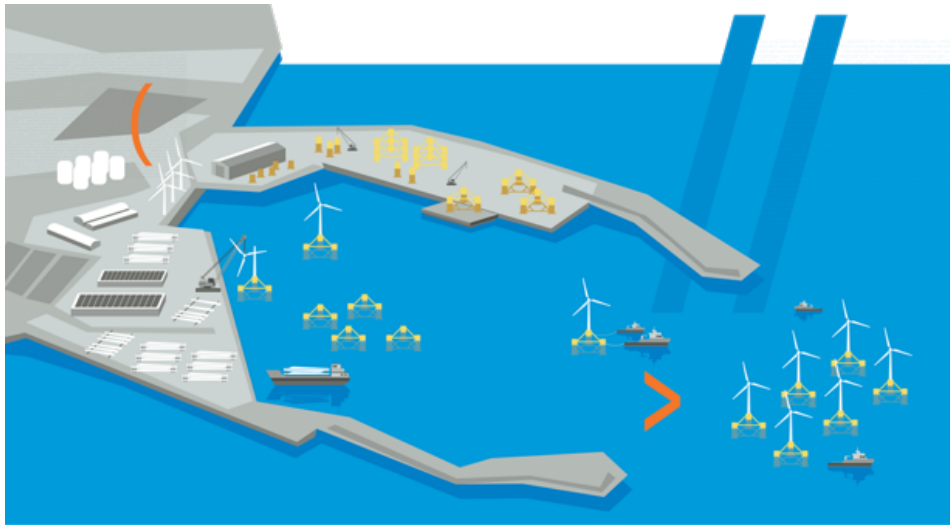


Figure 1.3: Final assembly and tow-out of FOWTs [50]

1.1.4. Wet storage of floating offshore wind foundations

Efficient logistical management is required for the commercial viability of FOWTs. Crane operations for turbine integration are highly weather-dependent, creating uncertainty in installation timelines. This adds pressure to the slow fabrication rate of floaters, which are expected to be produced at no more than one per week, leading to a supply chain bottleneck. As wind farms scale up in size and complexity, it becomes logistically useful to have a buffer of floaters stored in advance to manage these scheduling challenges. The less weather-dependent tow-out process allows for quicker installations once integration is complete.

Due to their large size, storing these foundations on land presents significant challenges. Fabrication yards typically lack space with sufficient load-bearing capacity to accommodate the semi-submersible floaters. Land-based storage is insufficient for the number of floaters that need to be stored, and the increasing scale of floating offshore wind projects exacerbates this issue.

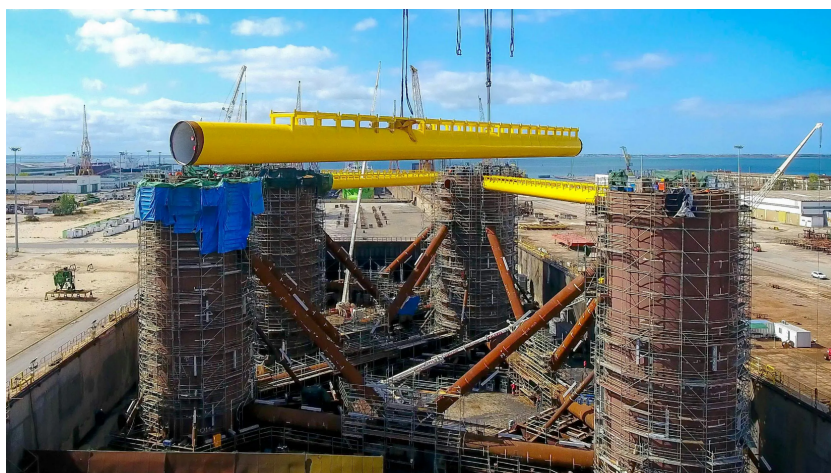


Figure 1.4: Final assembly of the primary structure of a steel semi-submersible [83]

This is where wet storage becomes an option. Wet storage involves the temporary mooring of FOWTs in coastal waters before their final deployment, effectively creating additional storage space on water rather than on land. This can be useful for managing installation schedules, optimizing harbor space, and ensuring that floaters are ready for integration when conditions allow. However, wet storage requires robust and adaptable mooring systems to secure the floaters against environmental forces such as wind, waves, and currents.

In summary, wet storage can be useful to create a logistical buffer to manage unpredictability and ensure continuous operations. The limitations of land-based storage make wet storage a practical and efficient solution to the challenges of FOWT fabrication and deployment.

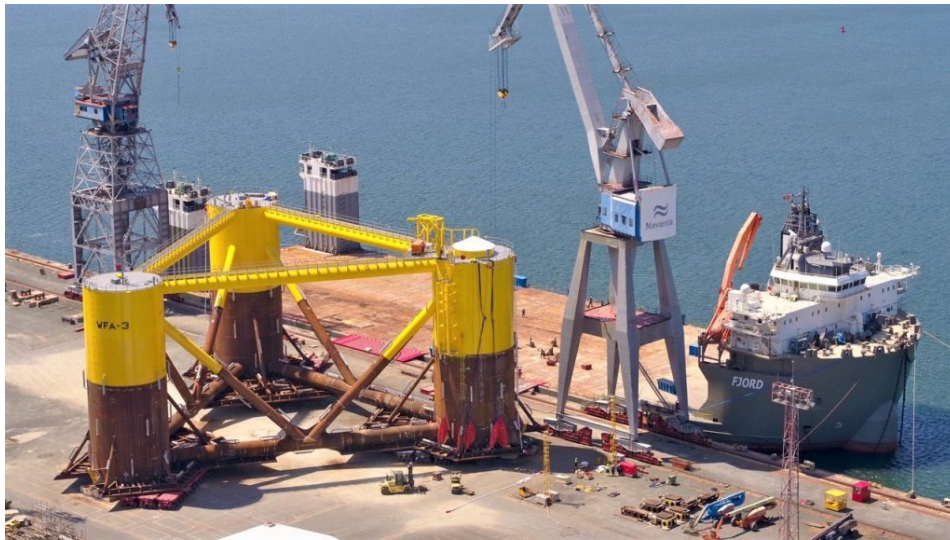


Figure 1.5: Load-out process of a semi-submersible foundation [3]

Possible wet storage locations are expected to be in harbors and bays, where conditions differ from offshore deployment sites. These differences which include water depths, tidal ranges and accessibility requirements impact mooring strategies and costs. While wet storage is a promising solution for managing the logistical challenges of FOWTs, there are currently no comprehensive studies addressing its implementation. This research aims to address this gap by investigating potential wet storage locations and assessing their suitability through dynamic analysis and other evaluations.

1.2. Knowledge gap

Though FOWTs are increasingly used to harness deep-water wind resources, wet storage for these structures is underexplored. A few knowledge gaps must be addressed to advance wet storage mooring systems for FOWTs.

Mooring system dynamics for nearshore wet storage have not been extensively analyzed, primarily because wet storage has not yet been applied in real-world scenarios. However, with the increasing likelihood of its use in the future, understanding these dynamics is important. Current mooring system designs are optimized for deep-water conditions [10, 106]. While the performance of mooring systems has been studied under offshore conditions, interactions with tidal ranges, wind, and waves in nearshore wet storage remain understudied, and the mooring of floaters in these environments requires further investigation [22]. Addressing this gap will support the commercialization of floating offshore wind turbines.

Second, while previous studies have examined floating offshore wind systems with integrated turbines [9, 54, 6], the behavior of standalone floaters is less understood. The absence of the turbine alters weight distribution, affects static offsets, and decreases floater draft, necessitating a reevaluation of the mooring system.

1.3. Problem statement

The rapid growth of offshore wind turbine installations creates significant challenges, particularly in the use of harbor space, both on land and in the water. As the demand for renewable energy increases, the efficient use of port spaces becomes critical [71]. This challenge is further intensified by the larger and heavier floating offshore wind turbines (FOWTs), which introduce new design and logistical complexities [58, 54]. A proposed solution to alleviate these pressures is wet storage, which temporarily keeps these structures afloat in sheltered locations, such as harbors or bays, using their buoyancy until turbine integration or offshore deployment. Wet storage not only relieves pressure on harbor space but also offers flexibility in scheduling installation and maintenance activities.

The feasibility of wet storage relies on the development of mooring systems that can securely anchor FOWTs under various environmental conditions. These mooring systems must be cost-effective, easy to deploy and retrieve, environmentally friendly, and occupy a minimal footprint. Although there has been substantial research on mooring systems for FOWTs with turbines [10, 106, 9, 54, 6], there is a lack of research on standalone floaters in nearshore conditions. Addressing this gap is essential for developing mooring solutions that support wet storage, ensuring a reliable FOWT supply chain and facilitating the large-scale deployment of offshore wind energy.

1.4. Research objectives and questions

The primary objective of this research is to develop a framework for designing and evaluating mooring systems for the temporary wet storage of floating offshore wind foundations. This framework aims to ensure technical feasibility and efficient spatial utilization, addressing the unique challenges posed by wet storage. The study intends to fill critical knowledge gaps in the application of FOWT mooring systems, particularly under different environmental conditions and operational states.

The main question guiding this thesis is formulated in the overarching research question:

How can mooring systems for the temporary wet storage of floating offshore wind foundations be designed to ensure technical feasibility and efficient spatial utilization?

To comprehensively address the overarching question, the research is guided by the following subquestions:

- *What are the key design objectives and criteria mooring system used in wet storage?*
- *Which environmental conditions at potential wet storage sites need to be considered when designing mooring systems?*
- *What are viable mooring system concepts for the wet storage of floating offshore wind foundations?*
- *How can different mooring configurations be modeled and verified?*
- *How do different mooring system designs compare quantitatively, and what are the associated trade-offs?*
- *How can the mooring design approach developed for semi-submersible platforms be applied to other floating offshore wind foundation types?*

These research questions investigate various aspects of the implementation of wet storage in floating offshore wind projects and form the foundation upon which the methodologies of this thesis are built.

1.5. Approach and methodology

Figure 1.6 shows the steps that the research has followed to develop and evaluate mooring systems for the wet storage of floating offshore wind foundations.

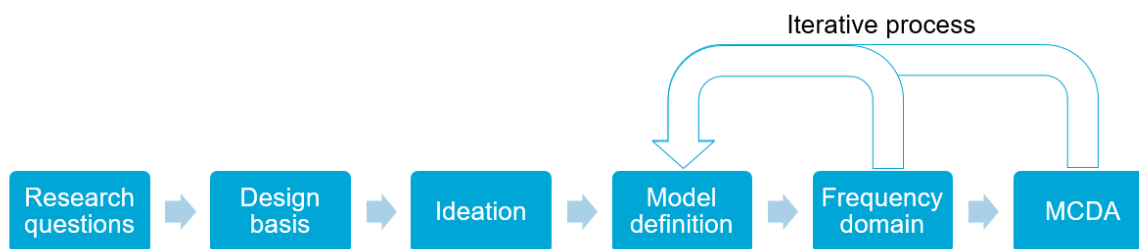


Figure 1.6: Research approach and methodology

The process begins with a review of the available literature, followed by the definition of the research questions that guide the subsequent steps. The next phase involves the derivation of a design basis, which includes listing all requirements for the mooring systems. This is followed by the ideation phase, where different mooring types and concepts are explored to identify potential solutions.

In the model definition phase, models of the mooring systems are developed, incorporating environmental conditions and floater characteristics. Potential flow-based diffraction analysis is used to calculate the loading and response of wet bodies as a result of surface water waves. This analysis defines the load response amplitude operators (RAOs), added mass, stiffness, and damping coefficients. This step is needed before proceeding to the frequency domain (FD) analysis, which assesses the dynamic behavior of the mooring systems. Dynamic analysis is used to understand how mooring systems respond to various environmental forces. FD analysis allows for rapid assessment of multiple mooring configurations, enabling adjustments of the designs based on initial results.

Upon achieving satisfactory results in the FD analysis, the study progresses to the Multi-Criteria Decision Analysis (MCDA) phase. This phase evaluates the mooring systems against multiple criteria to identify the most promising configurations. Further iterations may be required to refine the designs based on MCDA outcomes.

By following this methodology, the research aims to develop robust and efficient mooring systems for the temporary wet storage of FOWTs, addressing both theoretical and practical challenges.

1.6. Demarcation and scope

This thesis focuses on the semi-submersible foundations, examining the feasibility of wet storage for these structures. The emphasis is on storing floaters without turbines due to logistical reasons.

Excluded from the study's scope are financial modeling and economic analysis of installation methods, as these are not central to the technical exploration of FOWTs. The research also does not cover less developed turbine technologies like hydraulic, vertical-axis, and airborne wind turbines or multi-turbine platforms. Instead, it focuses on the established design of a 15 MW reference semi-submersible floater. This focus on larger turbines aligns with industry trends towards increasing turbine sizes for floating wind projects and the anticipated feasibility of floating offshore wind (FLOW) being more viable for high-capacity turbines.

This study does not explore the mathematical optimization of foundation designs specifically for wet storage, nor does it modify the fundamental design of the floaters. The floaters are designed for their full operational lifetime in offshore environments. Wet storage is considered a temporary solution to address land use constraints and is not intended for long-term use. Therefore, the focus is on designing mooring systems that work with the unaltered floater design.

Additionally, this research considers scenarios involving multiple floaters stored simultaneously but does not discuss specific assembly or maintenance activities during the storage phase. The primary focus is on the design and operational aspects of mooring systems for wet storage.

By defining these constraints, the research ensures a focused and detailed exploration of the critical aspects of the design of the mooring system for temporary wet storage, providing a solid foundation for subsequent studies and practical implementations.

1.7. Report structure

This thesis is structured to systematically explore the development and evaluation of mooring systems for the temporary wet storage of floating offshore wind foundations.

Chapter 1 provides the background, problem statement, knowledge gap, research objectives and questions, approach and methodology, demarcations, and an overview of the report structure.

Chapter 2 offers a comprehensive literature review covering the design basis for floater designs, offshore wind logistics, environmental loads and body motions, and mooring systems.

Chapter 3 details the development of a MCDA framework used to evaluate and compare different mooring system designs.

Chapter 4 describes the model setup, including the environmental conditions at the case study location, and details of the VoltturnUS-S floater, along with the diffraction analysis and mesh validation.

Chapter 5 presents the findings from the dynamic analysis of different mooring systems and the results of the MCDA, discussing the performance of various configurations.

Chapter 6 summarizes the primary findings, answers the research questions, and discusses practical implications.

Chapter 7 provides recommendations for further research and future work based on the findings of the thesis.

The References lists all sources referenced throughout the thesis, and the Appendices include additional data, detailed calculations, and supplementary material.

2

Theoretical background

2.1. Mooring systems

Floating offshore wind turbines (FOWTs) are secured to the seabed using mooring systems. These systems keep turbines in place despite dynamic environmental forces. Compliant support structures such as semi-submersibles can use catenary or taut mooring systems made of chain, wire, or fiber ropes [29]. For semi-submersibles and spars, mooring systems are not designed to counteract first-order wave-induced motions, as this causes excessive fatigue and is unnecessary for FOWT operation. Mooring systems are classified as temporary, semi-permanent, or permanent, each with specific challenges. Semi-permanent moorings, used for wet storage, require flexibility and robustness for station-keeping and easy retrieval and redeployment. Permanent installations need higher redundancy to ensure long-term safety according to DNV-ST-N001 [30].

2.1.1. Mooring profiles

The most common types of mooring profiles used for floating offshore wind turbines are [107, 98, 58]:

- Catenary mooring system
- Tension-leg (TLP) mooring system
- Taut mooring system
- Semi-taut mooring system

The catenary mooring system has a catenary-shaped profile with a part of the mooring line lying on the seabed in a static equilibrium position [11]. The self-weight of the mooring line forms the profile and generates the necessary restoring forces to counteract the FOWTs static offset and dynamic motions. The catenary mooring system is the most widely used in the oil and gas industry in shallow to medium-depth waters [68].

Tension-leg platforms (TLPs) use vertical moorings anchored to the seabed under constant tension. The high axial stiffness of the tubular steel pipe tendons minimizes vertical displacements, enhancing FOWT performance and longevity. Unlike chain moorings, TLP tendons demand precise installation and handling due to the required tension. Before tensioning, the platform is unstable, making them unsuitable for wet storage.

The taut leg mooring system does not have mooring lines lying on the seabed in the static equilibrium position. The mooring lines are taut from the anchor to the fairlead. This has the advantage that the anchor footprint is smaller and the mooring system uses less line material. This difference in anchor footprint is schematically shown in Figure 2.1. As the mooring lines are taut, the compliance to floater offset and dynamic response is mostly generated by line tensile stretch.

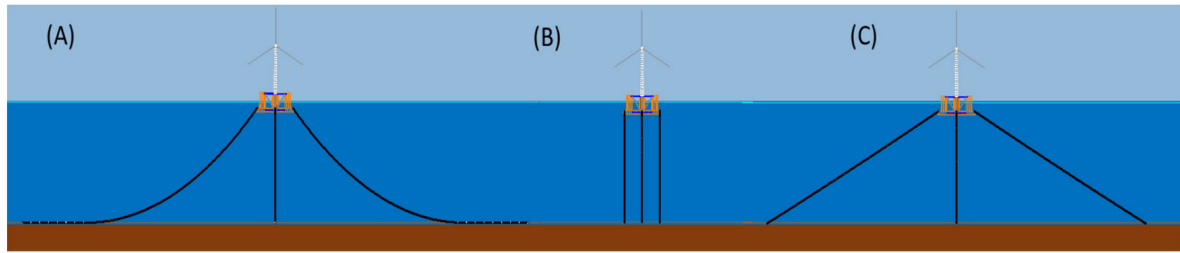


Figure 2.1: Schematic of three mooring systems: (A) Catenary, (B) TLP, (C) Taut [107]

The mooring system configuration can be selected by varying the system parameters until a system is found that complies with regulatory and functional requirements. This is typically done by iteration and varying parameters such as anchor radius, line size and number, grouping, and spread angles [68].

Catenary mooring system

For a simple catenary line configuration, the following equations are set up by Bartrop [8]. The ratio of the line length S and the line height H , with the tangent to the bottom at the line lower end, is given by:

$$\frac{S}{H} = \sqrt{2 \frac{T}{\omega H} - 1} \quad (2.1)$$

Where T is the fairlead tension and ω is the unit weight. The ratio S/d is the line slope, i.e., the ratio of the line length S to the water depth d , which can then be determined by:

$$\frac{S}{d} = \sqrt{\frac{2}{s_{coef}} \cdot \frac{Q}{\omega_r d} - 1} \quad (2.2)$$

Where s_{coef} is the minimum safety coefficient, ω_r is the line unit weight in water, and Q is the line breaking load [11][12]. For catenary mooring lines, a purely horizontal load at the anchor is often used, allowing drag embedded anchors (depending on seabed conditions) as detailed in subsection 2.1.5. This determines the allowable top load when the catenary is fully elevated.

The line breaking load Q for an R3 stud link chain cable, according to DNV-OS-E302 [24], is a function of the chain nominal diameter d_c (mm) and unit weight in air ω (kN/m):

$$Q = 103.84\omega(44 - 0.08d_c) \quad (2.3)$$

The mooring footprint is the horizontal distance between the anchor point and the fairlead when the catenary line is fully developed. This footprint defines the seabed area used by the mooring system and affects how many floaters can be accommodated in wet storage.

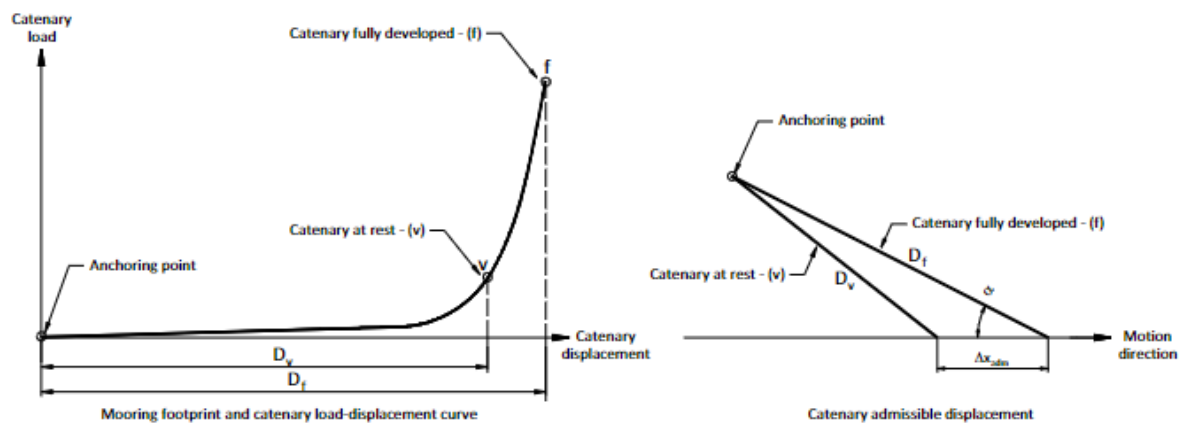


Figure 2.2: Characteristic points of a catenary line [11]

The horizontal projection D_f of the curve is reached when the allowable platform offset Δx_{adm} is reached by the most elongated line, in the plane with the lowest angle α to the motion direction. This angle α is shown in Figure 2.2. Therefore, the horizontal catenary length D_v in equilibrium under static forces only is:

$$D_v = D_f \sqrt{\sin^2 \alpha + \left(\cos \alpha - \frac{\Delta x_{adm}}{D_f} \right)^2} \quad (2.4)$$

Therefore, to minimize line weight, the following relationship must be satisfied:

$$\gamma_{\text{mean}} T_{c,\text{mean}} + \gamma_{\text{dyn}} T_{c,\text{dyn}} < S_c \quad (2.5)$$

Here, the characteristic line capacity S_c , defined as 95% of the minimum breaking load Q , must exceed the sum of the mean line tension ($T_{c,\text{mean}}$) multiplied by its load factor (γ_{mean}) and the dynamic contribution ($T_{c,\text{dyn}}$) multiplied by its load factor (γ_{dyn}). These load factors are determined by the consequence class of the mooring lines. The catenary systems counteract the offset caused by the turbine's mean thrust force during operations, resulting in mooring line uplift. In wet storage, without the mean thrust force, shorter catenary lines might be feasible.

Effect of shallow water on catenary mooring system Xu's research [105, 106] extensively covers the effects of shallow water on catenary mooring systems at depths of 50-80 m, unlike most studies on larger depths. This is relevant as wet storage is expected in even shallower waters.

The horizontal, geometric, in-elastic stiffness k_G of a catenary mooring line can be expressed as:

$$k_G = \frac{\partial T_H}{\partial x} = \omega \left[-\frac{2}{\sqrt{1 + 2\frac{T_H}{\omega h}}} + \cosh^{-1} \left(1 + \frac{\omega h}{T_H} \right) \right]^{-1} \quad (2.6)$$

where ω is the unit weight of the mooring line, x is the horizontal offset, h is the water depth, and T_H is the horizontal line tension [37]. For constant T_H , horizontal mooring stiffness decreases with increasing water depth, as shown in Xu's paper (Figure 2.3). In shallow waters, horizontal stiffness is relatively high. Horizontal wave-frequency motions of the floating wind turbine are mainly due to inertial forces. A stiffer mooring system results in higher natural frequencies for horizontal motions, potentially bringing them closer to the range of difference-frequency wave loads [106]. This can increase the likelihood of resonance and poses a design challenge for catenary mooring systems in shallow waters.

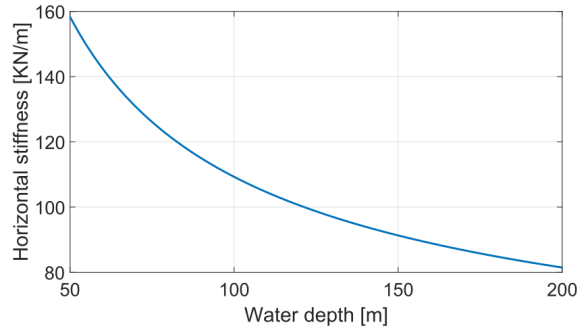


Figure 2.3: Influence of water depth on horizontal mooring stiffness for a specific case study [106]

Catenary mooring top angles α and β (see Figure 2.4) differ significantly in shallow waters. The catenary shape diminishes and stretches as shown in Figure 2.4.b. These angles are determined by the horizontal span s , effective water depth h , and the length of the suspended mooring line l_s . Thus, the following equations apply:

$$\beta = \text{atan} \left(\sinh \frac{2sh}{l_s^2 - h^2} \right) \quad \alpha = \frac{\pi}{2} - \beta \quad (2.7)$$

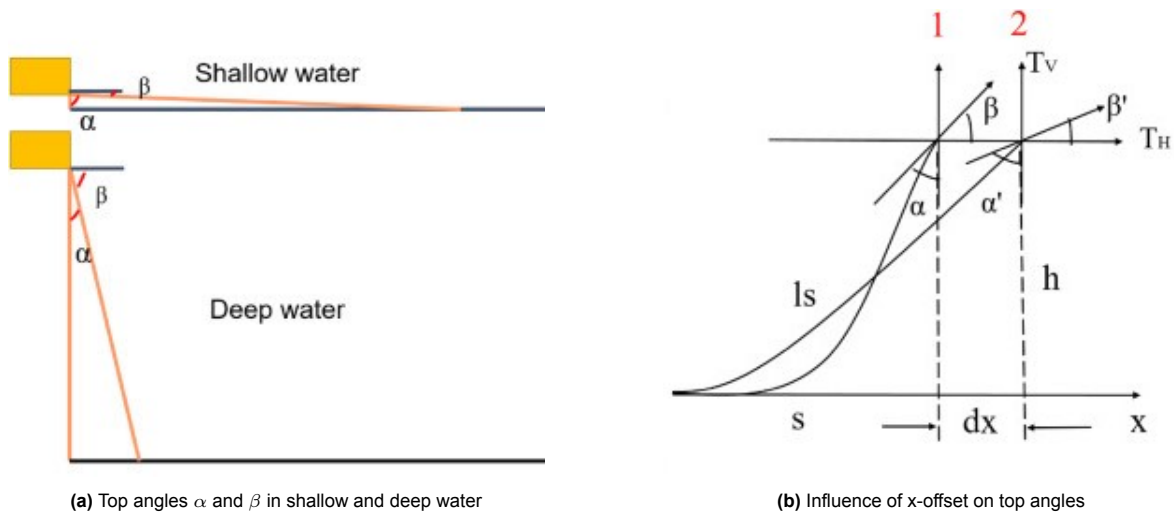


Figure 2.4: Top angles of catenary lines in shallow waters [106]

Taut mooring system

A taut mooring system employs tensioned lines, typically made from synthetic ropes or steel wire, to connect the floating substructure to the seabed anchors. Unlike catenary systems that rely on the weight of the lines for the restoring force, the restoring force in taut systems comes from the tension in the mooring lines. These lines run more vertically compared to catenary systems, allowing for a smaller mooring footprint. The compliance in the system is primarily provided by the elasticity of the ropes and, in some cases, load-reduction devices such as buoys or springs may be used to dampen loads and reduce tension peaks [19]. Due to the tension in the lines, vertical loads at the anchor points are significantly higher, often necessitating high-capacity anchors like piles or vertical load anchors to maintain stability.

The footprint radius of a taut mooring system is typically about twice the water depth, significantly smaller than that of catenary moorings, making it advantageous in areas with limited seabed space. This is useful in areas near fabrication yards, where the footprint reduction becomes more significant. However, the system requires a sufficient amount of tension to ensure stability under varying environmental conditions.

Effect of shallow water on taut mooring system Taut mooring systems are affected by shallow water conditions. In shallow waters, the proximity of the mooring lines to the seabed increases interactions with both the seabed and environmental forces such as currents and waves. These increased interactions generate higher dynamic loads on the system, which can complicate the design and performance of the mooring lines.

One key factor in the performance of taut mooring systems is line stiffness, which is determined by the material properties of the lines and the tension applied to them. In shallow waters, the stiffer the lines, the greater the resistance to displacement, but this comes at the cost of higher peak loads during dynamic events like storms or large waves. These peak loads can stress both the mooring lines and the anchors, leading to potential fatigue or failure over time.

On the other hand, using more flexible lines can help reduce these peak loads by allowing more movement and absorbing some of the energy from dynamic forces. However, the downside is that greater displacements can occur, which may result in the floating structure moving outside its operational limits. This is especially problematic in shallow water, where there is less space for movement before the structure comes into contact with the seabed or other obstacles.

Balancing these two factors, stiffness and flexibility, is required for the design of taut mooring systems in shallow waters. The system must be designed to minimize the dynamic loads while keeping the floater within its desired operational range.

Semi-taut mooring system

Certain designs use a semi-taut mooring system, combining catenary and taut features. These lines sag under their weight, allowing more vertical and horizontal movement than taut systems, reducing fatigue and needing shorter lines than catenary systems [46, 43].

Ji et al. propose adding clump weights to the bottom of the mooring lines to create a catenary shape near the bottom of the mooring line [59]. Therefore, the advantages of both mooring systems can be applied. This is shown in Figure 2.5.

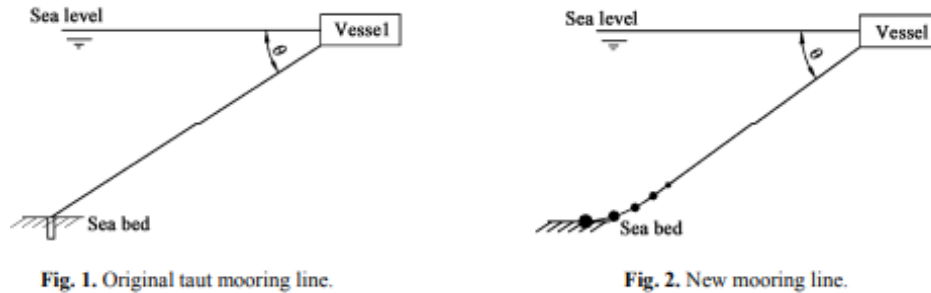


Figure 2.5: Clump weights added in taut mooring lines [59]

Single point mooring

Another notable mooring system is the Single Point Mooring (SPM), frequently used in the oil and gas industries [100]. SPM systems offer a central pivot for the floater, allowing it to rotate freely while maintaining its position. This configuration uses one main anchor connected to the floater, allowing weathervaning, which helps reduce mooring line loads. SPM systems are generally simpler in design compared to multi-point moorings, but they may offer less stability for certain applications. However, in sheltered environments, such as nearshore wet storage sites, SPM could be a suitable option depending on the site's environmental conditions.

Honeymooring

A novel approach that has been explored in the literature is the Honeymooring concept [49, 64]. This system arranges mooring lines in a honeycomb pattern, reducing spatial footprint while maintaining structural integrity. Honeymooring is particularly attractive for nearshore wet storage applications because it optimizes the use of limited space and reduces material costs. Its design aims to accommodate large numbers of floaters within a confined area, which is critical for optimizing wet storage logistics. While not yet widely implemented, Honeymooring represents a promising future direction for efficient mooring configurations in offshore wind energy.

2.1.2. Mooring components

Mooring systems are composed of components like mooring lines, anchors, and connectors that stabilize structures by resisting environmental forces. Their design considers environmental conditions, water depth, seabed characteristics, and dynamic loads. This section addresses key mooring components, their functions, types, and roles within the system.

2.1.3. Mooring lines

Mooring lines, integral to the stability and safety of marine structures, are designed based on the material's response to oceanic forces. Material choice is dictated by the application, each offering distinct advantages in their operational environment. Mooring lines are usually composed of metallic chains, metallic wires, or synthetic ropes [20, 106]. Mooring line materials can be classified by material type as shown in Figure 2.6.

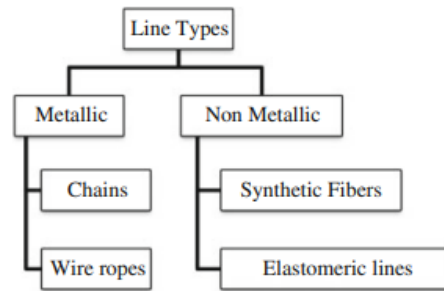


Figure 2.6: Mooring line types according to construction material [20]

Metallic chains Metallic chains, made primarily of steel, are durable and resistant to seabed contact. They come in studless and stud link varieties [98]. Stud link chains, with a bar (or 'stud') across the link, are used for shallow water mooring, offering ease of handling and a strong connection. Studless chains, lacking the bar, are preferred for permanent mooring due to their lighter weight and longer fatigue life, which is crucial in deep water applications where chain weight affects mooring dynamics and economics.

Metallic wires Steel wire ropes, due to their elasticity, are ideal for tensioned mooring systems, especially in deepwater applications where chain weight is prohibitive. Available in single-strand and multi-strand forms, their flexibility and stiffness can be customized. Protective coatings like polyurethane or zinc reduce corrosion and increase longevity.

Synthetic fiber ines Synthetic ropes made from nylon, polyester, polypropylene, Kevlar, or high-density polyethylene are highly elastic. Their stretchability under load provides damping beneficial for deepwater mooring with dynamic loads. This elasticity and their lightweight make them suitable for deepwater tether applications where traditional chain weight is a disadvantage.

Elastomeric lines Elastomeric mooring lines, made from natural or synthetic rubber, excel in elongation under load but are prone to abrasion and cutting, needing special attention in harsh environments.

A summary of the features of various line materials is given in Table 2.1.

Table 2.1: Mooring line materials, adapted from the oil and gas industry [20]

Material	Features	Comments
Chain	<ul style="list-style-type: none"> - Broad use experience - Readily available 	<ul style="list-style-type: none"> - Unsuitable for water depths greater than about 450 m - Susceptible to corrosion - Good abrasion resistance
Steel Wire Rope	<ul style="list-style-type: none"> - Broad use experience - Readily available 	<ul style="list-style-type: none"> - Unsuitable for water depths greater than about 900 m - Susceptible to corrosion
Polyester	<ul style="list-style-type: none"> - High dry and wet strength - Moderate stretch - Frequent use in deep water taut moorings 	<ul style="list-style-type: none"> - Most durable of all fibre line materials - Moderate cost
Nylon	<ul style="list-style-type: none"> - High dry strength - High stretch 	<ul style="list-style-type: none"> - Wet strength about 80% that of dry - Low fatigue life - Moderate cost
Polypropylene and Polyethylene	<ul style="list-style-type: none"> - Low weight - High stretch 	<ul style="list-style-type: none"> - Low strength - Low melting point - Susceptible to creep - Low cost
HMPE	<ul style="list-style-type: none"> - Low stretch - High strength to weight ratio 	<ul style="list-style-type: none"> - Replacing wire for towing-increased handling safety - High cost
Aramid	<ul style="list-style-type: none"> - Very low stretch - High strength to weight ratio 	<ul style="list-style-type: none"> - Minimum bending radius similar to steel wire rope - Low abrasion resistance - High cost
Elastomer	<ul style="list-style-type: none"> - Low weight - High elongation capacity - High tear strength 	<ul style="list-style-type: none"> - Susceptible to cutting and breaking

Falkenburg SYrope Model

Mooring system design must consider the stiffness of the mooring lines, as this parameter plays a critical role in determining the dynamic response of the system. The Falkenburg SYrope model provides an analytical framework for understanding the stiffness characteristics of mooring lines, with particular focus on synthetic fiber ropes such as nylon and polyester, which are commonly used in offshore applications. This model is especially relevant to Floating Offshore Wind Turbines (FOWTs), where environmental loads lead to significant elongation of the mooring lines.

As shown in Figure 2.7, the stiffness of polyester mooring lines is highly variable, depending on the amount of stretch. This variability is important for mooring systems subjected to both static and dynamic loads, as the stiffness will influence how the system responds to these different conditions.

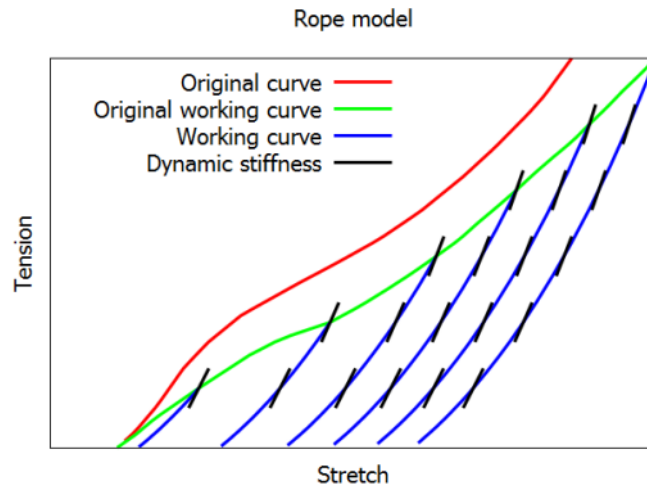


Figure 2.7: Variable stiffness characteristics of polyester mooring lines according to the Falkenburg SYrope model [36]

The Falkenburg model emphasizes the need to use dual stiffness values when analyzing mooring systems. In this approach, different stiffness parameters are applied for static offsets and for dynamic elongation, improving the predictive accuracy of mooring line behavior under varying load conditions. This dual-stiffness approach is particularly useful in scenarios involving large displacements, such as those experienced by FOWTs. Future studies should explore the application of this model in wet storage scenarios, where the static offset is typically smaller, to determine if multiple stiffness values are needed to enhance modeling accuracy in these conditions.

However, in the models used for this study, a single axial stiffness is employed, which is based on the line diameter. This simplified approach is common in early-stage analyses, where computational efficiency is a priority. As noted by Chang (2019), a frequency-domain approach with second-order transformations can be used to incorporate nonlinear dynamic effects in fully coupled analyses. Still, this study opts for a more streamlined model using a single stiffness value, recognizing that while this simplification may reduce accuracy, it remains sufficient for preliminary evaluations of mooring performance.

Both polyester and nylon mooring lines exhibit highly nonlinear axial stiffness, which is influenced by several factors:

- Mean loads acting on the mooring line
- Amplitude of dynamic loads
- Loading frequency

For polyester ropes, the influence of load amplitude and frequency on axial stiffness is relatively minor, allowing the stiffness to be approximated within reasonable bounds. Nylon ropes, on the other hand, are far more sensitive to these factors, necessitating the use of a nonlinear hysteretic stiffness model to accurately capture their behavior. This distinction is important in dynamic analysis, as nylon's lower stiffness can reduce peak loads during dynamic events, leading to smaller mooring components and potential cost savings [81].

Depalo (2022) further highlights the complexity of modeling dynamic stiffness in nylon ropes. His study shows that using a quasi-static stiffness model tends to underestimate peak mooring tensions by 30%–40% when compared to dynamic models that account for stiffness changes under varying loads. In simulations of a taut-moored wave energy converter (WEC), nylon ropes produced lower mooring tensions and allowed for greater WEC motions compared to polyester ropes, demonstrating nylon's advantages in certain applications. This underscores the importance of using dynamic stiffness models—especially for nylon ropes—to prevent underestimating the loads on mooring systems.

When selecting mooring line materials, it is important to consider not only the immediate performance

but also the long-term effects of usage. Synthetic fiber ropes, such as nylon and polyester, can experience stiffness changes over time due to factors like cyclic loading, internal heat generation, and fiber wear. These long-term effects must be accounted for in the design process, often necessitating conservative safety factors to ensure the durability and reliability of the mooring system over its operational life.

2.1.4. Auxiliary equipment

Auxiliary equipment such as buoyancy aids, clump weights, connectors, and tensioners can enhance the functionality and reliability of mooring systems. Buoyancy aids, such as in-line mooring buoys, help transfer loads through the connection system, enhancing overall fatigue resistance. However, while these aids improve fatigue resistance globally, they can also cause localized stress concentrations, potentially leading to fatigue reduction at specific points [7]. Clump weights assist in providing restoring forces and limiting floater displacements, but their use requires caution due to the risk of line failure at critical points such as the crown [38]. Additionally, in-line mooring load reduction devices are employed to lower peak tension, thus improving the durability and performance of the mooring system. Examples of such solutions include those offered by Dublin Offshore and TFI Marine [31, 95].

2.1.5. Anchors

At the end of a mooring line, various anchors can be used. The angle between the mooring line and the seabed determines the suitable anchor. A key difference between catenary and taut mooring systems is the vertical load on the anchor in taut mooring systems. An overview of a few anchor types is given in Figure 2.8.

A drag embedment anchor (DEA), shown in Figure 2.9a penetrates the seabed, generating holding capacity through soil resistance. DEAs are widely used and can resist large horizontal but not vertical loads. They are suitable for catenary mooring systems where the mooring line meets the anchor at a shallow angle [98].

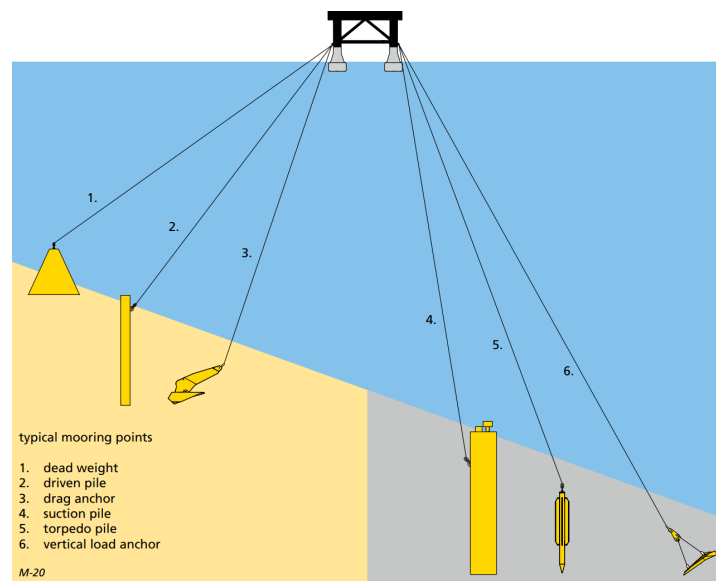


Figure 2.8: Overview of six different anchor types [98]

A vertical load anchor (VLA), shown in Figure 2.9b penetrates the seabed more deeply to resist vertical loads, making it ideal for taut leg mooring systems where the mooring line approaches at steep angles, like 45° .

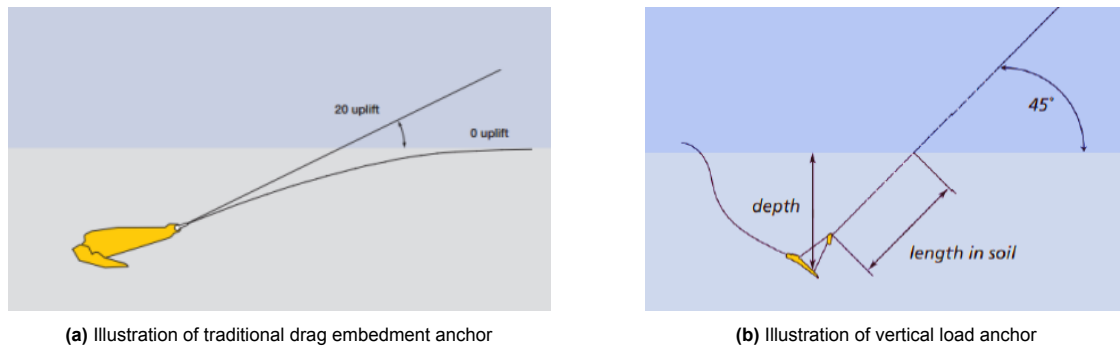


Figure 2.9: Comparison of drag embedment and vertical load anchors [74]

TLP systems depend largely on tendons and soil conditions. To improve them, redundant mooring lines and soil-insensitive anchors, such as concrete gravity anchors, suction, and pile-driven type anchors, can be used [63].

Suction pile anchors are hollow steel cylinders with a closed top and open bottom. They are installed by creating a pressure difference in the pipe, driving the pile to its target depth. Friction along the pipe walls and lateral soil resistance provide the holding capacity for horizontal and vertical loads [96].

Torpedo piles rely on kinetic energy to embed themselves at a target depth, making them suitable for deep water moorings due to their ability to withstand vertical and horizontal loads without mechanical handling [98].

Gravity or dead weight anchors rely on their weight and friction with the seabed for holding capacity and do not embed themselves into the seabed. Driven piles are installed using hammers or vibrators, and like suction piles, they rely on friction and lateral soil resistance for holding capacity [98].

Innovative anchors in development include dynamic tethers with springs, drilled anchors, and seabed anchored foundations templates (SAFT) [45]. As all anchors interact with the seabed, understanding soil mechanics is required. Standards like DNV-ST-N001 [30], DNV-RP-E301 [26], DNV-RP-E302 [27], DNV-RP-E303 [28], and EN 1537 [33] should be consulted for compliance. Choosing between anchors and piles is mostly an economic decision. Piles cost about 40% of equivalent capacity anchors but have higher installation costs. See Table 2.2 for a cost comparison.

Table 2.2: Cost comparison between anchors and piles, in which plus means less expensive and minus means more expensive, adapted from [98]

	Pile	Suction pile	Anchor
Soil survey	-	-	+
Procurement	+	-	-
Installation spread	-	-	+
Installation time	-	-	+
Pile hammer	-	+	+
Follower	-	+	+
Pump unit	+	-	+
Pretensioning	+	-	-
Extra chain	+	+	-
Rest value pile/anchor	-	+	+
Removal of anchor point	-	+	+
ROV	+	-	+

Another type of mooring used in nearshore settings is the pile field. This approach, more common in traditional harbor setups, involves a series of piles or dolphins arranged to secure vessels in place. When adapted for offshore or wet storage mooring, pile fields can provide robust and reusable anchoring points. This system is particularly suitable for shallow water locations where seabed penetration

is feasible. While less flexible compared to mooring line-based systems, pile fields offer stability and durability, especially in protected, low-energy environments.

Shared anchors

Offshore wind turbines are typically arranged so that multiple mooring lines can connect to a single anchor point. This setup, beneficial for wet storage, allows turbines to be placed closer together, reducing procurement costs and the number of offshore geotechnical investigations needed per anchor [23]. Additionally, a multiline anchor system increases redundancy in the mooring design at a relatively minor additional cost. By connecting each turbine to four anchors, as opposed to the more common three-anchor configuration, the system offers higher redundancy and improved load distribution. This additional anchor reduces the risk of mooring failure.

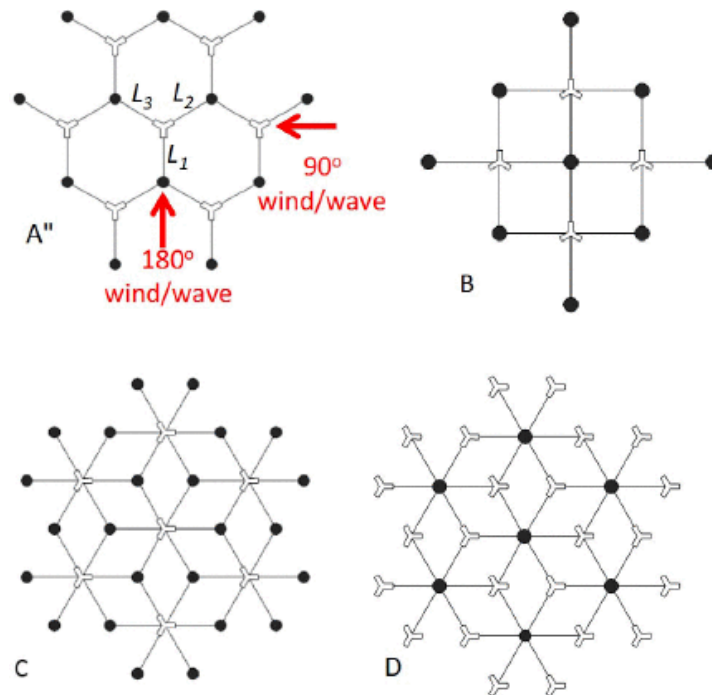


Figure 2.10: Potential wind farm configurations using multiline anchors [40]

Figure 2.10 shows wind farm configurations using multiline anchors, studied by Fontana et al. [40]. Their research shows anchor reductions up to 60% for 3-line and 79% for 6-line systems in a 100-turbine floating wind farm. Fontana's later study [39] with the NREL 5 MW turbine and OC4-DeepCwind semi-submersible found that multiline anchors affect the average maximum anchor force: 16% decrease for 3-line and 20% increase for 6-line anchors compared to single-line anchors. This impacts design strength due to multidirectional loading. The study calculated anchor forces using vector summation of line tensions at the shared anchor, considering both horizontal and vertical components. However, assumptions like large fairlead-to-anchor distances, minor platform motions, FOWT spacing over 500 meters, and independent wave fields may not apply to wet storage scenarios.

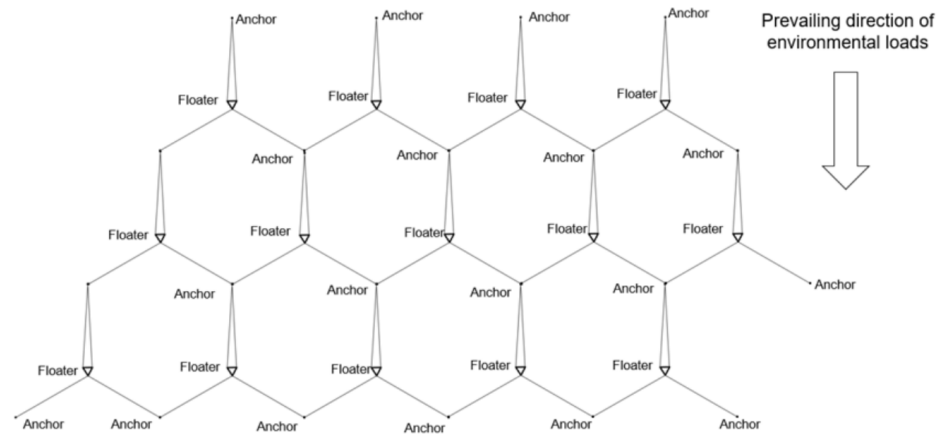


Figure 2.11: V-shape four-line mooring system for 14 turbines [104]

Wu et al. [104] propose a V-shape mooring system, shown in Figure 2.11, connecting mooring lines from all sides of a floater to one anchor, forming a honeycomb pattern. This system, with similar tension and platform offsets, and more stable yaw and heel angles, was tested in water depths of 250 to 1000 meters. Its use and behavior in shallower waters, relevant to wet storage, need further investigation.

2.2. Modelling of floating offshore wind foundations

This section outlines the techniques used for modeling mooring systems of floating offshore wind turbines (FOWTs), focusing on rigid body dynamics, hydrodynamics, and diffraction analysis.

Modeling FOWTs is commonly done in the time domain due to the nonlinearities involved, such as slow drift effects [87, 110, 29, 88]. Time-domain simulations are effective at capturing these nonlinear behaviors, leading to a more accurate representation of FOWT dynamics. Therefore, the equations of motion (EoMs) for FOWTs incorporate these nonlinearities to provide a complete description of the system's behavior [37, 86].

While frequency-domain modeling offers the advantage of reduced computation time, it requires the linearization of the system. This method is useful for initial assessments and comparative studies of mooring systems, as it allows for rapid evaluations. However, frequency-domain analysis can underestimate loads and responses because it neglects low-frequency second-order effects. A contributing factor to this underestimation is the use of the Newman approximation, which is known to undervalue the second-order response [94].

2.2.1. Hydrodynamics

The hydrodynamic behavior of floating platforms is governed by fluid-structure interactions, which include both forces acting on the structure and the motions of the structure in response. These interactions can be categorized into two primary components: diffraction, which accounts for the fluid's effect on the structure, and radiation, which considers the waves generated by the movement of the structure. Hydrostatics, on the other hand, deals with buoyancy and restoring forces that act to maintain the stability of the platform.

To estimate hydrodynamic loads, various theoretical models can be applied depending on the characteristics of the floating structure. For slender bodies such as SPAR platforms, where the diameter is much smaller than the wavelength, the Morison equation is often appropriate. This equation simplifies the hydrodynamic force into two components: drag and inertia, assuming that wave diffraction effects are minimal. However, for larger structures like semi-submersibles, diffraction and radiation effects dominate, making potential flow theory more suitable to accurately model the wave-structure interaction [97].

In deep water, the wave exerting hydrodynamic loads can be modeled using a harmonic function, and the wave dispersion relation is given by:

$$\omega^2 = gk \tanh(kh) \quad (2.8)$$

where ω is the angular frequency, g is gravitational acceleration, $k = \frac{2\pi}{\lambda}$ is the wave number, and λ is the wavelength.

The classification of water depth into shallow, intermediate, and deep waters depends on the ratio between water depth (h) and wavelength (λ):

$$\begin{aligned} \text{Shallow water: } & \frac{d}{\lambda} < 0.05 \\ \text{Intermediate water: } & 0.05 \leq \frac{d}{\lambda} < 0.5 \\ \text{Deep water: } & \frac{d}{\lambda} \geq 0.5 \end{aligned} \quad (2.9)$$

Understanding these classifications is essential for the selection of appropriate wave theories to model the behavior of floating structures in different environments. The applicability of wave theories is illustrated in Figure 2.12, which shows the range of non-dimensional wave heights and water depths where various wave theories apply. In the context of wet storage, extreme sea states are typically avoided, so not all wave theories will be relevant to this study. The figure serves as a guide to the selection of appropriate wave models for different hydrodynamic conditions.

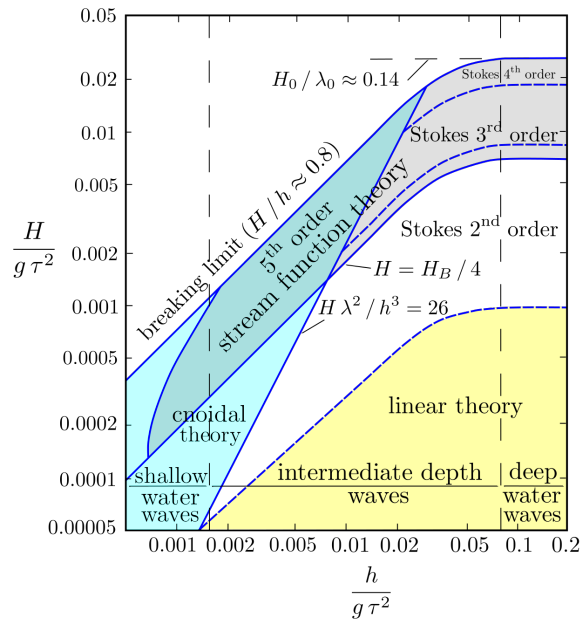


Figure 2.12: Applicability of wave theories [16]

In this thesis, wave loads are modeled using potential flow-based diffraction analysis, as it is well-suited for large offshore structures like semi-submersibles, where both diffraction and radiation play significant roles. The analysis incorporates wave interactions with the structure and their impact on platform motions, ensuring that the hydrodynamic response is well-represented for the expected environmental conditions in the wet storage site.

Potential flow theory

Potential flow theory describes the flow around a body as incompressible (though incompressibility is not strictly necessary), inviscid, and irrotational. The velocity field is represented as the gradient of a scalar function, known as the velocity potential.

The velocity potential ϕ is used to describe the fluid velocity vector $\mathbf{V}(x, y, z, t) = \langle u, v, w \rangle$ at time t at the point $\mathbf{x} = \langle x, y, z \rangle$ in a Cartesian coordinate system fixed in space [37].

$$\mathbf{V} = \nabla\phi = \mathbf{i}\frac{\partial\phi}{\partial x} + \mathbf{j}\frac{\partial\phi}{\partial y} + \mathbf{k}\frac{\partial\phi}{\partial z} \quad (2.10)$$

\mathbf{i} , \mathbf{j} , and \mathbf{k} are unit vectors along their respective axes. The velocity potential does not have physical meaning by itself but is used for the mathematical analysis of an irrotational fluid. This characterization of an irrotational velocity field stems from the fact that the curl of the gradient of a scalar is zero everywhere in the fluid. The vorticity vector $\boldsymbol{\omega}$ is obtained using the gradient operator ∇ and the velocity vector \mathbf{V} .

$$\boldsymbol{\omega} = \nabla \times \mathbf{V} = 0 \quad (2.11)$$

For floating structures, hydrodynamic loading typically consists of first-order and second-order wave loads.

First-order wave loads First-order wave loads, or linear wave loads, are the primary forces exerted on floating offshore structures due to incident waves. These loads cause the structure to oscillate with the same frequency as the waves, including incident, diffraction, and radiation wave loads. Mathematically, these forces are expressed as follows [37, 109]:

$$\mathbf{F}_{\text{wave}} = \mathbf{F}_{\text{incident}} + \mathbf{F}_{\text{diffraction}} + \mathbf{F}_{\text{radiation}} \quad (2.12)$$

where:

- $\mathbf{F}_{\text{incident}}$: force due to the incident wave potential.
- $\mathbf{F}_{\text{diffraction}}$: force due to diffraction potential, caused by wave field disturbance due to the structure.
- $\mathbf{F}_{\text{radiation}}$: force due to radiation potential, from waves generated by the structure's oscillations.

The incident and diffraction wave forces can be represented by:

$$\mathbf{F}_{\text{incident}} + \mathbf{F}_{\text{diffraction}} = -i\omega\rho \int_S \phi_{\text{incident}} \mathbf{n} ds - i\omega\rho \int_S \phi_{\text{diffraction}} \mathbf{n} ds \quad (2.13)$$

The radiation wave force is given by:

$$\mathbf{F}_{\text{radiation}} = -\mathbf{A}\ddot{\mathbf{q}} - \mathbf{B}\dot{\mathbf{q}} \quad (2.14)$$

Here, ω is the wave frequency, ρ the water density, ϕ_{incident} and $\phi_{\text{diffraction}}$ are the incident and diffraction potentials, \mathbf{n} is the normal vector to surface S , \mathbf{A} is the added mass matrix, \mathbf{B} is the radiation damping matrix, and $\ddot{\mathbf{q}}$ and $\dot{\mathbf{q}}$ are the acceleration and velocity vectors of the structure.

Diffraction analysis Diffraction analysis examines wave-structure interactions to assess hydrodynamic forces on floating offshore wind turbines (FOWTs). OrcaWave, utilizing potential flow theory, computes wave-induced loads and structural responses [67]. Linear diffraction methods, as used in OrcaWave, assume small wave amplitudes, whereas nonlinear methods handle large amplitudes but are computationally intensive [72].

In OrcaWave, the velocity potential ϕ is computed across mesh panels to evaluate the pressure on the structure's surface, leading to results such as added mass, damping, Load Response Amplitude Operators (RAOs), and Quadratic Transfer Functions (QTFs). These parameters inform the dynamic response of FOWTs under various wave conditions.

The physical problem to find the wave potentials ϕ_{incident} , $\phi_{\text{diffraction}}$, and $\phi_{\text{radiation}}$ involves solving a boundary value problem (BVP) based on Laplace's equation for an incompressible, irrotational flow:

$$\nabla^2 \phi = 0 \quad (2.15)$$

This equation must be solved subject to boundary conditions:

- At the free surface: The dynamic and kinematic free-surface boundary conditions need to be satisfied, which account for wave motion and the pressure continuity at the air-water interface.
- At the body surface: The Neumann boundary condition requires the normal velocity at the body surface to match the velocity of the body. This enforces the impermeability condition at the structure.
- At the seabed: The velocity normal to the seabed is zero, ensuring that there is no flow through the seabed.
- At infinity: A radiation condition ensures that waves radiate outward and do not reflect back into the domain.

Solving this boundary value problem yields the incident potential ϕ_{incident} , diffraction potential $\phi_{\text{diffraction}}$ (due to the presence of the structure), and radiation potential $\phi_{\text{radiation}}$ (due to the structure's own motion), which are then used to calculate the corresponding forces on the structure.

Load Response Amplitude Operators (RAOs) quantify the dynamic response of a structure to wave loads. In OrcaWave, RAOs are calculated using the Haskind relations or the diffraction load formula. They provide frequency-dependent response measures, which are critical for designing mooring systems and assessing how wave loads influence dynamic loads and mooring tensions.

Shallow waters alter wave behavior and hydrodynamic loading. As the depth decreases, wave speed, wavelength, and wave height change, which modifies diffraction patterns and the resulting forces on the structure. Though the change in wave height only occurs if the assumptions for deep water wave equations no longer hold. Separate diffraction analyses are necessary for different depths to accurately capture these effects.

Second-order wave loads Second-order wave loads are nonlinear forces at frequencies equal to the sum and difference of incident waves. Although marine structures are generally designed to avoid first-order wave energy, the second-order spectrum is harder to avoid and can excite the structure's natural frequencies, causing resonant response. These forces include mean drift, difference-frequency and sum-frequency wave loads [73].

The second-order wave forces can be decomposed into three components:

$$\mathbf{F}_{2\text{nd}} = \mathbf{F}_{\text{mean}} + \mathbf{F}_{\text{difference}} + \mathbf{F}_{\text{sum}} \quad (2.16)$$

where:

- \mathbf{F}_{mean} is the frequency-dependent mean force.
- $\mathbf{F}_{\text{difference}}$ is the difference-frequency wave drift force, which oscillates at difference-wave frequencies.
- \mathbf{F}_{sum} is the sum-frequency wave force, which oscillates at sum-wave frequencies.

The focus of this analysis is on difference-frequency forces, as sum-frequency forces are more relevant for very taut mooring systems or Tension Leg Platforms (TLPs). This is because sum-frequency forces oscillate at higher frequencies, which are more likely to excite the higher natural frequencies of taut systems like TLPs. These systems have higher stiffness and therefore higher natural frequencies, making them more susceptible to excitation by sum-frequency loads. In contrast, platforms like semi-submersibles or those with catenary mooring systems tend to have lower natural frequencies, making them more susceptible to difference-frequency forces, which oscillate at lower frequencies and align more closely with the natural periods of these platforms.

According to Pinkster (1975), the second-order wave forces determined by direct pressure integration can be expressed as [82]:

$$\mathbf{F}_{2nd} = \frac{1}{2} \rho g \int_{WL} \xi_r^{(1)} \cdot \xi_r^{(1)} \mathbf{n} dl + \int_{S_0} \left(\frac{1}{2} \rho \left(\nabla \phi^{(1)} \right)^2 \mathbf{n} + \rho \mathbf{X} \cdot \nabla \frac{\partial \phi^{(1)}}{\partial t} \mathbf{n} + \mathbf{M}_s \cdot \ddot{\mathbf{X}}_g + \rho \frac{\partial \phi^{(2)}}{\partial t} \mathbf{n} \right) ds \quad (2.17)$$

where ρ is water density, g is gravitational acceleration, \mathbf{n} is normal vector, $\phi^{(1)}$ is first-order velocity potential, $\xi_r^{(1)}$ is relative wave elevation, S_0 is mean wetted surface, \mathbf{X} is floating body motion, \mathbf{M}_s is mass matrix of the floating structure, $\ddot{\mathbf{X}}_g$ is center of gravity acceleration, and $\phi^{(2)}$ is second-order velocity potential.

Viscous load In potential flow theory, viscous effects are neglected. However, viscous drag forces can be for hydrodynamic loading on structures. These forces are calculated using the drag term of the Morison equation, accounting for the fluid force on a slender structural member's cross-section [70]. The viscous drag force is expressed as:

$$dF_{\text{viscous}} = \frac{1}{2} \rho C_d A |\mathbf{u}_f - \mathbf{u}_s| (\mathbf{u}_f - \mathbf{u}_s) dl \quad (2.18)$$

where C_d is the drag coefficient, A is the projected area of a unit length cylinder perpendicular to the flow, \mathbf{u}_f is the fluid velocity, \mathbf{u}_s is the structure's velocity, and dl is the differential length along the cylinder.

Mooring system load Mooring systems maintain the position of floating structures by providing restoring forces that counteract environmental loads. This study employs the lumped mass method to discretize cable dynamics along a mooring line. The mooring line is divided into N segments, each characterized by properties such as unstretched length, diameter, density, Young's modulus, and damping coefficient.

Hall et al. [48] describe the motion equation for each mooring line segment i as:

$$\underbrace{\mathbf{m}_i + \mathbf{a}_i}_{\text{mass and added mass}} \ddot{\mathbf{r}}_i = \underbrace{\mathbf{T}_{i+\frac{1}{2}} - \mathbf{T}_{i-\frac{1}{2}} + \mathbf{C}_{i+\frac{1}{2}} - \mathbf{C}_{i-\frac{1}{2}}}_{\text{internal stiffness and damping}} + \underbrace{\mathbf{W}_i + \mathbf{B}_i}_{\text{weight and contact}} + \underbrace{\mathbf{D}_{p_i} + \mathbf{D}_{q_i}}_{\text{drag}} \quad (2.19)$$

where \mathbf{m}_i is the mass of the i -th node, \mathbf{a}_i is the added mass at the i -th node, $\ddot{\mathbf{r}}_i$ is the acceleration vector of the i -th node, $\mathbf{T}_{i+\frac{1}{2}}$ and $\mathbf{T}_{i-\frac{1}{2}}$ are the tension forces at the nodes $i + \frac{1}{2}$ and $i - \frac{1}{2}$, $\mathbf{C}_{i+\frac{1}{2}}$ and $\mathbf{C}_{i-\frac{1}{2}}$ are the internal damping forces at the nodes $i + \frac{1}{2}$ and $i - \frac{1}{2}$, \mathbf{W}_i is the weight force, \mathbf{B}_i is the buoyancy force, \mathbf{D}_{p_i} is the transverse drag force, and \mathbf{D}_{q_i} is the axial drag force.

In OrcaFlex, lines are modeled using a lumped mass approach, representing the line as masses (nodes) connected by massless springs (segments), like beads on a necklace. Properties such as mass, buoyancy, and drag are concentrated at the nodes. The line, divided into sections of specified lengths, types, and segments, employs a finite element approach. The nodes aggregate the line's properties, while segments account for axial and torsional properties, allowing accurate simulation of mooring line dynamics [80]. Figure 2.13 illustrates the discretization of a physical object into nodes and segments, a technique employed in the modeling of mooring lines.

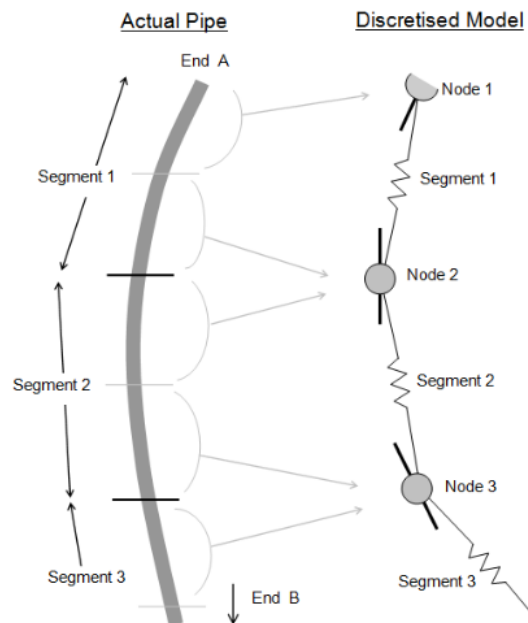


Figure 2.13: Discretized line model in OrcaFlex [80]

2.2.2. Differences between offshore and nearshore locations

Floaters are designed for offshore locations, which are different from wet storage locations. A key difference is water depth; nearshore locations have shallow waters, affecting wave behavior [53]. Nearshore wave conditions are shaped by shallower depths, leading to wave transformations such as refraction, shoaling, and breaking. Offshore waves are not affected by the seabed until they approach the coast. Refraction occurs as waves near a coastline at an angle are deflected due to decreasing wave celerity c with depth.

As shown in Figure 2.14, the wave direction changes, aligning the crests with the depth contours. Snell's law, which governs refraction at material boundaries, applies to shoaling when long-crested waves of constant period cross a bottom step from deeper to shallower water [47]. Waves are influenced by currents influenced by tidal, wind, or waves, and river flows. With the current, waves increase celerity, becoming longer and flatter, while opposing currents cause waves to break earlier, impacting mooring system design. Refraction can also occur if waves pass through areas with varying current velocity.

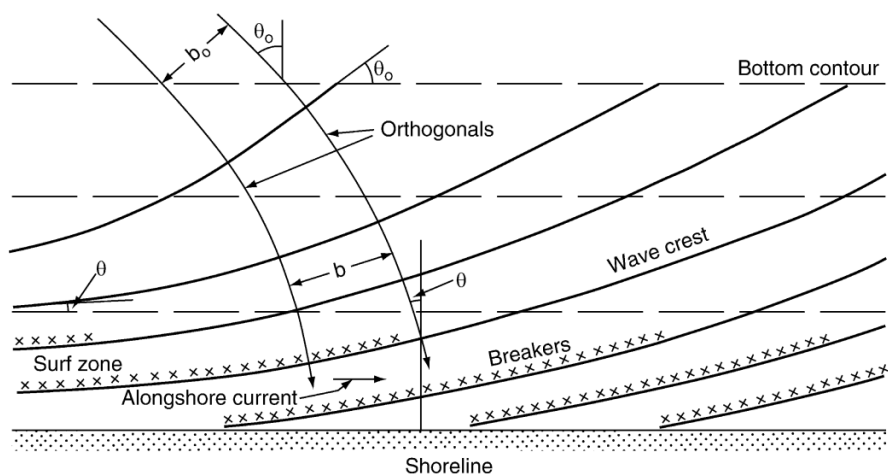


Figure 2.14: Wave refraction when waves approach a coast line [47]

Shoaling occurs as waves approach the shore. As waves move from deep to shallow water, their celerity and wavelength decrease, and wave height increases until they break [41]. Near the coast, nonlinear effects become significant [32]. The time-averaged energy in the control volume shown in Figure 2.15 should be conserved. The figure illustrates the shoaling effect with waves becoming shorter and taller.

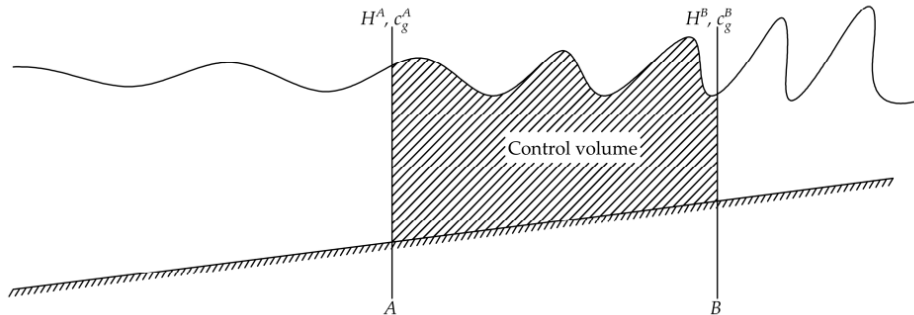


Figure 2.15: Conservation of mechanical energy flux between section *A* and *B* [32]

As wave energy passes through water, it sets water particles in orbital motion. Figure 2.16 shows wave energy changes over different depths as per Airy wave theory. In deeper waters, the circular orbital motion of water particles near the surface has diameters approximately equal to the wave height, and the energy decreases exponentially with depth; below a depth of half the wavelength ($D = 1/2 L$), the water is not affected by the wave [69]. In shallower water, seabed interaction flattens orbits. At intermediate depths, particles move elliptically, flattening and shrinking towards the seabed. At the bottom, particles move horizontally. In shallow water, the horizontal back-and-forth movements are uniform with depth.

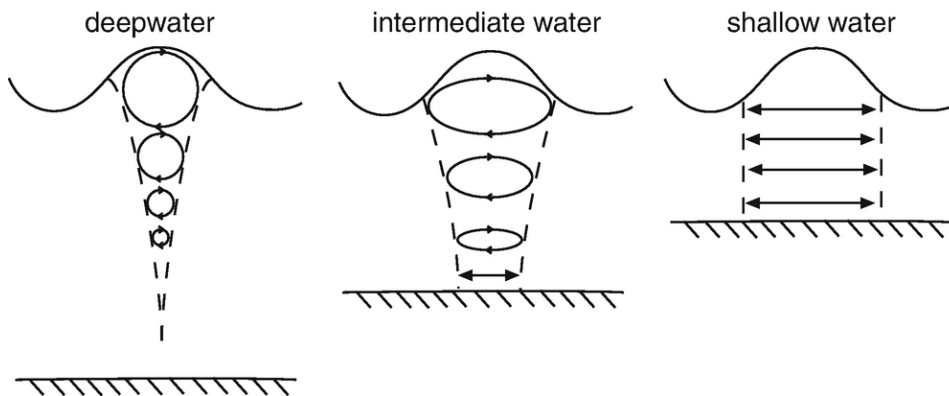


Figure 2.16: Squeezing of orbitals for shallower water and exponential decay of wave energy [69]

The wave energy distribution and changes in orbital motion from deep to shallow water significantly impact mooring system design. In shallow waters, wave energy is directed more horizontally, influencing the surge and sway degrees of freedom (DOFs) of moored bodies more than the heave, whereas in deeper waters, wave energy is distributed more uniformly across all directions. The load Response Amplitude Operators (RAOs) of a floating structure are influenced by variations in both draft and water depth. The draft of a moored body depends on its buoyancy, which is primarily determined by the displaced water volume and the structure's weight, not directly by wave-induced particle motion. However, for bodies with nonuniform shapes, such as floaters composed of columns connected by pontoons, the hydrodynamic effects on different parts of the structure (e.g., the pontoons) can vary significantly with water depth, influencing the dynamic behavior of the floater.

It is important to emphasize that nonlinear wave theories, such as Stokes theory, provide a more accurate description of water particle motions in shallow waters compared to Airy wave theory, especially when wave amplitudes are larger [69, 16].

2.2.3. Equations of motion

The floater supporting the wind turbine is treated as a rigid body. The complete nonlinear time-domain equations of motion of the coupled RNA, tower, floating platform, and mooring system are of the general form [61, 110]:

$$(M + A_\infty)\ddot{q} + C\dot{q} + Kq = F(t) \quad (2.20)$$

where:

- M is the mass matrix of the floater.
- A_∞ is the added mass at infinite frequency.
- \ddot{q}, \dot{q}, q are the acceleration, velocity, and displacement vectors of the platform in 6 degrees of freedom (DOFs).
- C is the damping matrix.
- K is the hydrostatic stiffness matrix.
- $F(t)$ represents the external forces acting on the system, including first-order wave-excitation forces, viscous drag forces, aerodynamic loads, mooring system restoring forces, and frequency dependent radiation forces.

The external forces $F(t)$ can be decomposed as follows:

$$F(t) = F_I(t) + F_{\text{Viscous}}(t, \dot{q}) + F_c(t, \dot{q}) + F_{\text{Aero}}(t) + F_m(t, q) \quad (2.21)$$

where:

- $F_I(t)$ are the first- and second-order wave-excitation forces.
- $F_{\text{Viscous}}(t, \dot{q})$ are the hydrodynamic viscous-drag forces.
- $F_{\text{Aero}}(t)$ are the aerodynamic loads.
- $F_m(t)$ is the force from the mooring system.
- $F_c(t, \dot{q})$ is the radiation force, which can be expressed as:

$$F_c(t, \dot{q}) = - \int_0^t R(t - \tau)\dot{q}(\tau)d\tau \quad (2.22)$$

where $R(t - \tau)$ is the retardation function, formulated as:

$$R(t) = \frac{2}{\pi} \int_0^\infty b(\omega) \cos(\omega t) d\omega \quad (2.23)$$

with b being the linear radiation damping matrix.

2.2.4. Frequency domain analysis

Although less accurate than time domain analysis, frequency domain (FD) analysis is highly valued for its computational efficiency. FD has been widely used in floating offshore wind (FOW) due to this efficiency. For example, Wang et al. [99] employ frequency domain models to predict FOWT responses by linearizing the governing equations, allowing for the efficient handling of complex hydrodynamic interactions. Similarly, Brommundt et al. [18] utilize frequency domain methods to optimize mooring systems, where linearization simplifies the dynamic behavior and reduces computational cost.

OrcaFlex solves the dynamic response at wave frequency by using linear mappings from the wave elevation process to the load process and from the load process to the response process [79]. This method involves deriving a complex vector-valued linear transfer function $\lambda(f_n)$, which maps the wave elevation process $\eta(f_n)$ to the load process $l(f_n)$. The wave elevation process $\eta(f_n)$ is calculated from the wave elevation spectrum $S_\eta(f_n)$ using the same discretization methods as available in the time domain.

Linear Airy wave theory is used to relate wave elevation to velocity and acceleration at model positions, considering added mass, linear damping, and viscous drag, resulting in a load on the object.

Next, OrcaFlex derives a complex matrix-valued linear transfer function $X(f_n)$ that maps the load process $l(f_n)$ to the response process $x(f_n)$:

$$X(f_n) = [-(2\pi f_n)^2 M + i2\pi f_n C + K]^{-1} \quad (2.24)$$

Here, M is the system inertia matrix, C is the system damping matrix, and K is the system stiffness matrix.

Finally, these transfer functions are combined to obtain the response process for each wave component f_n :

$$x(f_n) = X(f_n)\lambda(f_n)\eta(f_n) \quad (2.25)$$

The input and output of the frequency domain solver are stochastic, and the result process describes the statistics of the result over the whole ensemble of realizations, i.e., over all possible synthesized wave and wind realizations.

Linearization

In frequency domain analysis, equations are linearized around static equilibrium. OrcaFlex solves EoMs by discretizing time and using numerical integration. The system is linearized by approximating nonlinear behavior at the evaluation point. Nonlinearities in the OrcaFlex model, like hydrodynamic drag, radiation damping, aerodynamic loads, and mooring forces, need linearization.

The wave elevation-loading relation λ and loading-response relation X are nonlinear if second order wave loads are applied. They are linearized using the Jacobian matrix of the relationship, evaluated with the model in the static state. Essentially, the Jacobian is the first-order derivative of the function at the evaluation point. For instance, the system's stiffness is linearized using the tangent stiffness matrix calculated after statics.

The standard linearization procedure includes:

1. Static Analysis: Conduct a static analysis to determine the static equilibrium and operating point.
2. Jacobian Matrix Calculation: Calculate the Jacobian matrix, representing first-order partial derivatives of the equations at the operating point.
3. State-Space Representation: Use the Jacobian matrix to derive the linearized state-space representation.

Friction and Drag Linearization Unique methods are required to linearize friction and drag. Seabed friction is applied through the standard Coulomb friction model in the solid plane. Seabed friction for nodes is linearized using tangent stiffness, assuming nodes remain on the pre-slip curve. Other friction types are based on static positions and tangent stiffness. Drag linearization uses equivalent linearization, applying the Minimum Mean Square Error (MMSE) approach to minimize the mean square error between linear and nonlinear solutions.

Results extraction

To generate results in the frequency domain, OrcaFlex calculates the result process $r(f_n)$ for the specific result of interest, such as surge motion of the platform at a specific point. This involves applying a complex linear transfer function $\rho(f_n)$, which maps the response process $x(f_n)$ to the result process $r(f_n)$:

$$r(f_n) = \rho(f_n) * x(f_n) \quad (2.26)$$

The spectral density of the result process at frequency f_n is calculated as:

$$S_r(f_n) = \frac{r(f_n)r(f_n)^*}{df_n} \quad (2.27)$$

where $*$ denotes the complex conjugate. The spectral density plots help visualize how energy is distributed across different frequencies.

The RAO plots, represented as $|RAO|$, indicate the amplitude of the transfer function that maps the wave elevation process to the result process. It is given by the square root of the ratio of the spectra:

$$|RAO| = \sqrt{\frac{S_r(f)}{S_\eta(f)}} \quad (2.28)$$

These plots are used to understand the system's dynamics and identify resonant frequencies that could impact mooring system performance. Resonant frequencies can also be determined by modal analysis, where natural frequencies are derived by solving the eigenvalue problem using the system's mass and stiffness matrices.

Most Probable Maximum (MPM) The Most Probable Maximum (MPM) estimates the likely extreme value of a stochastic process in a given duration, important for mooring system safety and reliability. Calculated under a Rayleigh distribution for stationary Gaussian processes, the standard deviation σ is the square root of the zeroth moment of the spectral density [79].

$$\sigma = \sqrt{m_0} \quad (2.29)$$

where m_0 is the zeroth moment, calculated as:

$$m_0 = \sum_n f_n r(f_n)r(f_n)^* \quad (2.30)$$

The mean period of zero up-crossings T_z is calculated as:

$$T_z = \sqrt{\frac{m_0}{m_2}} \quad (2.31)$$

where m_2 is the second moment of the result spectral density.

The mean period of crests T_c is given by:

$$T_c = \sqrt{\frac{m_0}{m_4}} \quad (2.32)$$

where m_4 is the fourth moment of the result spectral density.

The spectral bandwidth ϵ is calculated as:

$$\epsilon = \sqrt{\frac{m_2^3}{m_0 m_4^2} \left(1 - \left(\frac{m_2^2}{m_0 m_4} \right) \right)} \quad (2.33)$$

The MPM of the dynamic part of the result process, occurring in duration T , is:

$$\text{MPM} = \sigma \sqrt{2 \ln \left(\frac{T}{T_z} \right)} \quad (2.34)$$

These statistical measures help in evaluating the performance and safety of mooring systems by predicting extreme responses under various conditions.

3

Framework development

This chapter introduces the methodology used to evaluate and compare mooring systems for the temporary wet storage of floating offshore wind turbines. It consists of three sections: the Multi-Criteria Decision Analysis (MCDA), the design basis, and the assumptions. The MCDA provides a framework for comparing different mooring concepts, the design basis establishes the essential parameters and environmental conditions for the mooring systems, and the assumptions clarify the constraints guiding the system design.

3.1. Multi-Criteria Decision Analysis

This section presents the framework to evaluate and differentiate mooring concepts using Multi-Criteria Decision Analysis (MCDA). MCDA sets out criteria for assessing and scoring concepts, typically applying the Weighted Sum Method (WSM). The WSM is particularly useful as it incorporates the importance of each criterion through weights, providing comparative results. Although WSM does not always lead to Pareto-optimal outcomes, as noted by Scott et al. [90], it is adequate for the early design stages of this analysis. Furthermore, the MCDA takes into account site-specific factors and focuses on minimizing computational time.

3.1.1. Criteria

The criteria are introduced and explained in the following subsections. A summary is given in Table 3.1. After that in subsection 3.1.2 the dependencies between the criteria are discussed.

Table 3.1: Criteria to access

Criterion	Unit
Dynamic behavior	Fairlead and anchor tensions & floater motions
Spatial utilization	Number of floaters per unit area
Accessibility	Distance between floaters
Hook-up efficiency	Time and equipment required for connection and disconnection
Cost	Total material costs

Dynamic behavior

Dynamic behavior refers to how the mooring systems respond to environmental variations, including waves, wind, currents, and tides. Key indicators include fairlead tensions, anchor tensions, and floater motions. Fairlead tensions represent the forces exerted at the floater's connection point with the mooring lines. Anchor tensions reflect the load transferred to seabed anchors, requiring larger anchors for higher forces. Floater motions, including displacements and velocities, are assessed as excessive motions increase the risk of collisions or structural failure.

This is the most important criterion. Only if dynamic behavior is deemed feasible can a mooring config-

uration be viable, and the other criteria become relevant.

Spatial utilization

Referring to the main research question (section 1.4), it is essential to ensure adequate spatial utilization. This can be measured by the number of floaters in an area defined by the mooring configuration's geometry and its seafloor footprint. Maximizing spatial utilization involves placing the floaters close together without causing collisions. Semi-submersible platforms are large, making spatial utilization important. For mooring line concepts, minimizing the anchor distance can enhance spatial use but may affect accessibility.

Aligned with the primary research question (section 1.4), spatial utilization is assessed to ensure efficient use of the designated area. The number of floaters within a specific area, defined by the mooring configuration and seafloor footprint, measures this criterion. Maximizing spatial utilization involves selecting configurations that accommodate the highest number of floaters without compromising accessibility or safety.

Accessibility

Accessibility is determined by the ability for tugs and other vessels to access the connection points of the design. Various types of tugs have been used in FOW projects, including Heavy Anchor Handling Tug Supply vessels (AHTSs) such as the BOKA Falcon, with an overall length of 93.4 m, for offshore transport [17]. Inshore harbour tugs, which typically range from 20 to 32 meters, have been utilized in sheltered areas [21]. The mooring configuration scores high on accessibility if there is enough room for tugs to maneuver. The required maneuvering room depends on the specific project and can be set as a constraint.

Accessibility is determined by the ease with which tugs and other vessels can access the connection points of the mooring configuration. Various types of tugs have been used in FOW projects, including Anchor Handling Tug Supply (AHTS) vessels, such as the BOKA Falcon [17]. Mooring configurations must ensure adequate room for vessel maneuvering. Larger floater displacements, as seen in catenary systems, can complicate access, whereas taut mooring systems provide more stable and predictable environments, improving accessibility for maintenance and operations

Hook-up efficiency

Hook-up efficiency assesses the complexity and time required to connect and disconnect the mooring system. Catenary systems generally offer higher hook-up efficiency due to lower pretension requirements and simpler connection procedures. In contrast, taut systems, which require precise tensioning, are more complex and time-consuming.

Cost

Cost is primarily determined by material requirements, including the number and length of mooring lines, line size, and additional hardware. Catenary systems, while more material-intensive due to longer lines, benefit from less expensive horizontal anchoring systems. Taut systems, on the other hand, rely on costlier vertical load anchors, which may increase total expenses.

3.1.2. Dependencies

Each criterion has varying degrees of interdependence with the others. For instance, there is often a trade-off between maximizing spatial utilization and maintaining accessibility. Placing floaters too closely to enhance spatial use can hinder tug maneuverability, reducing accessibility. Another example, improved dynamic behavior positively influences spatial utilization by allowing for tighter spacing of floaters. A positive sign pointing towards cost indicates that costs decrease, which is favorable.

Figure 3.1 illustrates these interdependencies.

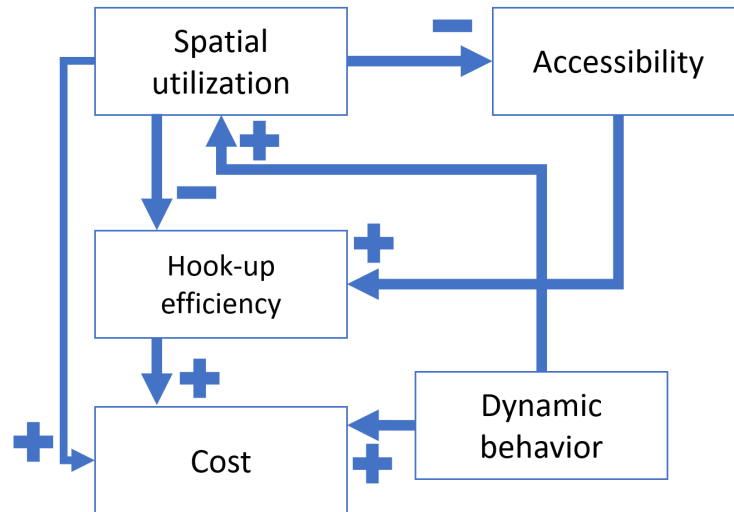


Figure 3.1: Interdependence of criteria

3.1.3. Weights

The criteria are assigned relative weights to reflect their importance. This weighting system ensures that concepts excelling in more important criteria achieve higher overall scores.

Dynamic behavior is the most important criterion and, thus, carries the most weight. Adequate spatial utilization follows, given its critical role in the congested sheltered areas where wet storage will take place, as reflected in the research questions. The other criteria, while still important, have comparatively lower weights.

Table 3.2: Weights

Criteria	Weight
Dynamic behavior	50
Spatial utilization	20
Accessibility	15
Hook-up efficiency	10
Cost	5
Total	100

3.2. Design basis

The design basis for the temporary mooring system of floating offshore wind turbines (FOWTs) is established by considering several categories: the floater, environmental conditions, mooring system configurations, and logistical requirements. These categories outline specific choices and constraints that guide the overall approach to the design and analysis of the wet storage mooring system.

A schematic representation of the design basis is shown in Figure 3.2.

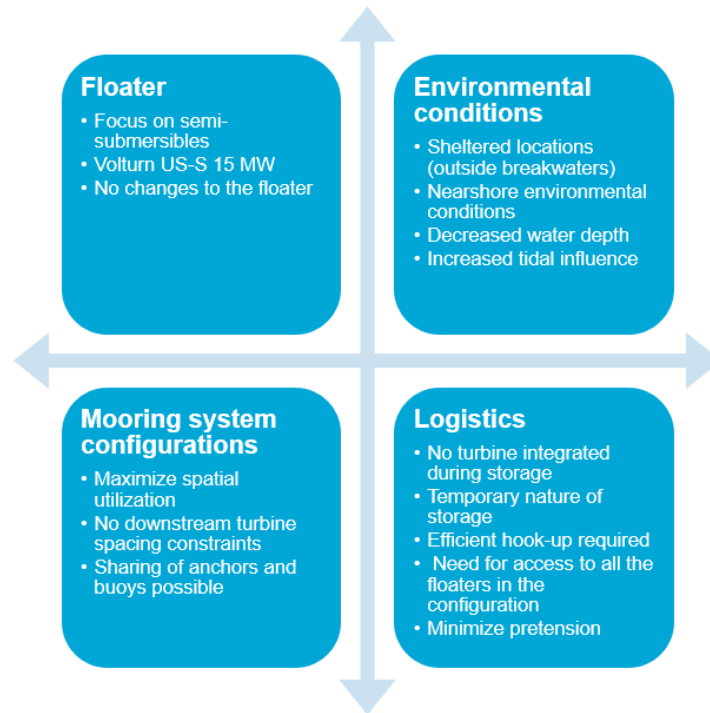


Figure 3.2: Design basis for a wet storage mooring system

The focus is on semi-submersible platforms, which present logistical challenges due to their large size and slow production rate. These platforms are selected because of their alignment with the industry's trend toward larger turbines for floating offshore wind projects. The VoltornUS-S 15 MW floater, an open-source and industry-aligned reference design, is chosen for this study [4]. No changes are made to the floater's original design, as the wet storage system must accommodate floaters designed for offshore operations. The floater draft can be varied using fluid ballast. Ballast fluids cannot be discharged due to environmental regulations. Grounding is avoided to minimize both environmental and structural risks, as the floater is not designed to withstand grounding or submerged loads.

The environmental conditions in this study are based on sheltered locations outside breakwaters to avoid harsh ocean conditions. These areas protect from direct waves, making them suitable for temporary storage. Nearshore conditions with shallow depths and high tidal influence are considered in the mooring system's performance. The environmental data is from existing sources and the analysis is based on one case study. All environmental forces are assumed to come from the positive Y direction, though future research may explore different wave headings to assess the system's yaw response.

Mooring configurations aim to maximize space use, ensure accessibility, and prevent floater collisions. Floater spacing allows close placement without affecting turbine power generation. The minimum anchor distance is 85 meters from the floater center, resulting in a 47-meter horizontal separation. This allows floater rotation and keeps mooring line tension within limits. Only fully installed mooring spreads are modeled in detail.

Logistical considerations are centered around the storage of floaters without turbines, as this reduces the complexity of operations and minimizes risks associated with WTG installation. The storage duration can vary from a few days to as long as one year, requiring a flexible and robust mooring system. The floater cannot leave the storage site if adverse weather is forecasted, and quick, easy hook-in and hook-out procedures are critical for efficient operations. Minimizing pretension in the mooring lines is essential to reduce handling difficulties and avoid delays in the deployment process. The design is intended to maintain access to all floaters throughout the storage period.

4

Model development and validation

The previous chapter outlined the design basis and assumptions for mooring systems in wet storage locations, focusing on stability, scalability, and environmental compatibility. This chapter focuses on the development and validation of the catenary and taut mooring models selected during ideation. Using the open-source VoltturnUS-S floating platform, the models simulate mooring system performance in various environments and validate the results against both literature and standards. The following sections describe the environmental conditions, the case study location, and the validation process, ensuring that the models are reliable for informed decision-making through the Multi-Criteria Decision Analysis (MCDA).

4.1. Environmental conditions

To describe a wet storage mooring configuration, the environmental conditions must be defined at a representative site. Wet storage is typically located near manufacturing/fabrication (MF) or staging and integration (S&I) harbors [93]. Due to limited space within harbors, storage is suggested outside harbor breakwaters.

Measured data is the most accurate source for environmental conditions, but long-term data collection is not available for every location worldwide [52]. Therefore, a variety of data sources are used in engineering contexts to obtain the necessary environmental information.

For wave data, measurements from wave buoys or higher fidelity models such as SWAN are recommended, particularly in shallow water applications [2, 1, 89]. In this modeling case, high-resolution refers to spatial and temporal resolutions fine enough to capture nearshore effects, such as wave refraction and diffraction in shallow waters. For wind data, global reanalysis datasets such as ERA-5 can be used due to their sufficient quality and coverage. The wind data from ERA-5 has been validated in various studies, demonstrating its reliability for engineering applications [52].

The effects of climate change on wind patterns in the North and Baltic Seas have been analyzed using ERA-5 reanalysis data, highlighting its applicability for regional studies [15]. Furthermore, global studies on port operability indicators, such as those conducted by Wiegel, have identified wind, short waves, and infragravity (IG) waves as critical factors. Wiegel's study utilizes ERA-5 reanalysis data and applies linear wave theory to translate this data to nearshore conditions [101].

To run the analysis for wet storage mooring configurations, the following environmental conditions are considered:

- Wind data from ERA-5, providing sufficient quality for engineering purposes.
- Wave data from high-resolution measurements, such as wave buoys, especially for shallow water applications.
- Tidal data specific to the site to account for water level variations.
- Local current profiles

Defining environmental conditions at a representative site ensures accurate and reliable mooring system performance analysis for wet storage.

4.1.1. Case study location

The focus on the Celtic Sea is driven by the extensive offshore development and the availability of environmental data, as illustrated in Figure 4.1. However, wet storage is expected to be in the Severn Estuary near these leasing zones, where harbors are located.



Figure 4.1: Celtic Sea FLOW leasing zones [65]

Waves and tides

The National Network of Regional Coastal Monitoring Programmes of England manages a network of nearshore wave buoys around England, some of which are in locations relevant to wet storage applications [85]. The locations of the wave measuring sites are shown in Figure 4.2. These Directional Waveriders are mostly deployed in 10 to 15 m water depths.

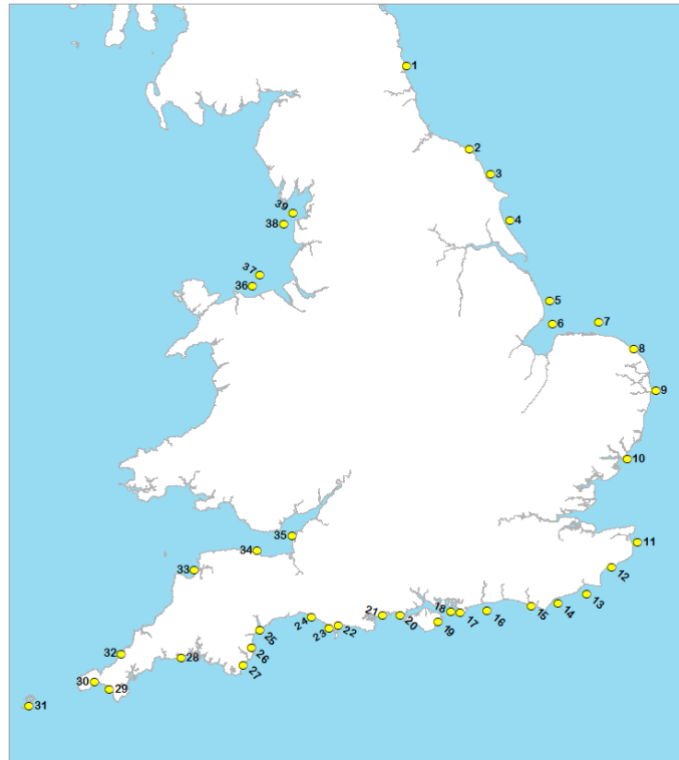


Figure 4.2: Locations of Directional Waveriders [85]

The buoys are placed between 0.4 and 16.2 km offshore, and the following buoys are of particular interest due to their proximity to offshore wind developments and sheltered locations:

- Buoy 34 in Minehead
- Buoy 35 in Weston Bay
- Buoy 36 in Rhyl Flats

From these options, the Minehead buoy was selected for analysis, as it is the most sheltered from long-period swell originating from the open sea. Its location within the Bristol Channel provides protection from significant offshore wave energy, making it representative of the type of nearshore environment that could be used for wet storage.

A storm analysis for the Minehead buoy was performed, as shown in Table 4.1. The wave periods T_p of 9.1 s and 8.3 s were observed, with the T_p of 9.1 s selected for a more conservative model, as it is closer to the expected natural frequencies of the floater. Furthermore, the highest significant wave height (H_s) of 3.08 m was chosen to ensure a conservative assessment.

Table 4.1: Storm analysis for the Minehead buoy [85]

Date/Time	H_s (m)	T_p (s)	T_z (s)	Dir. (°)	Water level elevation* (OD)	Tidal stage (hours re. HW)	Tidal range (m)	Tidal surge (m)	Max. surge (m)
18-Feb-2022 12:00:00	3.08	9.1	6.8	302	-2.65	HW +5	8.06	0.56	1.58
20-Feb-2022 23:00:00	3.00	8.3	6.9	300	1.34	HW	8.22	0.13	0.79

This case study uses a 10-meter tidal range over a 40-meter water depth, which is higher than the maximum tidal range observed at the Minehead buoy (8.22 meters). The 10-meter range was chosen to provide a more conservative estimate, taking into account the higher tidal ranges found in nearby areas of the Severn Estuary, where tidal ranges can reach up to 14 meters [13]. This ensures that the analysis covers a broader range of potential conditions in the region.

For the analysis, a JONSWAP spectrum was used to represent the irregular wave conditions, a standard approach in the industry [62]. The H_s of 3.08 m was selected as the higher value for conservatism, while the T_p of 9.1 s was chosen as it aligns the wave period closer to the expected natural frequencies of the floater, ensuring a more robust assessment.

The spectral density is shown in Figure 4.3. The model accounts for wave periods down to 2.5 s, capturing all significant wave energy. The wave energy peaks at 0.11 Hz (corresponding to T_p of 9.1 s) and follows a long-tail distribution toward higher frequencies. Frequencies up to 0.4 Hz are included, as wave energy beyond this point is considered negligible.

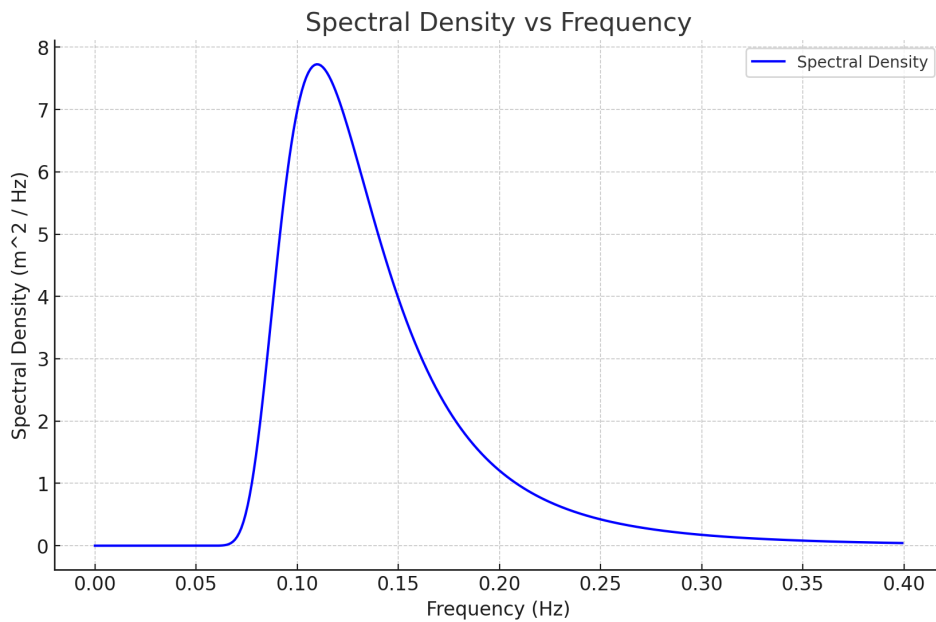


Figure 4.3: Spectral density wave train

Wind

DNV-ST-N001 provides guidance on the wind data required. The design wind speed is generally taken as the 1-minute mean velocity at a reference height of 10 m above sea level [30]. This can be derived from ERA-5 reanalysis data, resulting in a mean wind speed of 17.1 m/s, which is considered a conservative estimate for the design basis [52]. This wind speed value, sourced from the Global Wind Atlas, ensures the robustness of the system against extreme wind conditions. The NPD spectrum is used for representing the wind conditions in the modeling [75]. It is expected that the wave loads on the floaters will dominate compared to the wind loads.

How wind is modelled on floater Wind is modeled in OrcaFlex using the OCIMF method [76], which calculates surge, sway, and yaw drag loads on a stationary vessel. Although originally intended for tankers, the OCIMF method can be applied to other vessel types with appropriate adjustments.

Drag loads from relative velocities in the 6 degrees of freedom (DOFs) are expressed as:

$$\begin{aligned}
 f_x &= \frac{1}{2} C_{\text{surge}} \rho |\mathbf{v}|^2 A_{\text{surge}} \\
 f_y &= \frac{1}{2} C_{\text{sway}} \rho |\mathbf{v}|^2 A_{\text{sway}} \\
 f_z &= \frac{1}{2} C_{\text{heave}} \rho |\mathbf{v}|^2 A_{\text{heave}} \\
 m_x &= \frac{1}{2} C_{\text{roll}} \rho |\mathbf{v}|^2 A_{\text{roll}} \\
 m_y &= \frac{1}{2} C_{\text{pitch}} \rho |\mathbf{v}|^2 A_{\text{pitch}} \\
 m_z &= \frac{1}{2} C_{\text{yaw}} \rho |\mathbf{v}|^2 A_{\text{yaw}}
 \end{aligned} \tag{4.1}$$

With:

- f_x , f_y , and f_z : drag forces in the x-, y-, and z-directions.
- m_x , m_y , and m_z : drag moments about the x-, y-, and z-directions.
- C_{surge} , C_{sway} , C_{heave} , C_{roll} , C_{pitch} , and C_{yaw} : the surge, sway, heave, roll, pitch, and yaw coefficients relative to the vessel's heading.
- ρ : water (current) or air (wind) density.
- \mathbf{v} : relative velocity of sea or air past the vessel. For wind, \mathbf{v} is based on wind velocity at 10m above mean water level. For current, it is based on velocity at the load origin's instantaneous position. \mathbf{v} includes the translational velocity of the load origin.
- A_{surge} , A_{sway} , A_{heave} , A_{roll} , A_{pitch} , and A_{yaw} : surge, sway, heave areas and roll, pitch, yaw area moments. For current, these are the areas below waterline; for wind, above waterline.

Wind area and coefficients In this analysis, only surge and sway provide significant contributions due to the wind direction from the positive Y-direction (sway). The central column is shielded by one of the outer columns, so the effective area is calculated for the unshielded outer columns. The floater draft is set to 14 m, with a column height of 21 m above water.

The frontal area per column is calculated as:

$$A_{\text{frontal,cyl}} = b \times h \tag{4.2}$$

with $b = 12.5$ m and $h = 21$ m, giving:

$$A_{\text{frontal,cyl}} = 262.5 \text{ m}^2 \tag{4.3}$$

The total frontal area, considering three columns, is:

$$A_{\text{frontal,tot}} = 3 \times A_{\text{frontal,cyl}} \tag{4.4}$$

which results in:

$$A_{\text{frontal,tot}} = 787.5 \text{ m}^2 \tag{4.5}$$

To determine the drag coefficient of a column in air, the Reynolds number is calculated using a column diameter of 12.5 m, an air velocity of 17.1 m/s, an air density of 1.225 kg/m³, and a dynamic viscosity of air at 1.81×10^{-5} Pa·s [34]. The Reynolds number is approximately 10^7 . Empirical data for cylinders in crossflow suggest a drag coefficient of around 0.5 for Reynolds numbers higher than 10^4 [5].

Currents

The design current speed is 1.5 m s⁻¹, supported by Severn Estuary Partnership studies indicating peak coastal currents can reach this speed during spring tides [91].

How currents are modeled on the floater Currents are modeled in OrcaFlex using the same OCIMF method as for wind. The drag area is calculated similarly to the wind analysis. The frontal area is determined based on the submerged parts of the floater, yielding a frontal area of 960.9 m². The Reynolds number is estimated to be approximately 10⁷. The load coefficient is more complex to determine, as the floater has an irregular underwater shape with many hard angles that disturb the water flow. Although some papers provide drag coefficients for semi-submersibles, these values are highly dependent on the specific design of the floater [57, 14]. Based on these sources, an estimated drag coefficient (C_d) of 0.5 was adopted for this analysis. Further research is recommended to refine this value.

4.2. Floater definition

The VoltturnUS-S [4] is a semi-submersible floating platform designed for the IEA 15-MW reference turbine [42]. This floater was chosen for the model due to its open-source nature and compatibility with the expected turbine size. The general configuration and sizing of the VoltturnUS-S, including key dimensions and characteristics such as draft, overall dimensions, and mass distributions, are illustrated in Figure 4.4. The platform has a draft of 20 meters when fully installed with the turbine placed on top and fully ballasted. It has dimensions of 100 meters by 90 meters and a total platform mass of 18,000 tonnes, which includes hull steel mass, fixed ballast mass, and fluid ballast mass.

The VoltturnUS-S [4] is a semi-submersible floating platform designed for the IEA 15-MW reference turbine [42]. The open-source nature and compatibility with the expected turbine size make it an ideal candidate for this model. Key dimensions and characteristics of the VoltturnUS-S platform include a 20-meter draft when fully installed and ballasted, with overall dimensions of 100 meters by 90 meters and a total platform mass of 18,000 tonnes, comprising hull steel, fixed ballast, and fluid ballast. These details are illustrated in Figure 4.4.

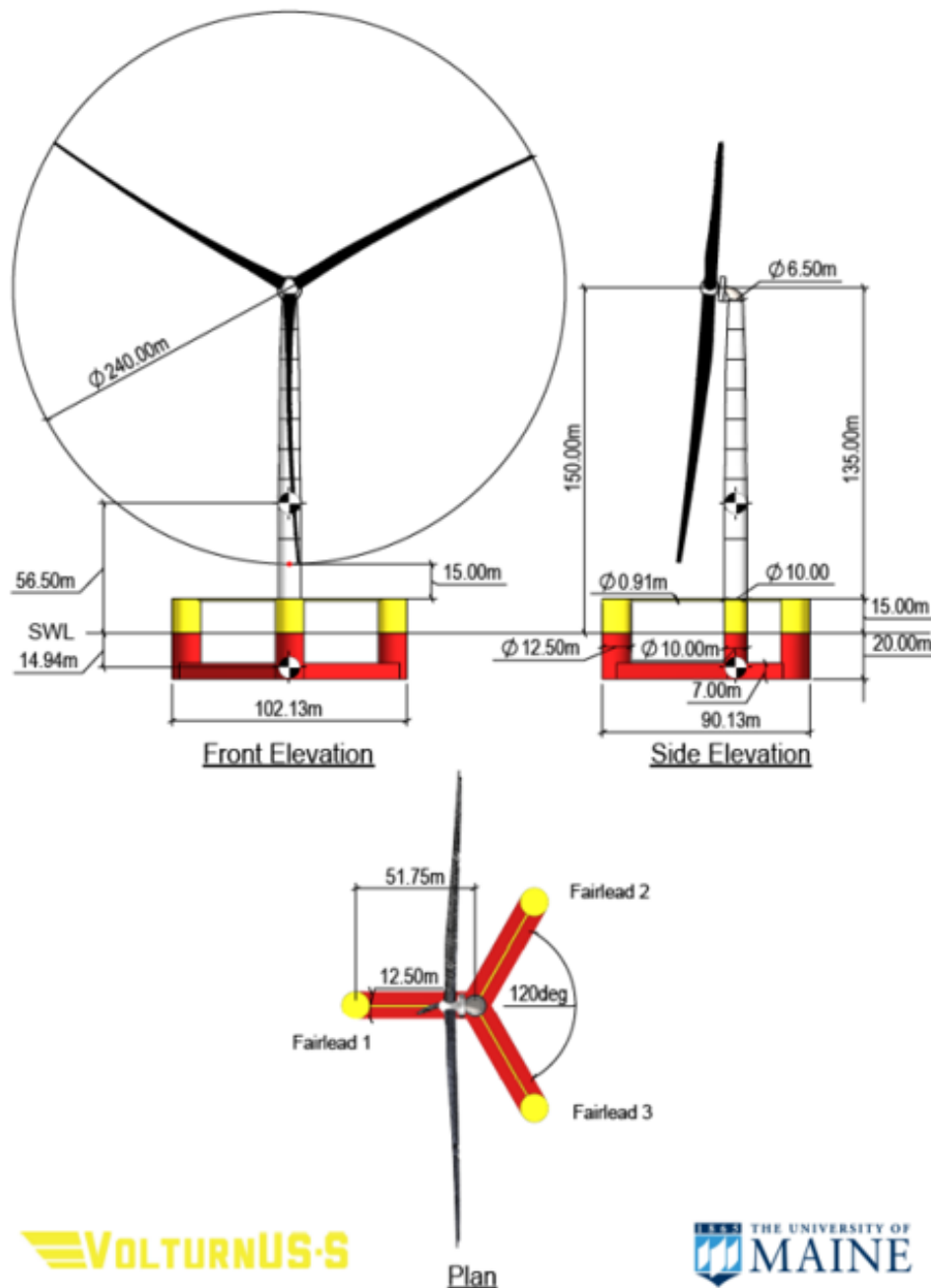


Figure 4.4: General configuration of VoltturnUS-S floater designed for the IEA 15-MW reference turbine [4]

4.2.1. Diffraction analysis

OrcaWave is a diffraction analysis program that calculates loading and response to waves. It uses potential flow theory, which is further highlighted in chapter 2, to determine added mass, stiffness, damping coefficients and load RAOs. The results of a diffraction analysis depend on, among others, floater draft, mass and water depth.

These values vary with different configurations, necessitating multiple diffraction analyses including four water depths and four drafts. The mooring system affects the floater draft, and the turbine, which constitutes about 10% of the total system mass, also influences the draft. This makes for a total of 16 different diffraction analysis.

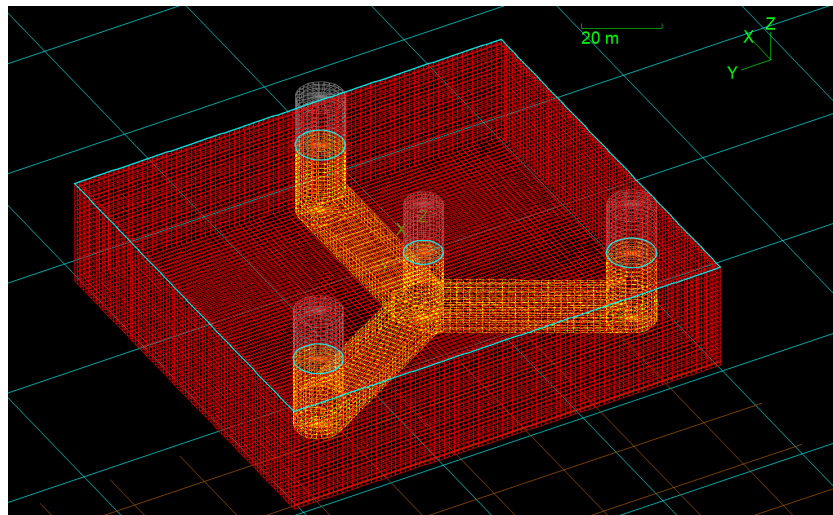
Table 4.2: Draft and water depth configurations for diffraction analysis

Draft	Shallow low tide (35 m)	Shallow no tide (40 m)	Shallow high tide (45 m)	Deep (200 m)
14 m	No Turbine	No Turbine	No Turbine	No Turbine
15 m	No Turbine	No Turbine	No Turbine	No Turbine
16 m	No Turbine	No Turbine	No Turbine	No Turbine
20 m	Turbine	Turbine	Turbine	Turbine

Mesh validation

Mesh validation is critical to ensure that the diffraction analysis produces accurate results. Without proper validation, the diffraction analysis can yield imprecise predictions, for example when calculating first-order potential flow solutions. According to DNV standards, the diagonal length of the mesh panels should be less than 1/6 of the smallest wavelength analyzed to achieve sufficient precision in the results [25].

The mesh file provided by Orcina, shown in Figure 4.5, serves as the foundation for this analysis [77]. The characteristics of this mesh must be validated to ensure it can accurately capture the wave interactions within the defined range of frequencies.

**Figure 4.5:** Overview of VoltumUS-S mesh [77]

For this study, the maximum frequency considered is 0.4 Hz, which corresponds to the smallest wavelength to be modeled. The smallest wavelength is found by determining the wavelength at this frequency for the four water depths under consideration (35 m, 40 m, 45 m, and 200 m).

Wavelength calculation The wavelength is calculated iteratively using the dispersion relation:

$$\omega^2 = gk \tanh(kh) \quad (4.6)$$

where ω is the angular frequency, g is gravitational acceleration, $k = \frac{2\pi}{\lambda}$ is the wave number, h is the water depth, and λ is the wavelength. The calculation was validated by comparing the code-generated results with reference data from Sheng et al. [92], though for this context, we will focus only on the code-generated results.

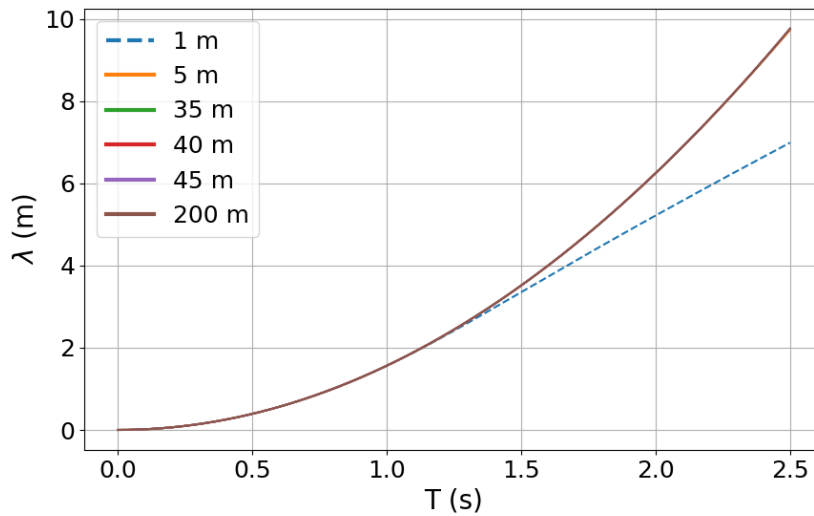


Figure 4.6: Wavelength over wave period for various water depths

The plot in Figure 4.6 shows that for all water depths considered in this study, the wavelengths fall on the same line. From this plot, the wavelength at 0.4 Hz is found to be 9.76 meters for all water depths.

According to DNV standards, the maximum allowable panel size for mesh validation is 1/6 of the wavelength. Therefore, the maximum panel size is calculated as:

$$\text{Max panel size} = \frac{9.76}{6} = 1.63 \text{ m} \quad (4.7)$$

OrcaWave is used to verify that all panels in the mesh are smaller than 1.63 meters, confirming that the mesh is valid for first-order diffraction analysis.

The validated mesh is suitable for modeling first-order wave interactions up to the target frequency of 0.4 Hz. However, for second-order analysis, which requires the calculation of Quadratic Transfer Functions (QTFs) for time-domain simulations, a significantly finer mesh would be needed. The current mesh is sufficient for the first-order analysis performed in this study, but further refinement is recommended for more complex second-order analyses.

4.3. Mooring system definition

This section defines the catenary and taut mooring system models, building on the environmental conditions and floater definition outlined earlier. The simulations are conducted in the frequency domain (FD), which is explained in detail in subsection 2.2.4. Frequency domain analysis is well-suited for early-stage design as it allows for rapid computation and the exploration of various design variations. Although FD analysis primarily captures first-order wave loading, it is sufficient for understanding the primary behavior of mooring systems under typical conditions, such as those expected for wet storage.

The focus of this chapter is on two types of mooring systems: catenary and taut. These mooring systems were selected based on the design criteria for wet storage and are described in detail in section 2.1. Here, we translate these theoretical concepts into practical inputs for OrcaFlex simulations and explore the impact of key parameters, including water depth and line diameter, on system performance.

4.3.1. Governing parameters

The mooring system performance is primarily influenced by two governing parameters: water depth and mooring line diameter. These parameters were identified as having the most significant impact on the motion and tension characteristics of the system. Water depth varies based on tidal fluctuations

and site-specific conditions, while line diameter affects the weight, stiffness, and tension in the mooring lines.

To evaluate these influences, parametric studies are conducted across a range of water depths and line diameters for both catenary and taut mooring systems. These variations help identify the viable configurations that meet performance requirements while complying with design constraints.

Influence of water depth

Water depth, which fluctuates due to tides, plays a crucial role in determining the tension and geometry of the mooring lines. In this study, tidal variations between 35 m and 45 m are considered, corresponding to the tidal ranges observed in the Severn Estuary.

As the water depth changes, several key factors influence the mooring system's behavior. First, the floater's draft remains constant at 14 m, while the anchor point and line length are held fixed. Second, as the water level rises or falls, the touchdown point of the mooring line shifts, changing the shape of the catenary curve that the line forms. Third, this movement causes the angle of the mooring line at the fairlead to change, which in turn affects the tension distribution along the mooring line. These tidal effects are illustrated in Figure 4.7, which shows how the mooring line geometry adapts to changing water depths.

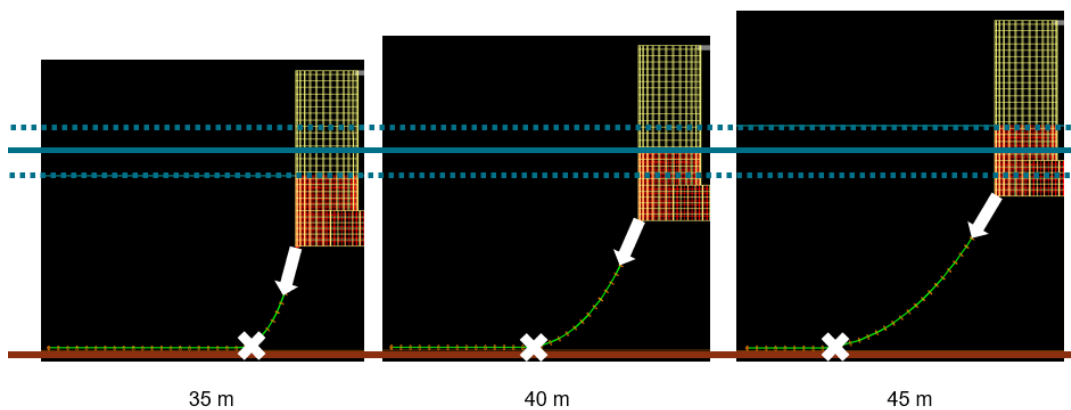


Figure 4.7: Tidal influence on mooring line

Influence of line diameter

The diameter of the mooring lines is another critical parameter affecting the system's performance. Line diameter influences the line's weight, stiffness, and tension capacity, all of which have a direct impact on the system's stability. In this study, line diameters ranging from 50 mm to 300 mm are analyzed.

When the line diameter increases, the weight of the mooring lines affects the overall tension distribution, which in turn influences the required anchor distance and line length. Although the floater's draft would theoretically vary from 13.8 m to 14.2 m due to line diameter changes, the draft itself does not affect the system performance in this case. Therefore, all models use a constant draft of 14 m to align with the values from the diffraction analysis, simplifying the analysis while maintaining accuracy for comparison purposes. The shape of the catenary curve and the angle at the fairlead are also influenced by the line diameter, which affects the tension profile along the line. The effects of line diameter on mooring performance are illustrated in Figure 4.8, showing how different line diameters affect the system's geometry.

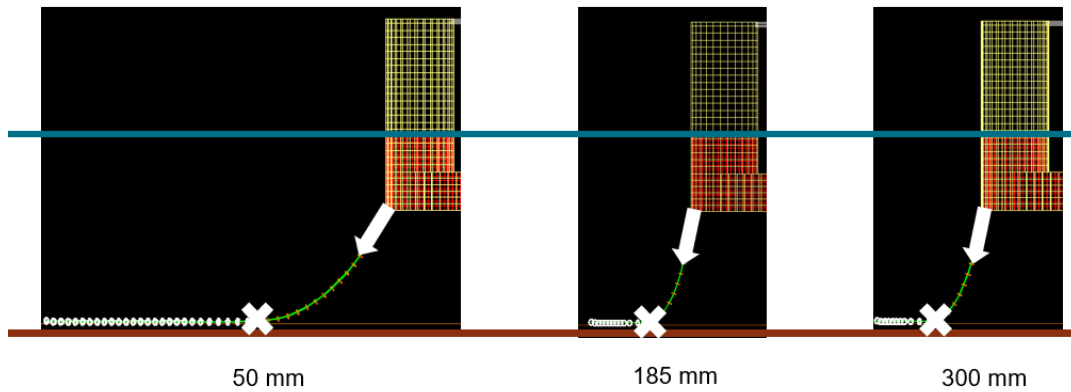


Figure 4.8: Influence of line diameter on mooring system

4.3.2. Anchor distance and line length algorithm

To determine the minimum anchor distance and line length for each mooring system, an algorithm is employed that balances performance with compliance to design constraints. This algorithm is designed to calculate the shortest possible anchor distance while ensuring that all constraints are met for each configuration.

The algorithm begins by defining the mooring system type (catenary or taut) and setting the parameters for water depth and line diameter. Based on these inputs, the algorithm systematically searches for valid anchor distances and line lengths. It starts with a coarse search to identify potential solutions, followed by a finer search to improve the selection. The algorithm checks for compliance with design constraints such as maximum tension, minimum slack, and prevention of anchor uplift.

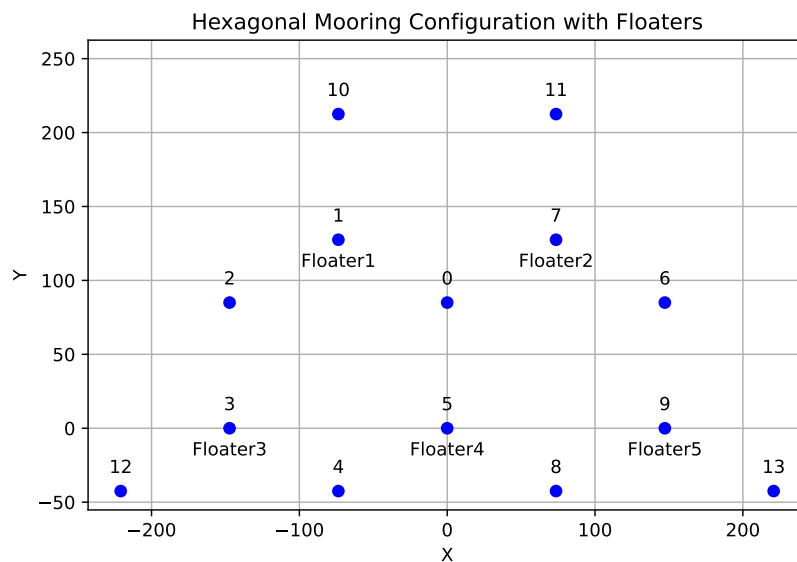


Figure 4.9: Node locations for an anchor distance of 85 m

Figure 4.9 shows an example hexagonal mooring configuration, which is created based on the anchor distance. The layout utilizes nodal points to create an efficient arrangement for the floaters while maintaining compliance with design constraints.

For a more detailed breakdown of the algorithm, please refer to Appendix A.

4.3.3. General constraints for mooring systems

Both catenary and taut mooring systems must adhere to a set of general constraints. These constraints are critical to maintaining the performance and stability of the system under various environmental conditions:

- The maximum fairlead tension must stay within allowable limits to prevent overstressing the mooring lines and connections.
- Uplift at the anchor may or may not be allowed depending on the type of anchor used. For systems utilizing drag anchors, uplift is not permissible, as it would cause the anchor to lose its holding capacity. However, for systems using vertical load anchors, uplift is acceptable.
- The mooring line angle in the horizontal plane, which is spanned by the seabed, must remain within acceptable ranges at both the fairlead and the anchor. Excessive angles could reduce stability and affect system performance.
- Line tension must remain within designed limits to avoid slack or overly taut conditions, ensuring the integrity and functionality of the mooring system.
- A minimum separation distance of 45 m between floaters is required to avoid interference or collisions between mooring systems.

4.3.4. Catenary mooring system

The catenary mooring system is characterized by slack lines that form a curved geometry, relying on the weight of the mooring lines to maintain tension. The system has several concept-specific constraints:

- Uplift at the anchor is not allowed, meaning the system must be designed to keep the anchor securely on the seabed across all tidal variations.
- The maximum tension in the mooring lines must not exceed the allowable limits set by the line diameter and material properties.
- The anchor distance and line length are calculated for a base water depth of 45 m, ensuring that the system remains stable without uplift even under high tidal conditions.

The catenary model features a 5-floater layout arranged in a hexagonal pattern to maximize spatial efficiency. Each floater is anchored by three lines, with the anchors designed to accommodate forces from multiple directions. This layout is shown in Figure 4.10. It is important to note that there is no hydrodynamic interaction between the floaters in the model. For instance, no shielding effect is considered, meaning each floater is treated as an independent entity in terms of wave and current loading.

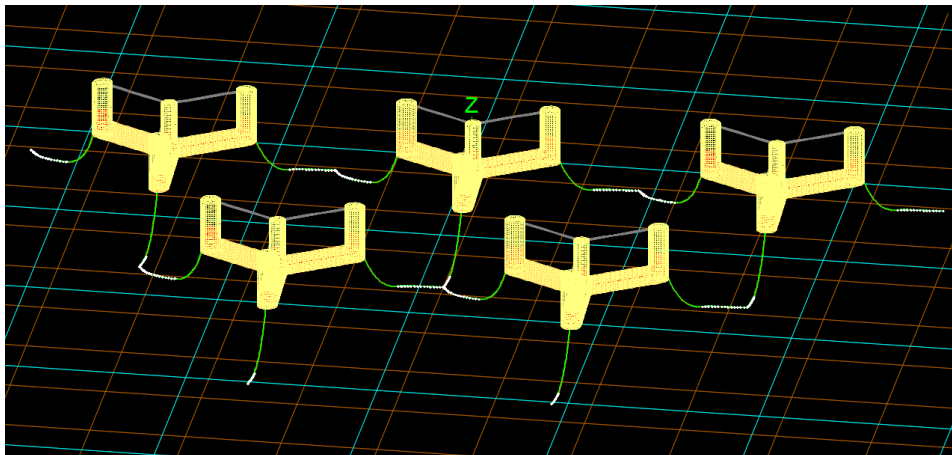


Figure 4.10: Catenary mooring system layout

4.3.5. Taut mooring system

The taut mooring system relies on the tension in the lines rather than their weight to provide stability. The system uses mooring lines that are more vertical, allowing for some uplift at the anchor. The

concept-specific constraints for the taut system are as follows:

- Uplift at the anchor is allowed because the system relies on vertical tension to maintain stability, rather than the weight of the lines.
- The tension in the mooring lines must remain below the maximum allowable limits, as determined by the line diameter and material.
- Anchor distance and line length are calculated for a base water depth of 35 m, ensuring that no slack occurs in the lines, even at low tidal levels.
- Mooring angle allowance is set to 90 degrees in the horizontal plane. This constraint limits the angle the mooring line can make, with a window of 45 degrees to both sides of the line between the nodes. This ensures that, even when environmental forces elongate the mooring lines, the floaters remain within their intended footprint. Preventing the floaters from moving far beyond the anchors helps avoid excessive displacement that could lead to collisions when environmental conditions change direction.

The taut model shares a similar layout to the catenary model but uses stiffer lines made of materials such as polyester or nylon. This makes it particularly well-suited for compact configuration applications. The layout is shown in Figure 4.11.

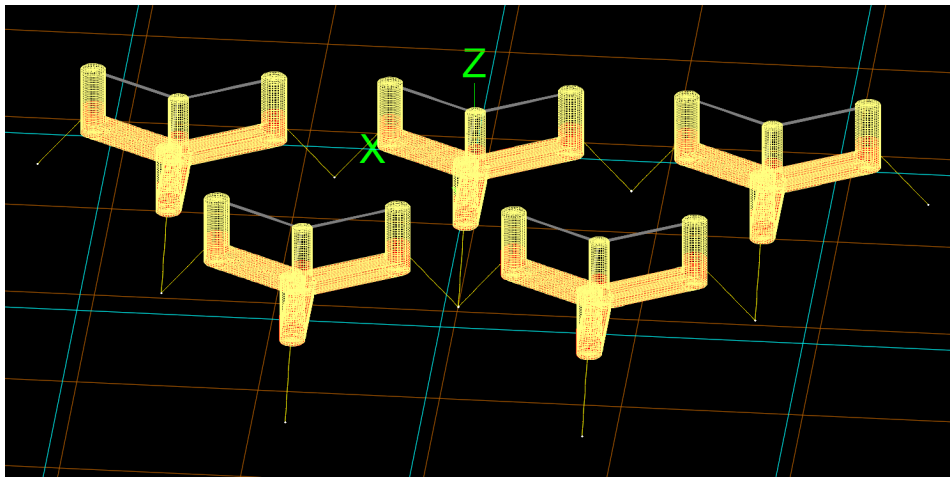


Figure 4.11: Taut mooring system layout

4.4. Model validation

The validation of the mooring system models developed in this thesis is required to ensure their accuracy and alignment with real-world conditions. The validation process focuses on two main aspects: the Load Response Amplitude Operators (Load RAOs) and the system's natural frequencies. The following sections outline the approach taken to validate the mooring system models, comparing them against reference literature, such as the floater definition [4] and established standards.

4.4.1. Load Response Amplitude Operators (RAOs)

In this thesis, Load RAOs are used to validate the behavior of the modeled system, as calculated in the Orcina model, by comparing them with NREL reference data. Load RAOs represent the ratio of the load (force or moment) applied to the floater due to wave excitation to the wave amplitude. The units in this context are expressed in N/m for translational degrees of freedom (DOFs), indicating the force applied per meter of wave amplitude. For rotational DOFs (roll, pitch, yaw), the units are expressed in N-m/m, indicating the moment applied per meter of wave amplitude. This concept allows for a direct comparison of the forces and moments acting on the system in response to different wave conditions.

This analysis focuses on the heave, pitch, and surge DOFs as they are the most significant due to the expected loading conditions and the symmetry of the platform.

First, the base case is used as a control to assess whether the models resemble the NREL data. Then, the effects of varying floater drafts and water depths are analyzed to assess the model's sensitivity to these factors.

NREL extraction and conversion

The WAMIT output from the VoltturnUS-S platform, provided in non-dimensional form, is converted to first-order wave excitation coefficients with physical units using the following formula:

$$\tilde{X}_i = \frac{X_i}{\rho g A L^m} \quad (4.8)$$

where \tilde{X}_i is the non-dimensional excitation force or moment from WAMIT, X_i is the desired dimensional excitation force or moment, ρ is the water density, g is the acceleration due to gravity, A is the waterplane area of the structure, and L is the characteristic length of the structure. The exponent m is 2 for translational DOFs (surge, sway, heave) and 3 for rotational DOFs (roll, pitch, yaw).

To carry out this conversion, we assume the values for ρ , g , and A as follows:

- The density of seawater (ρ) is 1025 kg/m³.
- The acceleration due to gravity (g) is 9.81 m/s².
- The waterplane area (A) and characteristic length (L) are set to 1 for the normalized values from the NREL output.

This conversion process aligns the non-dimensional WAMIT output with the dimensional units used in the Orcina results, allowing for a direct comparison of the load RAOs. For the rotational DOFs, the units are converted to N-m/m to match the outputs for moments.

Comparison with available literature The base case model was designed to closely replicate the NREL VoltturnUS 15 MW reference platform [4], utilizing the same parameters, including a water depth of 200 meters, a floater draft of 20 meters, and the same mooring system. Comparing the Load RAOs between the Orcina model and the NREL reference serves as a benchmark for validating the model.

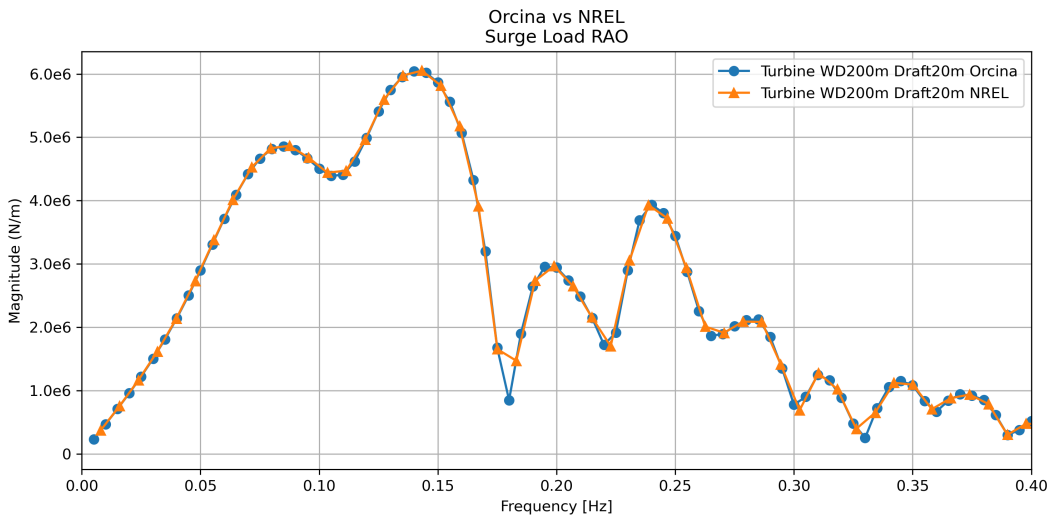


Figure 4.12: Comparison with NREL reference platform for the surge direction

Figure 4.12 shows that the Load RAOs from Orcina's diffraction analysis align well with the reference data for the surge direction. Similar agreement is found for other degrees of freedom (DOFs), including heave and pitch, as shown in Appendix B.

Effect of the draft Figure 4.13, Figure 4.14 and Figure 4.15 show the Load RAOs for a floater with the turbine integrated and the turbine removed. Removing the turbine reduces the draft of the floater from 20 m to 14 m, increasing the magnitude of the load response in the studied degrees of freedom (DOFs). This change impacts the loads on the floater, as illustrated in Figure 2.16, showing the squeezing of orbitals for shallower water. The pontoons move more towards the wave energy zone, leading to higher loads in surge and heave, as explained by the exponential decay of orbitals down the water column.

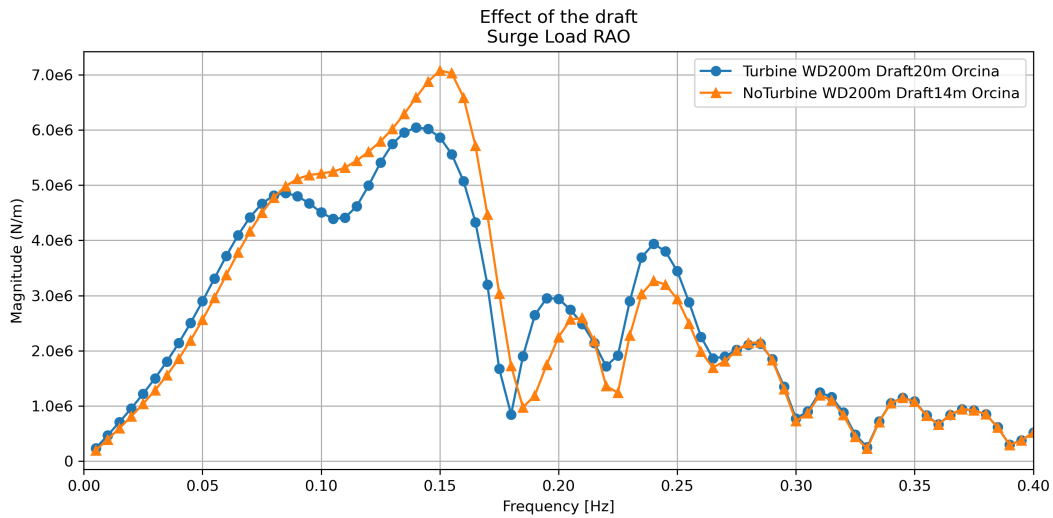


Figure 4.13: Effect of draft on surge direction

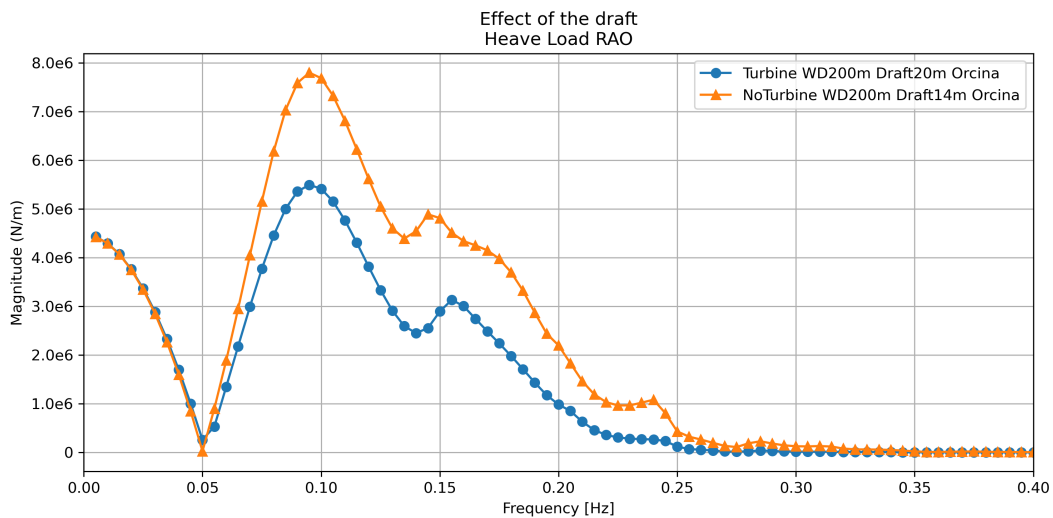


Figure 4.14: Effect of draft on heave direction

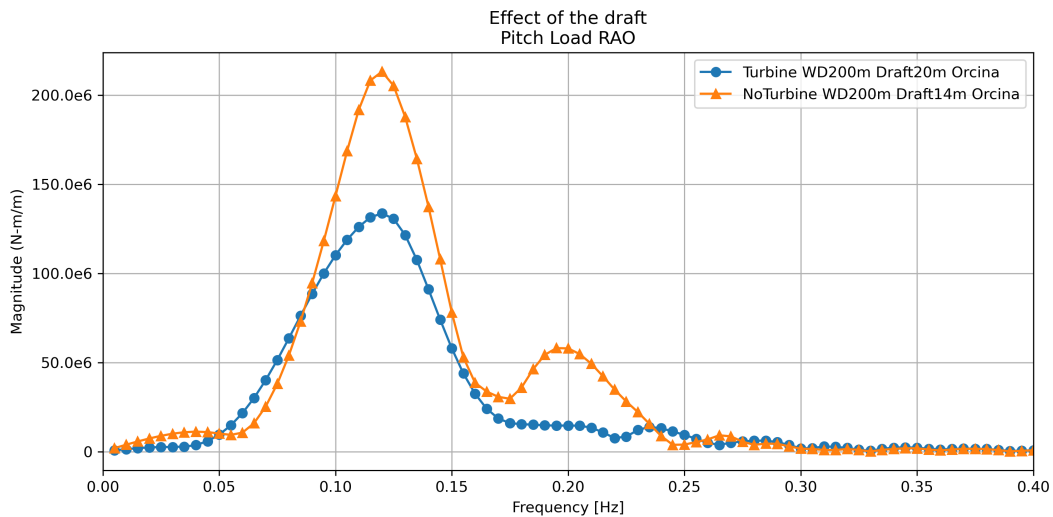


Figure 4.15: Effect of draft on pitch direction

It is important to note that for shorter waves with frequencies higher than 0.26 Hz, the differences in Load RAOs due to draft variations are negligible, as the floater's response in these high-frequency conditions remains consistent across draft configurations. This is because short, high-frequency waves do not significantly impact the large floater differently in surge, as the draft change only slightly decreases the amount of the columns subjected to loads in surge. However, the pontoons remain fully submerged for both drafts. In heave and pitch, the response is near zero for high-frequency waves, as the large size of the floater minimizes the effects of these waves.

The effect of varying moored drafts (14 m, 15 m, and 16 m) mirrors that of the 14 m and 20 m comparison. As draft increases, pontoons sit deeper, reducing wave interaction at lower frequencies. At higher frequencies, load responses converge due to less surface interaction. In the heave direction, shown in Figure 4.16, increased draft lowers the load response by reducing surface wave energy impact.

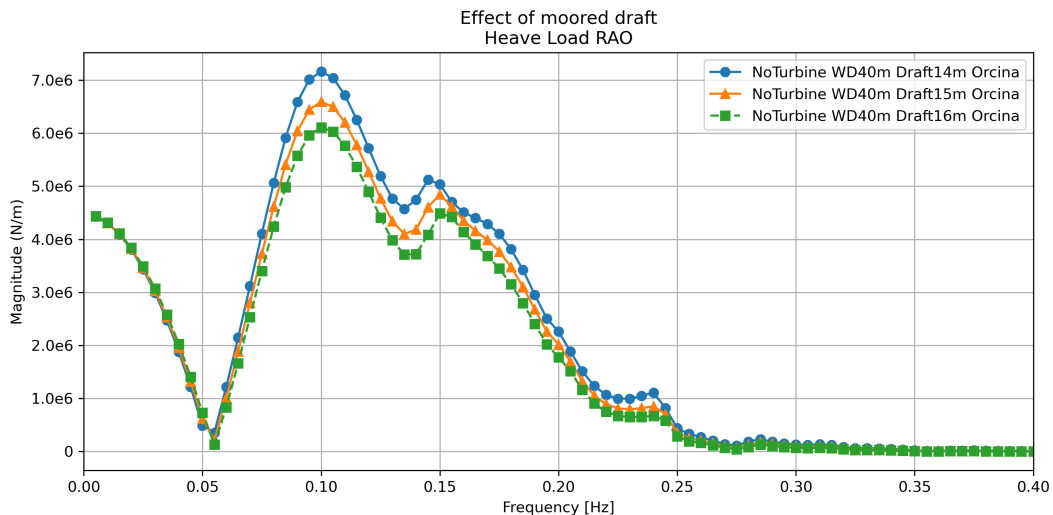


Figure 4.16: Effect of moored draft for the heave direction

Comparison of water depths Figure 4.17 and Figure 4.18 show the Load RAOs for water depths of 200 m and 40 m. As the water depth decreases, the load response in the surge direction increases, primarily due to stronger wave-seabed interaction in shallower waters. This effect is more pronounced

at lower frequencies, where the waves interact with a larger portion of the submerged structure. Figure 2.16 illustrates the squeezing of orbitals in shallower water depths, altering the direction of wave energy and amplifying the surge response. The wave energy becomes more horizontally directed in shallower waters, leading to an increase in surge response and a reduction in heave response, as further explained in subsection 2.2.2.

At higher frequencies, waves behave as if they are in deep water, regardless of water depth. The transition from shallow to deep water behavior occurs when the water depth (D) exceeds half the wave's wavelength (L), following the criterion $D > 0.5L$. For waves with frequencies higher than 0.12 Hz, the influence of water depth diminishes, and the load responses converge across all water depths. This is because shorter, high-frequency waves primarily interact with the floater's surface, reducing seabed effects.

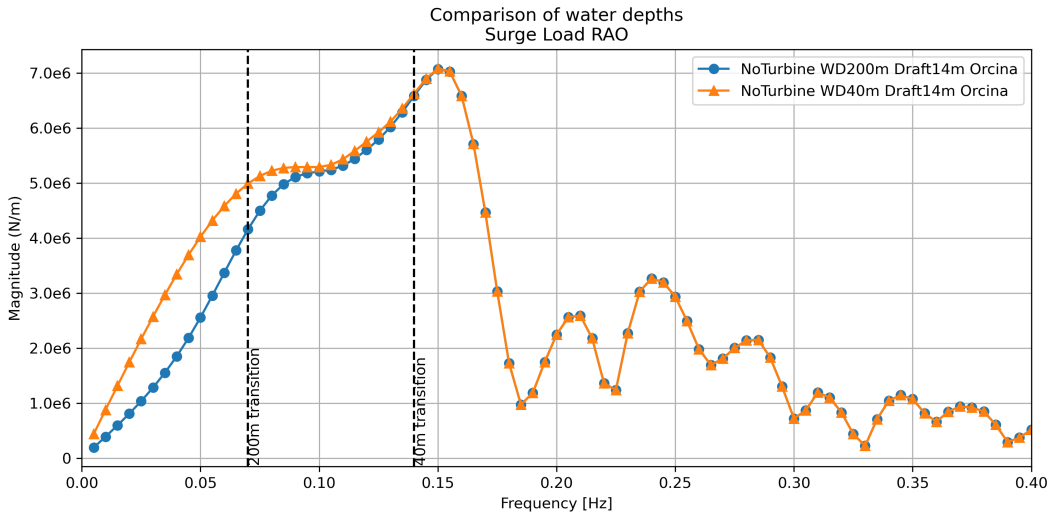


Figure 4.17: Effect of water depth on surge direction

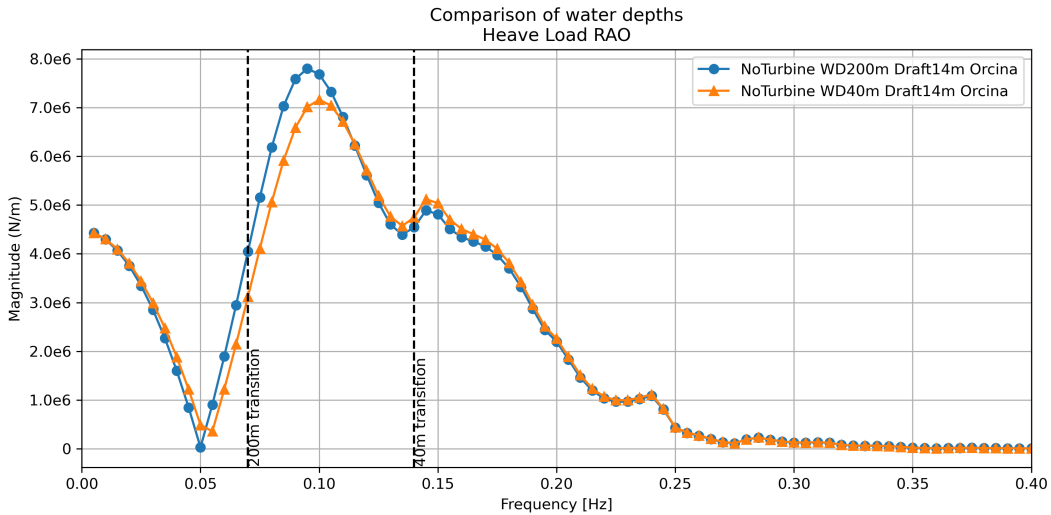


Figure 4.18: Effect of water depth on heave direction

The transition lines in the plots mark the frequencies where waves begin to behave as deep-water waves. These transition frequencies are calculated using the deep-water wavelength formula:

$$\lambda = \frac{g}{2\pi f^2} \quad (4.9)$$

For each water depth, the transition frequency is determined by checking when $D > 0.5L$, which marks the shift to deep-water behavior. This transition leads to converging responses in the surge and heave directions at higher frequencies.

Tidal range effects on Load RAOs are minimal, with only minor differences observed across the degrees of freedom. As shown in Figure 4.19, the impact of tidal variations on the heave direction is negligible, confirming that tidal changes do not significantly alter the load response in this study.

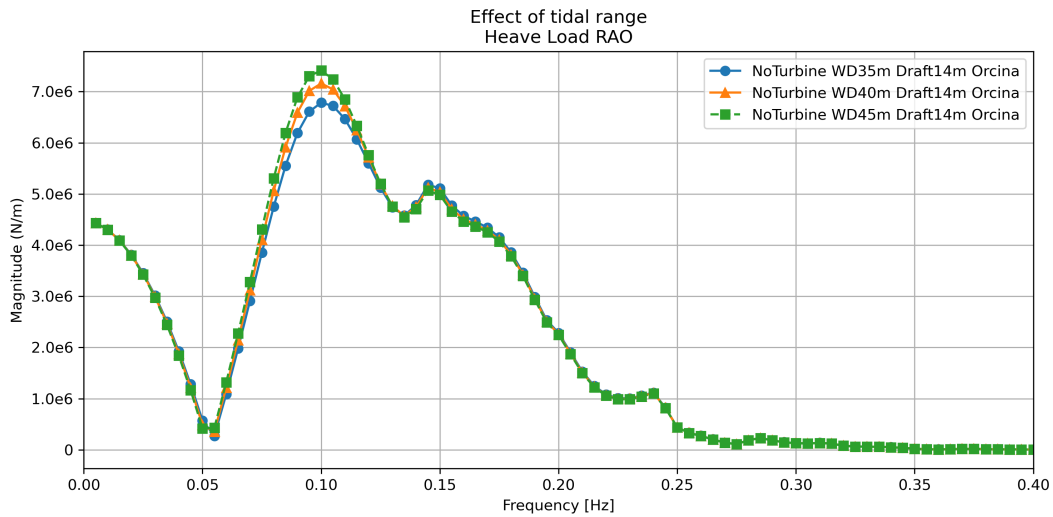


Figure 4.19: Effect of tidal range on heave direction

4.4.2. Natural frequencies

Understanding the natural frequencies of the floating platform is useful for predicting its dynamic behavior and ensuring its stability. This section explores these frequencies through free-decay tests and modal analysis, offering insights into how the mooring system affects platform dynamics.

Free-decay tests

Free-decay simulations were conducted using an Orcina file called K03 15MW semi-sub FOWT, built to represent the VoltturnUS 15 MW reference floater [77]. These simulations were modified to isolate the rigid body modes by removing all external forces, such as wind, waves, and currents, allowing the platform to oscillate freely and revealing its natural frequencies.

Figure 4.20 shows the platform just before it is released in the pitch degree of freedom, initiating the free-decay response.

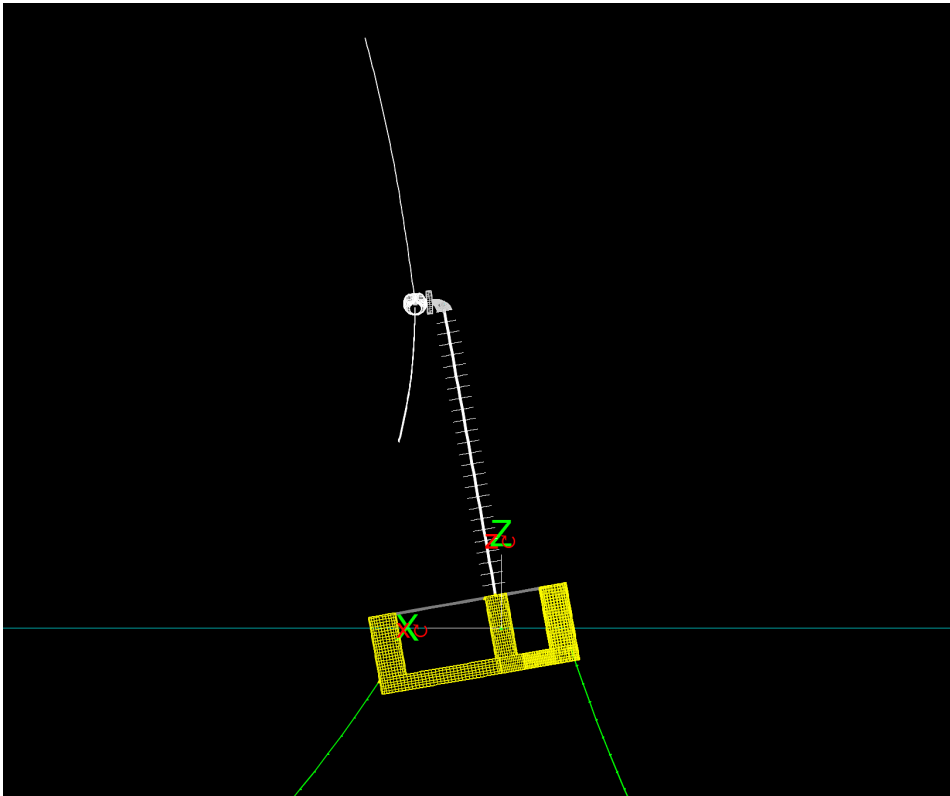


Figure 4.20: Model constraint just before release for pitch DOF

The initial displacements for each degree of freedom (DOF) used in the simulations are presented in Table 4.3.

Table 4.3: Initial displacements for free-decay simulations

DOF	Initial Displacement
Surge [m]	30
Sway [m]	30
Heave [m]	5
Roll [deg]	10
Pitch [deg]	10
Yaw [deg]	15

The results of these free-decay tests were compared to NREL reference data from the VolturnUS-S platform [4], revealing small discrepancies, particularly in the mooring-sensitive DOFs.

Table 4.4: Free decay of mooring system sensitive DOFs

	NREL	Orcina	Difference
Surge [s]	142.9	133.4	-6.7%
Sway [s]	142.9	132.8	-7%
Yaw [s]	90.9	84.3	-7.2%

Table 4.5: Free decay of mooring system insensitive DOFs

	NREL	Orcina	Difference
Heave [s]	20.4	20.7	1.3%
Roll [s]	27.8	27.2	-2.0%
Pitch [s]	27.8	27.2	-2.0%

The most significant deviations occur in the mooring-sensitive DOFs (surge, sway, and yaw), as shown in Table 4.4. These differences highlight the influence of mooring stiffness and hydrodynamic properties on the natural periods of the platform. Conversely, the mooring-insensitive DOFs (heave, roll, and pitch) exhibit much closer agreement between the models, with discrepancies within 2%, as shown in Table 4.5.

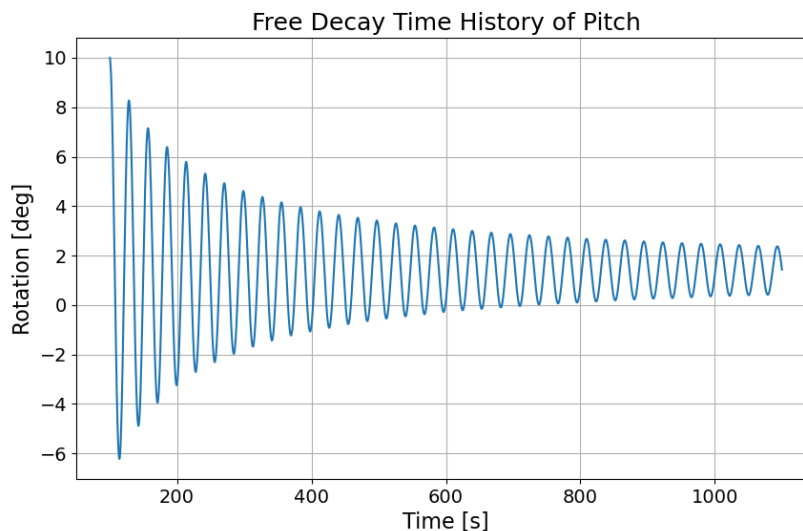
**Figure 4.21:** Response and free decay for pitch DOF

Figure 4.21 illustrates the platform's free-decay response in the pitch DOF, showing how the oscillation dampens over time. Additional plots for all DOFs are available in the Appendix C.

The observed discrepancies can be explained by several factors:

- Slight variations in the platform's center of mass (COM) can significantly affect the natural periods of the structure. These differences impact how the platform responds to external forces and can explain some of the discrepancies between the Orcina and NREL results.
- The exclusion of off-diagonal damping terms in the Orcina model may contribute to differences in overall damping behavior. This can lead to variations in the system's response, particularly in terms of how it handles coupled motions between different degrees of freedom.
- Differences in platform volume between the models lead to variations in buoyancy and hydrodynamic properties. These variations affect the natural frequencies of the floating structure by altering how it interacts with water forces.
- The way hydrodynamic damping from mooring lines is modeled can also influence the results. Differences in how damping is handled between the Orcina and NREL models may contribute to the observed discrepancies in natural periods, especially for mooring-sensitive degrees of freedom.
- In the NREL simulations, aerodynamic drag was minimized by adjusting the orientation of the blades to reduce resistance during decay tests. This step was not replicated in the Orcina simulations, which may explain some of the differences in the results.

Modal analysis

Modal analysis was conducted to investigate the platform's natural frequencies. The damping-free analysis was compared to free-decay test results to examine the damping impact on natural periods. Both modal and frequency domain analyses in this thesis use a constant added mass, as software limitations prevent the use of frequency-dependent added mass.

The added mass matrix is a 6x6 matrix, representing the inertia induced by the surrounding water. In this analysis, only the diagonal terms (surge, sway, heave, roll, pitch, and yaw) are considered, as these dominate the dynamic response. Off-diagonal terms (e.g., surge-pitch coupling) are typically less significant, although pitch-surge coupling may be an exception due to the floater's geometry and the influence of the mooring system, which can induce pitch motion when surge displacement alters the mooring line tension.

Table 4.6: Modal analysis of mooring system sensitive DOFs

	Free decay	Modal analysis	Difference
Surge [s]	133.4	129.8	-2.7%
Sway [s]	132.8	128.9	-2.9%
Yaw [s]	84.3	84.3	0%

Table 4.7: Modal analysis of mooring system insensitive DOFs

	Free decay	Modal analysis	Difference
Heave [s]	20.7	20.6	-0.3%
Roll [s]	27.2	28.3	3.9%
Pitch [s]	27.2	28.3	3.9%

The discrepancies between the modal analysis and free-decay tests, shown in Table 4.6 and Table 4.7, can largely be attributed to the exclusion of damping effects in the modal analysis. While modal analysis assumes no damping, real-world systems, like the one simulated in the free-decay tests, experience significant damping, particularly from hydrodynamic sources such as mooring line drag and viscous effects. This explains the slightly shorter periods observed in the free-decay tests for surge, sway, and heave.

To further understand the system's dynamic characteristics, the added mass over frequency for the surge DOF was examined. Figure 4.22 shows that for frequencies of 0.12 Hz or lower, the added mass remains almost constant. This observation supports the use of a constant added mass in the frequency domain analysis for low-frequency excitations, which dominate the platform's response. This constant added mass assumption holds true for other DOFs as well, as shown in the detailed graphs in Appendix D. For higher frequencies, the added mass is less significant, and the impact on the natural periods is lower.

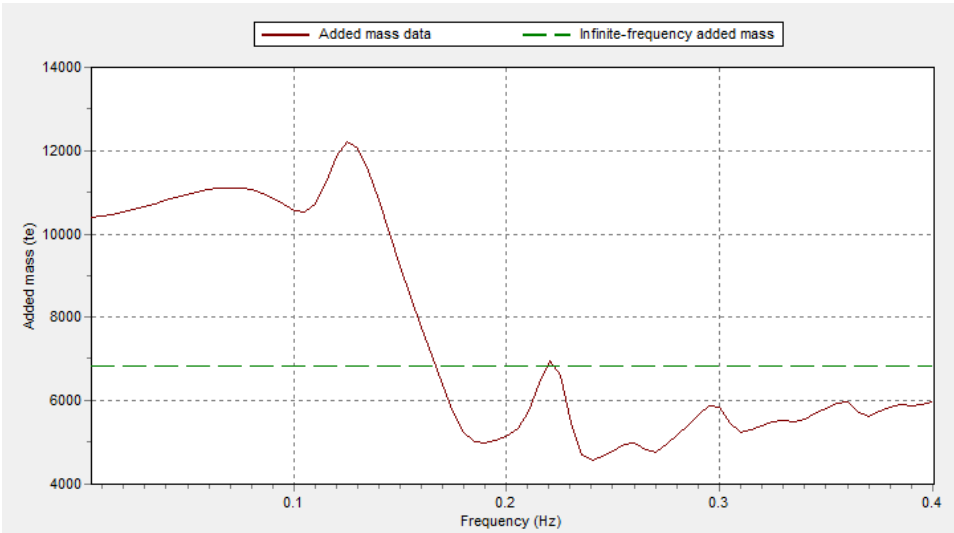


Figure 4.22: Added mass as a function of frequency for surge-surge

The natural frequencies derived from both free-decay tests and modal analysis highlight the complexities involved in accurately modeling the dynamic behavior of floating offshore platforms

5

Results

This chapter presents the analysis of mooring systems designed for the temporary wet storage of floating offshore wind foundations. It evaluates mooring configurations under various environmental conditions, focusing on dynamic behavior, spatial utilization, accessibility, hook-up efficiency, and cost-effectiveness. These results offer insights into the feasibility and performance of different mooring concepts. A Multi-Criteria Decision Analysis (MCDA), as introduced in chapter 3, is employed to compare and assess the mooring systems against defined criteria, ensuring a comprehensive evaluation of their performance.

5.1. Dynamic behavior

The dynamic behavior of mooring systems is critical in ensuring safe and reliable storage of floating offshore wind foundations. This section focuses on results extracted from both catenary and taut mooring system simulations. These results include:

- Fairlead tensions are the forces exerted on the fairlead, which are the connection points between the mooring lines and the floater. Fairlead tensions indicate the load that the floaters fairlead must withstand, and excessive tensions may lead to mooring line failures.
- Anchor tensions are the forces transferred to the seabed anchors. A higher anchor tension necessitates a larger anchor to counteract these forces.
- Floater motions encompass the movements of the floating structure, including both displacements and velocities. Horizontal displacements are especially important, as excessive movement could lead to operational risks such as collisions with neighboring floaters, while increased velocities or accelerations can impose additional loads on the mooring lines.

Both static and dynamic analyses are conducted to assess system performance. The static analysis provides an initial understanding of how the mooring system behaves under constant environmental forces, establishing a baseline for system performance. In contrast, dynamic analysis in the frequency domain evaluates the system's response to various environmental loads, including wave and wind spectra. This approach provides insights into how the mooring system reacts to different environmental forces based on their respective spectra.

5.1.1. Catenary mooring systems

The catenary configuration relies on gravity to form its characteristic free-hanging shape, with the end of the mooring lines lying horizontally on the seabed. Selected for its robustness and simplicity in handling environmental forces, this section presents key results on anchor distance, line length, fairlead and anchor tensions, and floater motions, highlighting performance across different water depths and mooring line diameters.

Anchor distance and line length

The required anchor distance and line length are calculated for various line diameters, using the algorithm outlined in subsection 4.3.2, for a base water depth of 45 meters. This depth represents the water level at high tide, ensuring that the calculated distances and lengths prevent uplift under all tidal conditions. If a lower water depth had been used as the base, there would be a risk of uplift occurring when these distances and lengths are applied to greater depths.

The anchor distance is defined as the horizontal distance between the center of the floater and the anchor point. As shown in Figure 4.4, the three fairleads are located 58 meters from the center point of the floater. Thus, the horizontal distance that the mooring line spans can be calculated as the anchor distance minus the distance between the center of the floater and the fairlead.

For six different line diameters, the anchor distance and line length were evaluated to understand their impact on the overall mooring system. Figure 5.1 presents the results, showing the relationship between anchor distance, line length, and line diameter.

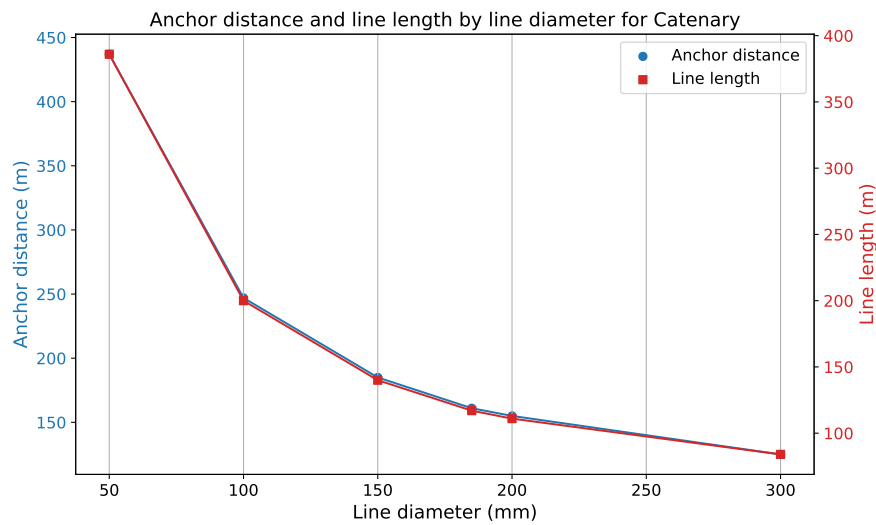


Figure 5.1: Anchor distance and line length over line diameter

As shown in Figure 5.1, both the anchor distance and line length decrease as the line diameter increases. Heavier mooring lines provide larger restoring forces, which allows for shorter anchor distances and line lengths while still maintaining the necessary mooring system performance. For the largest line diameter, the shortest anchor distance of 135 meters is observed.

The model remains insensitive to the minimum anchor distance constraint of 85 meters, meaning this limit does not affect the results in the tested range. However, future research or specific operational requirements could impose a different minimum anchor distance, in which case the anchor distance and line lengths will need to be adjusted accordingly.

Although longer anchor distances may offer more operational flexibility, they result in reduced spatial utilization and increased material use, both of which need to be considered in the final mooring system design. Therefore, the strategy here is to select the shortest anchor distance that meets all design constraints.

Fairlead tensions

Fairlead tensions represent the forces exerted on the mooring lines at the floater's connection point (the fairlead). These tensions can be decomposed into static and dynamic components influenced by factors such as the diameter of the mooring line, the anchor distance, and environmental conditions.

Tension in a mooring line is balanced by line weight, anchor holding capacity, uplift, and seabed friction. Seabed friction represents the friction of the mooring line from the anchor until the line touch-down

point and is represented by the Coulomb friction model. Mooring line tension can be decomposed into horizontal (T_H) and vertical directions (T_V). The vertical tension is offset by line weight and uplift. The model finds the first valid solution with zero static uplift, but as noted in DNV-RP-E301 [26], some uplift may occur, especially with larger chain diameters. Horizontally, forces are balanced by anchor capacity and horizontal tension, favoring lower tensions to minimize anchor size and capacity. This balance of forces is shown in Figure 5.2.

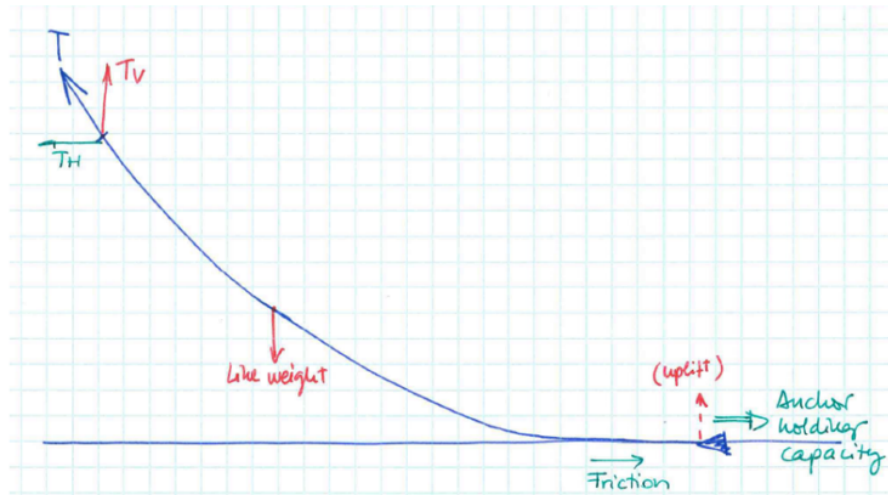


Figure 5.2: Schematic of a catenary mooring line [51]

Pretensions and declinations Figure 5.3 shows pretensions on the fairlead side for various line diameters and water depths. The pretension refers to the baseline tension in the mooring lines due to the weight of the mooring lines and the floater, without any environmental loading (i.e., wind, waves, or currents). This tension is purely a result of gravitational forces. The x-values of the nodes represent the line diameters, and the three lines represent the water depths. Tension increases with both line diameter and water depth due to heavier lines and more suspended mooring lines, resulting in greater loads at the fairlead. It can also be observed that the lines representing different water depths diverge as the line diameter increases. This is because the tension increases with the weight of the mooring line, and the weight scales approximately with the square of the diameter.

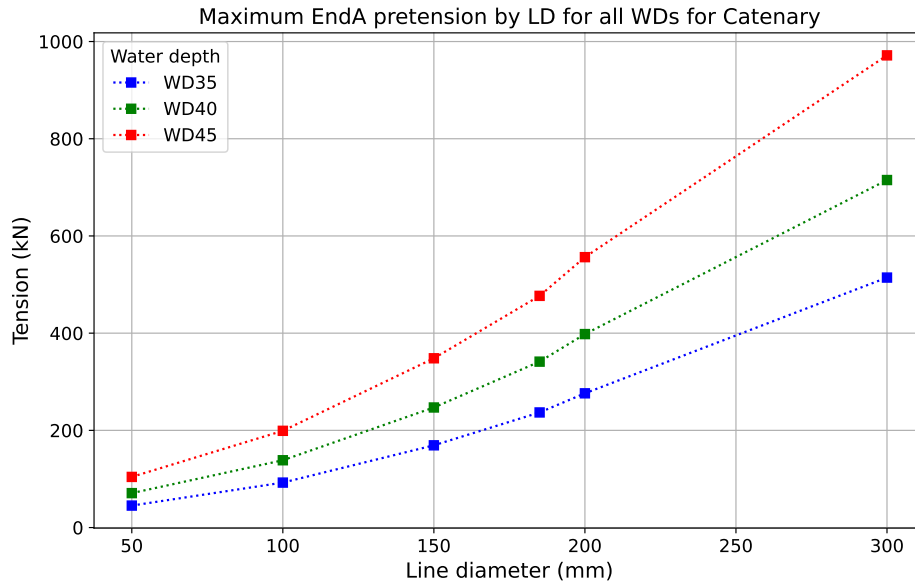


Figure 5.3: Pretensions for the fairlead side of the mooring lines

The declination angle of the fairlead, depicted in Figure 5.4, shows that larger line diameters result in steeper angles, implying a more vertical orientation of the mooring line and increased vertical tension at the fairlead. In addition, the declination angles increase slightly with greater water depth, as the mooring line spans a greater vertical distance, creating a more pronounced vertical load component.

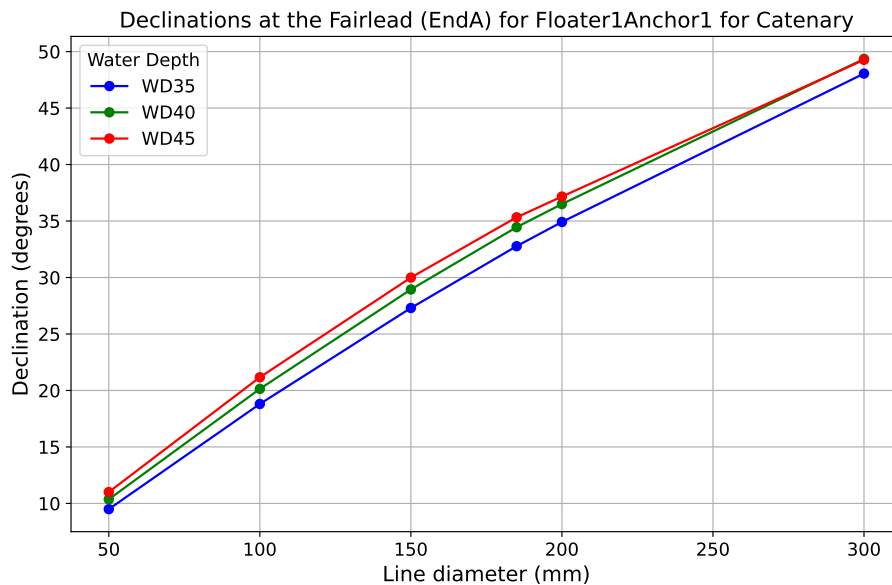


Figure 5.4: Declinations on the fairlead side for an upwind line

Feasibility of hook up using tugs The pretensions depicted in Figure 5.3 represent calm sea conditions, which resemble those encountered during installation. Table 5.1 compares pretension values to the bollard pull capacity of offshore assets, including typical harbor tugs and Anchor Handling Tug Supply (AHTS) vessels.

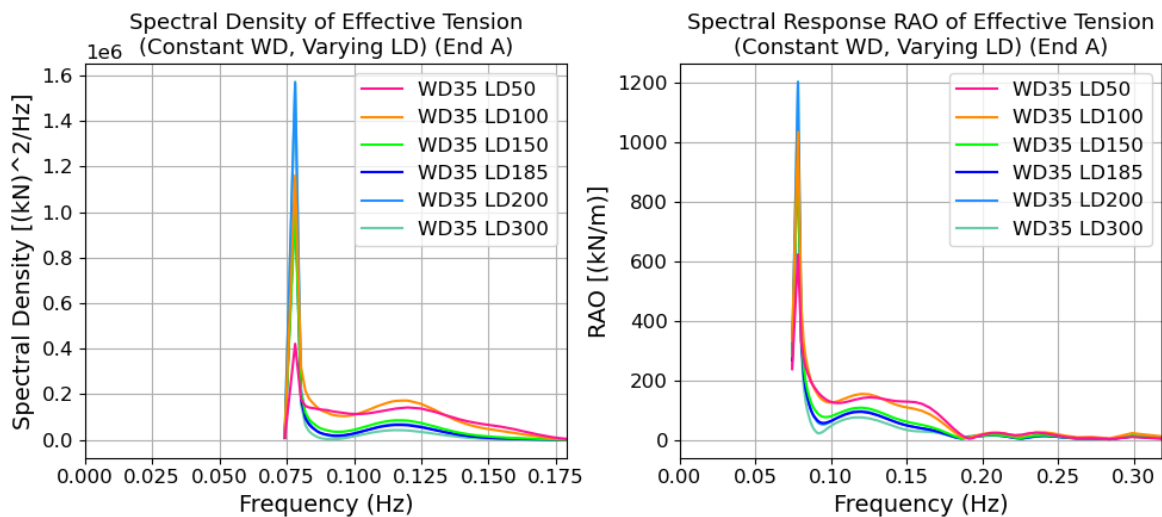
Table 5.1: Bollard pull data for selected ships [17]

	Weight	Force
Typical harbour tug	50 metric tonnes	500 kN
Typical AHTS	65 to 200+ metric tonnes	600 to 2000 kN
Largest AHTS	477 metric tonnes	4700 kN

The feasibility of installing the mooring system using tugs is primarily dependent on the duration of the hook-up procedure and the environmental conditions. If the procedure can be completed within a timeframe significantly shorter than the tidal period (approximately 12 hours), harbor tugs with a bollard pull of 500 kN can handle all mooring line diameters. For longer installations, where tidal fluctuations may introduce additional challenges, tugs are capable of managing line diameters up to LD200.

The results indicate that additional in-line tensioners are not generally required for installations under these calm conditions, further supporting the feasibility of using standard tugs for the majority of the hook-up process.

Spectral density and response After assessing the pretensions and declinations in the previous section, it is important to analyze the dynamic tensions to understand how waves, wind, and currents affect the mooring system. These tensions depend on environmental loading, mooring line diameter, and water depth. Figure 5.5 compares the power spectral density (PSD) and response amplitude operator (RAO) of effective tension in an upwind line with constant water depth and varying line diameter.

Figure 5.5: Floater1Anchor1 Overlay Plots for Constant WD, Varying LD**Figure 5.5:** Spectral density and RAO of effective tension of an upwind line

The *power spectral density (PSD) plot* on the left side of Figure 5.5 shows the distribution of tension energy across different frequencies. The spectral density highlights how much energy is present at each frequency, offering insight into which frequency ranges have the greatest influence on the mooring line tensions.

- The largest peak in the spectral density occurs at 0.078 Hz, corresponding to the natural frequency of the system. At this frequency, the mooring system is most susceptible to large displacements and forces.
- For all line diameters, this peak is prominent, but the magnitude is highest for larger line diameters (LD300). This is because larger lines have increased mass, which amplifies resonant behavior, leading to higher tension amplitudes at the natural frequency.

- Beyond the natural frequency, the spectral density decreases for all line diameters. However, smaller line diameters (e.g., LD50 and LD100) exhibit higher energy levels in the higher frequency ranges (above 0.1 Hz). This occurs because smaller lines, being lighter, provide less resistance to short-period waves, making them more vulnerable to higher-frequency wave loading, while larger lines are better at attenuating these forces.

The *response amplitude operator (RAO) plot* on the right side of Figure 5.5 shows the transfer function that relates the wave-induced motions to the resulting tensions in the mooring line. The RAO provides a measure of how the system amplifies or attenuates wave-induced forces at different frequencies.

- The RAO plot also shows a significant peak at 0.078 Hz, where the system exhibits resonant behavior. Larger mooring line diameters (LD300) show the highest RAO values at this frequency, indicating greater amplification of wave-induced forces. This is consistent with larger lines amplifying resonant behavior due to their increased mass.
- At higher frequencies (above 0.081 Hz until 0.16 Hz), the RAO values decrease significantly as the line diameter increases. This suggests that larger, heavier mooring lines are more effective at dampening wave-induced forces in the higher frequency range. The increased mass of the larger lines provides more resistance, thereby reducing system motion at these higher frequencies.

The fluctuating tails observed in both the PSD and RAO plots above the natural frequency arise from variations in the load RAOs, which represent the first-order wave forces on the vessel. These fluctuating tails indicate dynamic responses to short-period waves and align with the input load RAOs shown in subsection 4.4.1.

- The fluctuating behavior from 0.15 Hz to 0.03 Hz seen in the spectral response RAO plot can be directly observed in the load RAO plots. This shows that the dynamic behavior at these frequencies is influenced by the load RAOs.
- A bump or peak in both the PSD and RAO plots at 0.12 Hz is also observable in the load RAOs. This behavior highlights that the lower line diameters (LD50 and LD100) are more susceptible to wave frequencies in the 0.08 Hz to 0.18 Hz range. The lower tension resistance of these smaller line diameters explains this vulnerability to dynamic forces in these higher frequency ranges.

Static and dynamic tensions Following the analysis of pretensions, we expand the study to include environmental loading, introducing two additional types of tension: static tension, representing the equilibrium tension under constant environmental forces such as wind and waves, and the Most Probable Maximum (MPM) tension, which accounts for the dynamic maximum tensions during a 3-hour storm event. The MPM includes both the static component and the dynamic loading effects caused by waves and wind. Figure 5.6 illustrates these two additional types of tension.

The general trend in Figure 5.6 reveals that larger line diameters result in increased tensions due to the greater mass and length of submerged mooring lines. Additionally, a divergent pattern between the water depths is observed, both of which are similar to the trends seen in the pretension analysis.

For smaller line diameters, the static tension represents around 66% of the MPM tension; for instance, if the MPM tension is 1200 kN, the static tension is approximately 800 kN. As the line diameter increases, this proportion rises, with the static tension representing around 85% of the MPM tension for larger diameters. This trend results from the larger mass of the lines, which dampens the dynamic response to environmental forces and reduces the difference between static and MPM tensions. Consequently, the static component becomes more dominant in the total tension for larger line diameters.

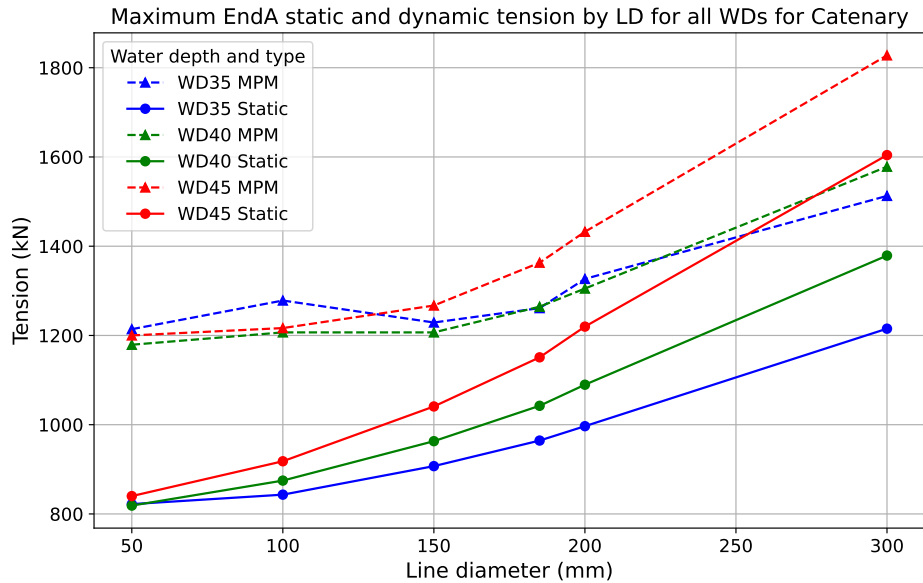


Figure 5.6: Fairlead tensions for various environmental conditions

An notable behavior is observed in the MPM for WD35, where the tension fluctuates before aligning with the expected trend of lower tensions relative to the other water depths. This anomaly may be attributed to numerical inaccuracies in the MPM calculation, as OrcaFlex employs statistical approximations to estimate MPM values during storm events. Further investigation could clarify whether these fluctuations are caused by specific environmental inputs or are inherent in the numerical methods used.

Given that static tension alone underestimates the total tension, particularly for smaller line diameters where dynamic effects are more significant, the MPM provides a more accurate reflection of the system's performance under extreme environmental conditions. Therefore, the MPM is the most relevant measure for design and safety considerations.

Anchor tensions

Anchor tensions, representing the forces transmitted to the seabed anchors, show trends similar to fairlead tensions. However, notable differences arise due to the interaction between the mooring line and the seabed, and the distribution of the line's self-weight.

Figure 5.7 shows the pretensions on the anchor side for different line diameters and water depths. Anchor pretensions increase with line diameter, as seen with the fairlead tensions, but the values are generally lower. While seabed friction does contribute to this reduction, a more important factor is the self-weight of the mooring line. The tension at the fairlead must support the full suspended weight of the mooring line, while the tension at the anchor is lower because the line's weight is largely supported by the seabed.

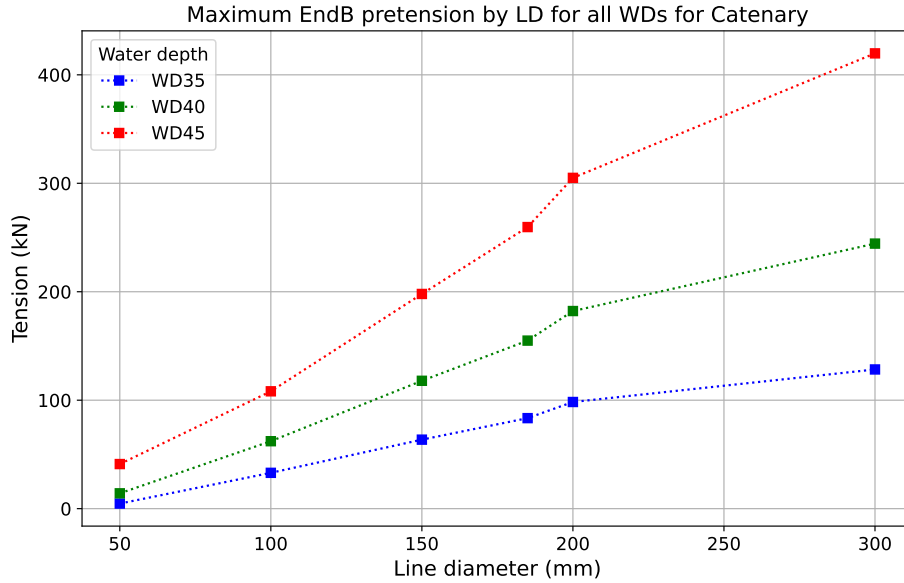


Figure 5.7: Static tensions for the anchor side of an upwind mooring line

Figure 5.8 presents both static and MPM tensions for the anchor side. Unlike the fairlead, there is no strong correlation between line diameter and MPM tension on the anchor side. This is due to the horizontal orientation of the mooring line near the anchor, which causes environmental forces to be transmitted to the anchor, but without the significant self-weight component affecting the MPM. Furthermore, the fluctuations in the MPM lines are likely due to numerical approximations in the OrcaFlex model used to estimate these maximum tensions during storm events.

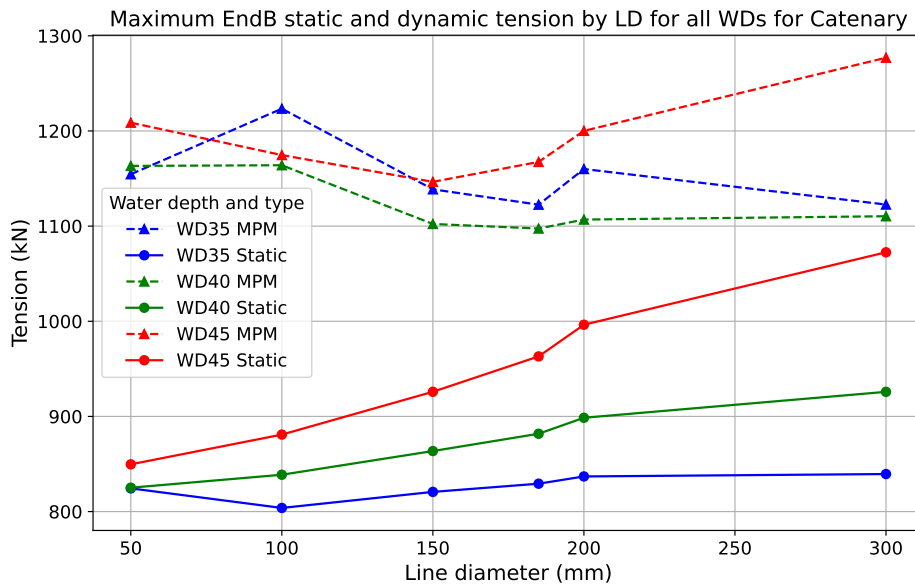


Figure 5.8: Static and MPM tensions for the anchor side of an upwind mooring line

Figure 5.9 illustrates the vertical force component (E_z) at the anchor under static and dynamic conditions. Under static conditions, a minor uplift force is observed at the anchor, which can be attributed

to modeling constraints in OrcaFlex. The declination constraint in the model allows the mooring line to have a small upward angle (approximately 88-89 degrees) near the anchor, resulting in a slight uplift. However, the observed uplift force is minimal, with values around 45 kN for the largest line diameters, which accounts for less than 5% of the total static tension at the anchor.

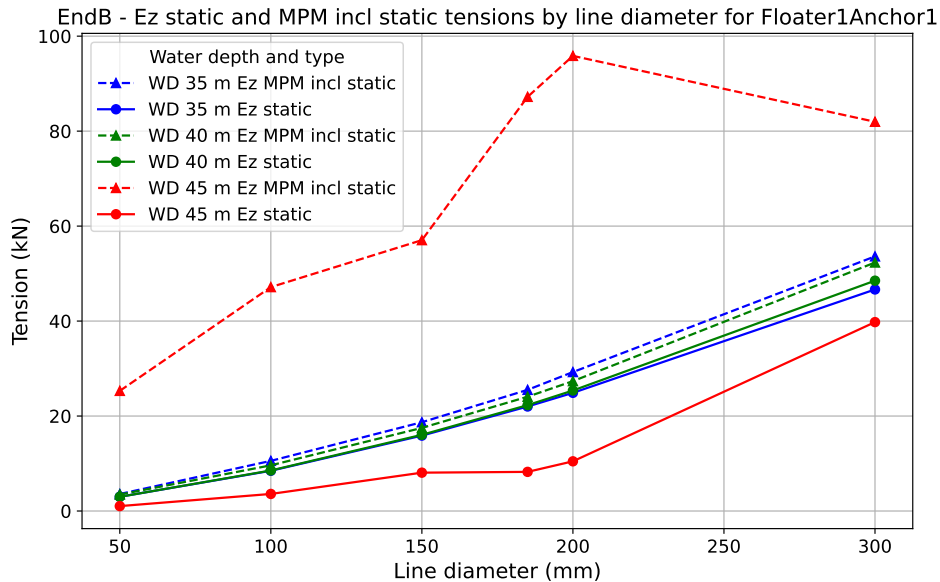


Figure 5.9: Vertical force component (E_z) at the anchor

During dynamic loading conditions, represented by the MPM tension, a more pronounced vertical force component (E_z) appears for the WD45 case. This is due to the larger vertical distance that must be spanned at this water depth, despite the same amount of line length being available. Although the observed uplift occurs during these dynamic conditions, DNV-RP-E301 [26] provides guidance on the use of drag anchors with slight amounts of uplift under certain conditions. Therefore, the anchor system is expected to manage these forces during extreme environmental loading, but further investigation is required to ensure compliance.

Floater motions

Floater motions, including displacements, velocities, and accelerations, are key indicators of the dynamic performance of the mooring system. The environmental forces -wind, waves, and currents- are applied in the Y direction, resulting in most displacements along this axis. The large size and buoyancy of the floater limit Z-axis displacements, while the lack of environmental forces in the X direction prevents noticeable motion in that direction.

Analysis of floater displacements, shown in Figure 5.10 reveals that displacements are primarily static (approximately 90%). In shallower water depths, the mooring line assumes a more vertical orientation, reducing the horizontal restoring force, which increases displacements. Heavier chains create greater horizontal restoring force due to their weight, but their vertical orientation limits this effect. The current has a greater influence on displacement than wave conditions, with waves only slightly affecting the floater due to its large mass and inertia.

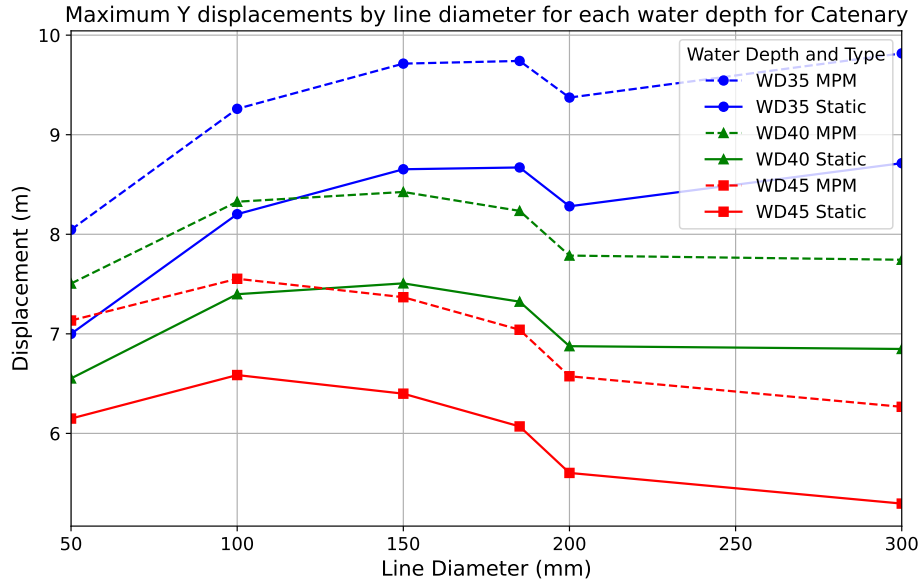


Figure 5.10: Y displacements

Floater velocities and accelerations are summarized in Table 5.2 and Table 5.3. MPM values are consistent across LDs, with higher values in shallower water due to a more vertical mooring line and reduced tension. The maximum acceleration of 0.563 m/s^2 for WD35 LD200 (about 0.05 g) is well below the tower-top axial acceleration limits of 0.2 to 0.3 g [84]. Note that no tower is installed on the floater in this study, and there are no formal limits for standalone floater accelerations, which are usually constrained by tower-top axial acceleration when integrated with a turbine.

Table 5.2: Velocities in Y direction for different line diameters and water depths

Water depth (m)	Y velocity (m/s)					
	LD50	LD100	LD150	LD185	LD200	LD300
35	0.73	0.73	0.73	0.73	0.74	0.74
40	0.69	0.68	0.67	0.67	0.66	0.66
45	0.69	0.69	0.69	0.69	0.69	0.69

Table 5.3: Accelerations in Y direction for different line diameters and water depths

Water depth (m)	Y acceleration (m/s^2)					
	LD50	LD100	LD150	LD185	LD200	LD300
35	0.56	0.56	0.56	0.56	0.56	0.56
40	0.54	0.53	0.53	0.53	0.53	0.53
45	0.54	0.54	0.54	0.54	0.54	0.54

5.1.2. Taut mooring systems

The taut mooring system was analyzed similarly to the catenary system, varying both line diameters and water depths. This analysis included two types of mooring lines: Nylon and Polyester. These materials, discussed in detail in the theoretical background (chapter 2), were chosen for their distinct mechanical properties. Nylon exhibits greater elongation under tension compared to Polyester, which is more rigid and frequently used in permanent mooring applications. As highlighted in subsection 2.1.3, the nonlinear stiffness of these materials was not included in the current simulations. As explained in subsection 2.1.3, omitting nonlinear stiffness may result in underestimating tensions by 30%-40%, particularly for Nylon. This underestimation arises because advanced models like the Falkenburg SYrope

model account for dynamic stiffness changes under load, which are not captured by a static stiffness approximation. Consequently, the results presented here should be interpreted with caution.

The anchor distance and line length are constant for all Polyester mooring systems, with an 85 m anchor distance and 34 m line length. This line length is then stretched to span the distance between the anchor and the fairlead. Similarly, the anchor distance and line length for Nylon mooring systems are set at 85 m anchor distance and 24 m line length, which is also stretched.

The declination angle of the fairlead, depicted in Figure 5.11, shows that larger line diameters result in steeper angles due to the lower displacements associated with higher line diameters. This will be shown later in Figure 5.1.2. Additionally, the declination angle increases with greater water depths as the mooring line needs to make a sharper angle toward the anchor. The deeper the water, the more vertical the mooring line becomes

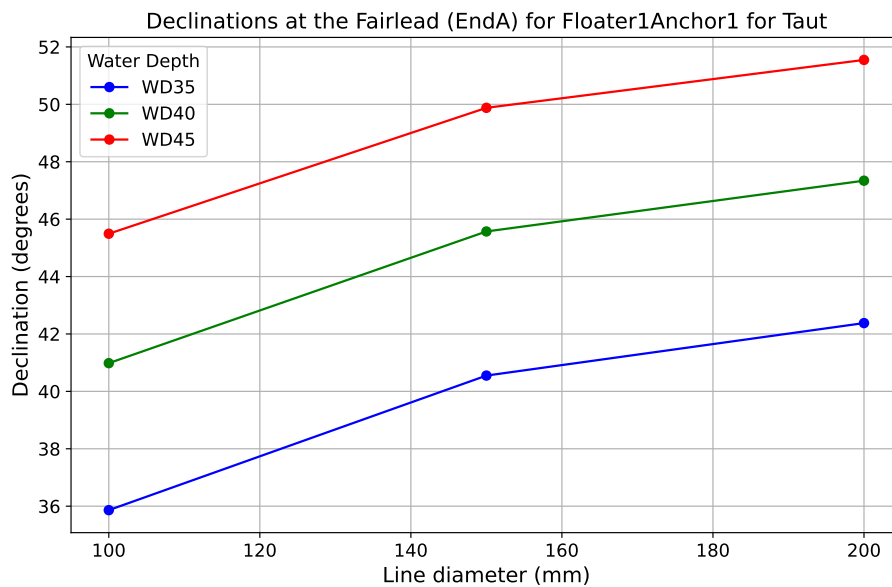


Figure 5.11: Declinations on the fairlead side for an upwind line

Fairlead tensions

The pretension, static, and dynamic tensions at the fairlead for the taut mooring system were computed. For both Nylon and Polyester lines, the solver first uses the lowest water depth to determine a valid anchor distance and line length, ensuring the lines remain taut and free from slack. As shown in Table 5.4, the breaking strengths of the mooring lines increase rapidly with diameter, likely due to the fact that breaking strength scales with the cross-sectional area, which grows with the square of the diameter.

Table 5.4: Line breaking strengths for Polyester and Nylon [78]

Line Diameter (mm)	Polyester (kN)	Nylon (kN)
50	426	348
100	1704	1393
150	3535	3135
200	6818	5574

Figure 5.12 presents the pretensions for Polyester lines at three different water depths, with the crosses indicating the breaking strengths for the four modeled line diameters. In shallow water (the blue line), the pretensions stay below the breaking strengths for all line diameters, satisfying the design constraints.

However, as the water depth increases, the pretensions exceed the breaking strengths, particularly at greater depths, making the solution invalid. To obtain valid solutions for Polyester lines at these depths, certain constraints would need to be adjusted. Since slack is not allowed in the mooring system, primarily to avoid dangerous snap loads, other parameters such as the material properties of the mooring lines need to be modified. This could involve selecting materials with higher tensile strength or utilizing other materials with increased stiffness to prevent excessive elongation under load.

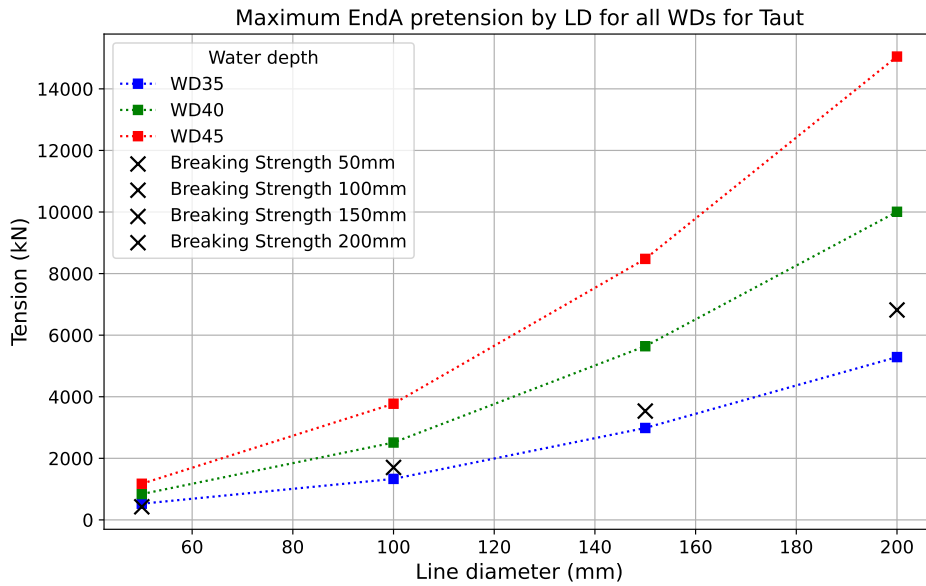


Figure 5.12: Static tensions for the fairlead side of the mooring lines (Polyester)

Given the invalid results for Polyester, the analysis proceeds with Nylon mooring lines. Figure 5.13 shows the pretensions for the Nylon mooring lines.

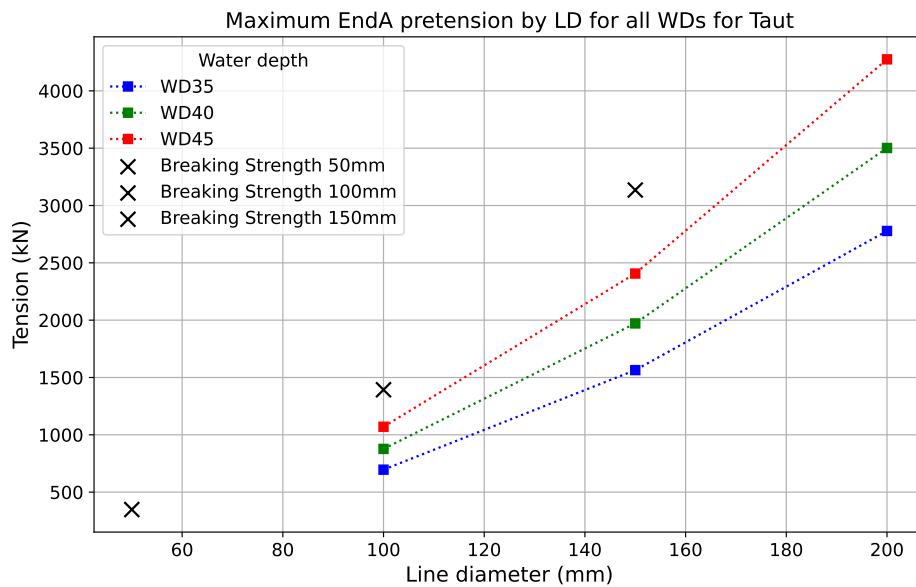


Figure 5.13: Pretensions for the fairlead side of the mooring lines (Nylon)

LD50 shows no valid static solutions due to the constraints set in the model, which were not met for this configuration. This is attributed to the minimum anchor distance and line length requirements, which the model could not satisfy under the given loading conditions.

Similar trends to the catenary system are observed. However, most of the additional tension arises not from increased weight but from the greater water depth, which stretches the lines further and results in higher pretensions. As the water depth increases, the mooring lines must cover a longer distance between the anchor and the floater, which increases the tension required to maintain a taut configuration.

For this case, the pretension required during hook-up at low tide in calm waters was 2800 kN. This high pretension is a notable disadvantage for taut systems, as specialized equipment would be required for tensioning. However, the displacements for WD45 LD200 are modest, at 4.5 meters, due to the high tension reducing displacements.

Figure 5.14 presents both static and MPM tensions for different line diameters. The dynamic tensions are close to the static tensions for WD35 and WD40, as these cases involve less line stretch due to the shallower water depths. The solver uses a base water depth of 35 m, ensuring taut lines across all depths. However, in WD45, the dynamic response becomes proportionally larger, likely due to the higher overall tension amplifying the effects of environmental loads. Caution is required when interpreting these results, especially for highly elongated lines, as non-linear stiffness effects become more pronounced under such conditions.

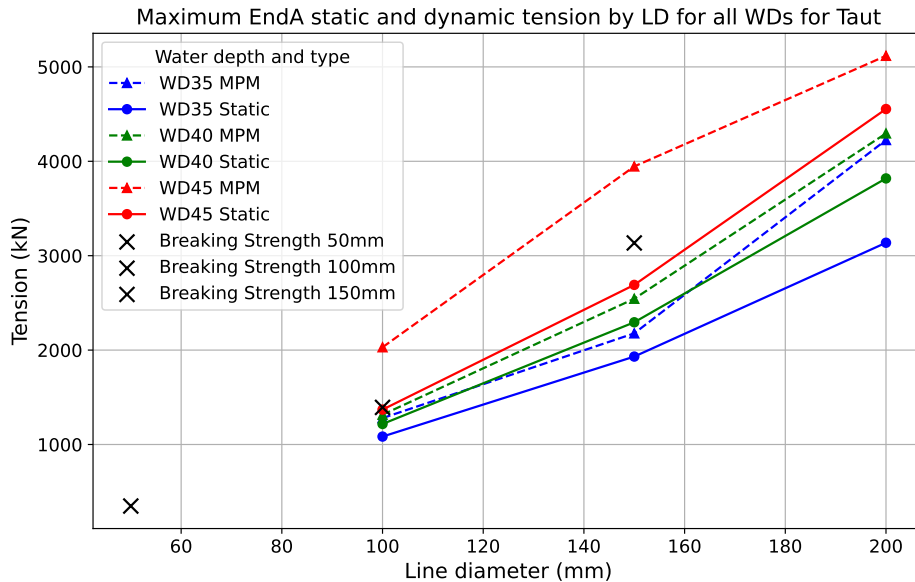


Figure 5.14: Static and MPM tensions for the fairlead side of the mooring lines (Nylon)

Anchor tensions

In taut mooring systems, anchor tensions are nearly identical to fairlead tensions due to the direct load path and low line weight in water. Both the anchor and fairlead are modeled as points and a uniform current is used. In practice, the tension difference is within 0.2 kN, negligible for this model’s accuracy.

The most important components to consider are the vertical and horizontal forces on the anchor. The horizontal component (E_y) directly affects the anchor’s holding capacity, while the vertical component (E_z) impacts the uplift forces. Figure 5.15 shows the MPM horizontal and vertical anchor forces for Nylon mooring lines at different line diameters for a water depth of 45 m. This water depth is governing for anchor sizing due to the increased forces associated with deeper waters.

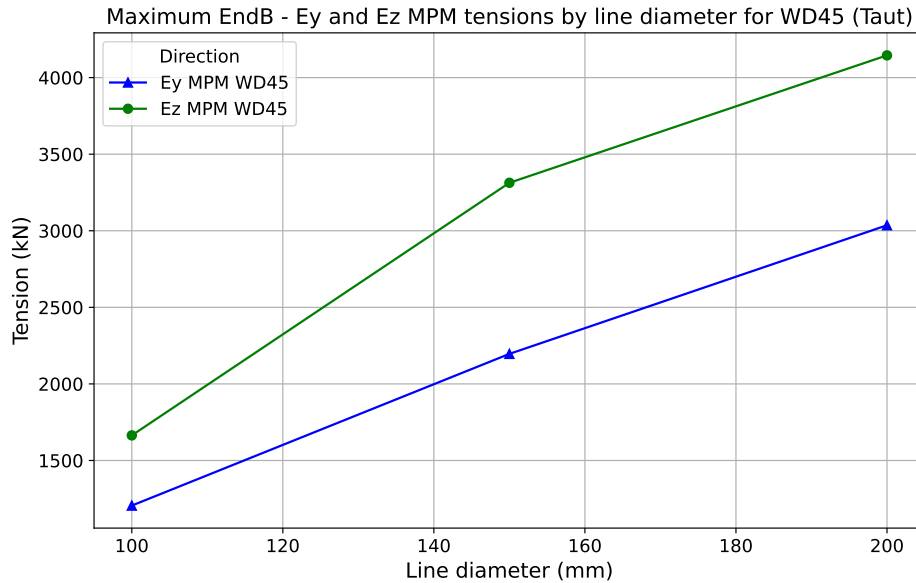


Figure 5.15: Horizontal (E_y) and vertical (E_z) forces at the anchor for Nylon mooring lines at WD45

In Figure 5.15, two lines are presented: one for the horizontal force component (E_y) and one for the vertical force component (E_z). The vertical force (E_z) line is higher than the horizontal force (E_y), indicating that at a water depth of 45 m, more vertical tension is expected at the anchor. Both force components exhibit an upward trend with increasing line diameter, which aligns with earlier observations in the catenary mooring results.

The horizontal force component increases with both line diameter and water depth. From 1205 kN to 3036 kN for WD45. As the line diameter increases, the stiffness of the mooring line also increases, necessitating greater horizontal forces to achieve the required elongation for the taut configuration. Deeper water depths increase the vertical distance, causing more line stretch and higher horizontal tensions. This relationship indicates a trade-off between tensions and displacements: lower line diameters (less stiff lines) result in higher displacements but lower tensions, while higher line diameters (stiffer lines) lead to lower displacements but higher tensions.

The vertical force component represents the uplift acting on the anchor. This uplift force is significant in taut mooring systems due to the steep angle of the mooring lines. As water depth and line diameter increase, so does the vertical force, potentially requiring anchors capable of handling substantial uplift. The higher E_z values indicate that vertical forces are more dominant than horizontal forces at the anchor point in WD45. For example, at LD200, the vertical force of approximately 4145 kN exceeds the horizontal force of about 3036 kN.

Substantial uplift and horizontal forces require robust anchoring solutions capable of withstanding high vertical and horizontal loads. Vertical load anchors (VLAs), as discussed in subsection 2.1.5, are suited to handle the uplift forces present in taut mooring systems at shallow waters. Selecting and designing anchors carefully is important to maintain the integrity of the mooring system, considering the increased tensions with larger line diameters and deeper waters.

Floater motions

As mentioned in the catenary mooring system analysis, the floater's motions are predominantly along the Y-axis due to environmental forces being applied from this direction. The large hydrostatic stiffness of the floater and the symmetry of the loading result in negligible motions in the X and Z directions.

Figure 5.16 presents the maximum Y-direction displacements of the floater for Nylon mooring lines across different LDs and WDs. Both static and MPM displacements are shown, with the MPM displacements accounting for dynamic environmental loading.

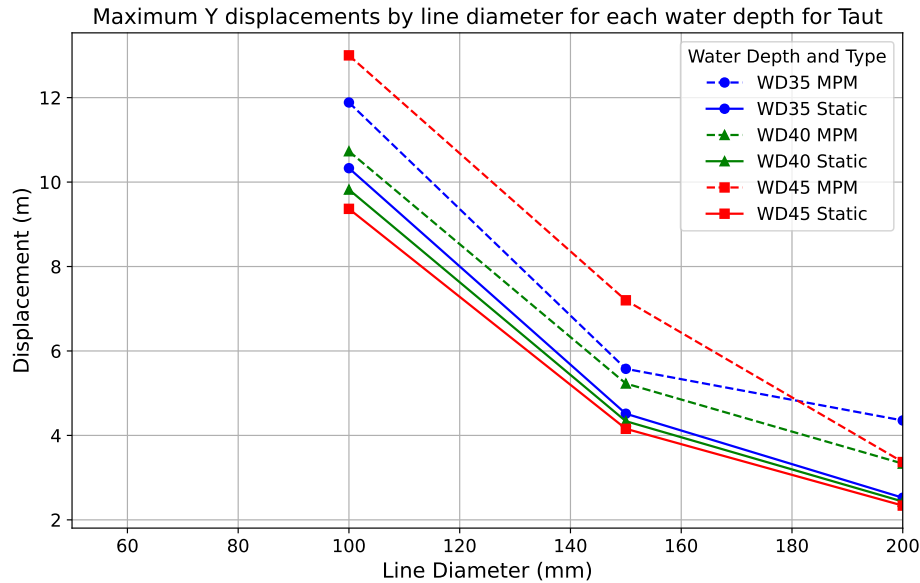


Figure 5.16: Maximum Y-direction displacements of the floater for Nylon mooring lines

The results indicate that the maximum displacements decrease with increasing line diameter due to the higher stiffness and restoring force provided by larger mooring lines. A larger line diameter increases the axial stiffness of the mooring line, which reduces the amount of stretch under load. Consequently, the floater experiences smaller excursions under the same environmental conditions. For example, at WD35, the MPM displacement reduces from approximately 10.00 m for LD100 to around 5.00 m for LD200.

Displacements increase with water depth because deeper waters require the mooring lines to span a greater vertical distance, resulting in more line stretch and reduced horizontal stiffness. This leads to larger floater excursions under environmental loading. At WD45, the MPM displacement for LD100 increases to about 12.00 m, compared to 10.00 m at WD35.

Velocities and accelerations of the floater are summarized in Table 5.5 and Table 5.6. The MPM values are provided for different line diameters and water depths.

Table 5.5: MPM velocities in Y direction for Nylon mooring lines

Line Diameter (mm)	WD35 (m/s)	WD40 (m/s)	WD45 (m/s)
100	0.92	0.67	1.86
150	0.73	0.67	1.62
200	1.07	0.68	0.73

Table 5.6: MPM accelerations in Y direction for Nylon mooring lines

Line Diameter (mm)	WD35 (m/s ²)	WD40 (m/s ²)	WD45 (m/s ²)
100	0.62	0.53	1.01
150	0.57	0.53	0.92
200	0.70	0.54	0.57

Generally, velocities and accelerations decrease with increasing line diameter, consistent with the expectation that stiffer mooring lines limit floater motions. Larger line diameters provide greater restoring force, which not only reduces the maximum displacement but also dampens the floater's motion, re-

sulting in lower velocities and accelerations. For example, at WD45, the MPM acceleration decreases from 1.01 m/s² for LD100 to 0.57 m/s² for LD200.

The observed increase in velocities and accelerations with water depth, particularly for smaller line diameters, is due to the increased line stretch and reduced stiffness in deeper waters. The longer mooring lines in deeper waters allow for greater floater motions under dynamic loading. This effect is more pronounced for lines with lower stiffness (smaller diameters), leading to higher velocities and accelerations.

These trends influence the design and performance of the mooring system. Higher velocities and accelerations can lead to increased dynamic loads on the mooring lines and the floater, potentially affecting structural integrity and fatigue life. Therefore, selecting an appropriate line diameter is influential to balance the floater motions and the resulting tensions in the mooring lines. While larger diameters reduce floater motions, they also result in higher pretensions and require stronger anchors, as discussed earlier. The choice of line diameter must consider these trade-offs to ensure the safety and reliability of the mooring system.

5.1.3. Comparison of catenary and taut concepts

Varying line diameters (LDs) were evaluated for both mooring systems, revealing considerable differences in performance. Only specific configurations were acceptable, as all polyester lines produced invalid outcomes, while only one nylon line diameter (LD200) yielded satisfactory results.

Catenary systems experience lower pretensions, ranging from approximately 500 kN to 1500 kN, making them easier to install without the need for specialized equipment. The anchor loads are primarily horizontal, which allows for the use of conventional drag anchors. In contrast, taut mooring systems have higher pretensions, reaching up to 2800 kN for larger line diameters and deeper water. These higher tensions require specialized tensioning equipment during installation and demand anchors capable of resisting vertical loads, such as vertical load anchors (VLAs).

In terms of floater motions, the catenary system generally shows larger displacements, up to 14 m for smaller line diameters, due to its inherent compliance, allowing more horizontal movement. Maximum accelerations in the catenary system reach around 0.56 m/s², or approximately 0.057 g, which is well within operational limits. In comparison, the taut system, with its higher stiffness and restoring force, limits floater displacements more effectively, reducing them to approximately 5 m to 12 m depending on line diameter and water depth. However, maximum accelerations can reach up to 1.01 m/s², or approximately 0.10 g, which is still within acceptable limits.

5.2. Other criteria

In addition to dynamic behavior, several other criteria are evaluated to assess the suitability of mooring systems for temporary wet storage of floating offshore wind foundations. These criteria include spatial utilization, accessibility, cost, and hook-up efficiency. Each of these criteria is discussed in detail below.

5.2.1. Spatial utilization

Spatial utilization refers to the efficiency with which the available area is used for mooring the floaters. In the context of temporary wet storage, maximizing spatial utilization means accommodating the highest number of floaters within a given area without causing collisions or operational hindrances. For the catenary mooring system, the anchor distance must be sufficiently large to ensure stability and prevent collisions. However, for chain diameters of 150 mm and larger, the spatial utilization becomes constrained by accessibility limits, resulting in no significant difference compared to the taut mooring system. The taut mooring system generally allows for better spatial utilization due to its vertical load distribution, which requires less horizontal space compared to catenary systems. Nevertheless, in shallow water depths, the taut system will always remain on the limit of the accessibility constraint, balancing spatial utilization and accessibility effectively.

5.2.2. Accessibility

Accessibility is a critical criterion that evaluates the ease with which tugs and other vessels can maneuver around and access the moored floaters. Both catenary and taut mooring systems have the same

45 m minimum distance constraint between floaters to ensure adequate maneuverability for tugs. However, the catenary system, due to its higher displacements, poses more challenges for accessibility compared to the taut system. The taut mooring system, with its lower displacements and velocities, scores better in terms of accessibility as it provides a more stable and predictable environment for tugs to operate safely and efficiently.

5.2.3. Hook-up efficiency

Hook-up efficiency assesses the complexity involved in connecting and disconnecting the mooring lines. Catenary mooring systems have an advantage in this aspect due to their reduced need for high tension in the mooring lines. This makes the process of putting in and taking out the mooring system simpler and faster. Taut mooring systems, while offering better dynamic stability and spatial utilization, require more precise tensioning and handling during the hook-in and hook-out procedures, thus increasing the complexity and time required for these operations.

5.2.4. Cost

Cost is evaluated based on the amount of material required and the complexity of the mooring system. Catenary mooring systems typically use more expensive chain materials due to the need for heavy chains that can handle the dynamic loads effectively. On the other hand, taut mooring systems require vertical load-carrying anchors, which are more expensive than the horizontal anchors used in catenary systems. Consequently, the overall cost comparison between catenary and taut mooring systems is dependent on the specific configurations and materials used. While catenary systems might incur higher material costs, taut systems may balance out these costs with more expensive anchoring solutions.

5.3. Multi-Criteria Decision Analysis

The Multi-Criteria Decision Analysis (MCDA) integrates the evaluated criteria to compare the catenary and taut mooring systems systematically. The criteria and their respective weights, as introduced in chapter 3, are summarized in Table 5.7.

Table 5.7: Criteria and weights for MCDA

Criterion	Weight (%)
Dynamic behavior	50
Spatial utilization	20
Accessibility	15
Hook-up efficiency	10
Cost	5
Total	100

5.3.1. Scoring of mooring systems

Each mooring system is scored on a scale from 1 to 5 for each criterion, where 1 represents poor performance and 5 represents excellent performance. The scores are based on the analysis conducted in the previous sections, translating physical observations into quantitative assessments.

Table 5.8: MCDA scores for catenary and taut mooring systems

Criterion	Catenary Score	Taut Score
Dynamic behavior	4	2
Spatial utilization	3	4
Accessibility	3	4
Hook-up efficiency	4	2
Cost	3	2

Dynamic Behavior

- **Catenary (Score: 4):** The catenary mooring system exhibits acceptable dynamic behavior, with velocities and accelerations well below critical thresholds. Floater displacements are moderate,

up to 14 m, depending on line diameter and water depth. The system effectively manages dynamic loads with lower tensions.

- **Taut (Score: 2):** The taut mooring system has mixed performance in dynamic behavior. While it can limit floater displacements effectively with the larger line diameters, the system shows poor performance for certain configurations. Specifically, all polyester line configurations did not yield valid results, and only one nylon line diameter provided acceptable performance. The higher pretensions and sensitivity to material properties reduce its dynamic performance score. Selecting the appropriate line diameter is crucial, as the system behaves differently across tested diameters.

Spatial Utilization

- **Catenary (Score: 3):** The catenary system requires longer anchor distances and larger mooring footprints due to the horizontal extent of the mooring lines. For example, with a 150 mm chain diameter, the anchor distance can be around 135 m, reducing spatial efficiency.
- **Taut (Score: 4):** The taut system, with steeper mooring lines, requires less horizontal space, improving spatial utilization. Reduced floater displacements allow for closer spacing between floaters, enhancing the number of units that can be stored in a given area.

Accessibility

- **Catenary (Score: 3):** Larger floater displacements in the catenary system may pose challenges for vessel maneuvering and access, particularly in tight mooring fields. The minimum spacing between floaters may need to be increased to maintain safe access routes.
- **Taut (Score: 4):** Reduced displacements and a smaller mooring footprint in the taut system improve accessibility for tugs and support vessels, facilitating operations such as maintenance and hook-up.

Hook-up Efficiency

- **Catenary (Score: 4):** Lower pretensions in the catenary system simplify the hook-up process, requiring less specialized equipment and shorter installation times. For instance, tensions are within the capability of standard harbor tugs with a bollard pull of around 500 kN.
- **Taut (Score: 2):** High pretensions in the taut system complicate the hook-up procedure, necessitating specialized tensioning equipment and longer installation durations. Pretensions can reach up to 2800 kN, exceeding the capacity of typical installation vessels.

Cost

- **Catenary (Score: 3):** The use of heavier chains and longer mooring lines increases material costs. However, conventional anchors are less expensive, and installation procedures are simpler, potentially offsetting material costs.
- **Taut (Score: 2):** Material costs may be lower due to lighter mooring lines, but the requirement for specialized anchors capable of handling high vertical loads increases overall costs. Additionally, higher installation complexity can add to operational expenses.

5.3.2. Weighed scores

The weighted scores for each mooring system are calculated by multiplying the criterion weight by the system's score for that criterion. The total score is the sum of the weighted scores.

Table 5.9: Weighted MCDA scores for catenary and taut mooring systems

Criterion	Catenary weighted score	Taut weighted score
Dynamic behavior (50%)	$4 \times 50 = 200$	$2 \times 50 = 100$
Spatial utilization (20%)	$3 \times 20 = 60$	$4 \times 20 = 80$
Accessibility (15%)	$3 \times 15 = 45$	$4 \times 15 = 60$
Hook-up efficiency (10%)	$4 \times 10 = 40$	$2 \times 10 = 20$
Cost (5%)	$3 \times 5 = 15$	$2 \times 5 = 10$
Total score	360	270

The total scores indicate that the catenary mooring system outperforms the taut system based on the weighted criteria. The catenary system's advantages in dynamic behavior and hook-up efficiency outweigh its disadvantages in spatial utilization and accessibility.

5.3.3. Sensitivity analysis

To assess the robustness of the weighed scores, a sensitivity analysis is performed by varying the weights of the criteria. This analysis examines how changes in the importance assigned to each criterion affect the overall ranking of the mooring systems.

Scenario 1: Increased importance of spatial utilization If spatial utilization is deemed more critical, its weight can be increased from 20% to 30%, with corresponding adjustments to other criteria.

Table 5.10: Adjusted criteria weights for scenario 1

Criterion	Adjusted weight (%)
Dynamic behavior	45
Spatial utilization	30
Accessibility	15
Hook-up efficiency	5
Cost	5
Total	100

Recalculating the weighted scores:

Table 5.11: Weighted MCDA scores for scenario 1

Criterion	Catenary weighted score	Taut weighted score
Dynamic behavior (45%)	$4 \times 45 = 180$	$2 \times 45 = 90$
Spatial utilization (30%)	$3 \times 30 = 90$	$4 \times 30 = 120$
Accessibility (15%)	$3 \times 15 = 45$	$4 \times 15 = 60$
Hook-up efficiency (5%)	$4 \times 5 = 20$	$2 \times 5 = 10$
Cost (5%)	$3 \times 5 = 15$	$2 \times 5 = 10$
Total score	350	290

In this scenario, the total scores are closer, with the taut mooring system's improved spatial utilization making it more competitive, but the catenary system still maintains a higher total score.

Scenario 2: Increased importance of hook-up efficiency Alternatively, if hook-up efficiency is critical, its weight can be increased from 10% to 20%, with adjustments to other criteria.

Table 5.12: Adjusted criteria weights for scenario 2

Criterion	Adjusted weight (%)
Dynamic behavior	45
Spatial utilization	15
Accessibility	15
Hook-up efficiency	20
Cost	5
Total	100

Recalculating the weighted scores:

Table 5.13: Weighted MCDA Scores for Scenario 2

Criterion	Catenary weighted score	Taut weighted score
Dynamic behavior (45%)	$4 \times 45 = 180$	$2 \times 45 = 90$
Spatial utilization (15%)	$3 \times 15 = 45$	$4 \times 15 = 60$
Accessibility (15%)	$3 \times 15 = 45$	$4 \times 15 = 60$
Hook-up efficiency (20%)	$4 \times 20 = 80$	$2 \times 20 = 40$
Cost (5%)	$3 \times 5 = 15$	$2 \times 5 = 10$
Total score	365	260

In this scenario, the catenary system's advantage in dynamic behavior and hook-up efficiency further increases its total score, reinforcing its preference when installation simplicity is a priority.

5.3.4. Discussion

The sensitivity analysis demonstrates that the choice between catenary and taut mooring systems is sensitive to the weighting of the criteria based on project priorities. When spatial utilization and accessibility are highly valued, the taut mooring system becomes more competitive but still does not surpass the catenary system in total score. Conversely, when dynamic behavior and hook-up efficiency are prioritized, the catenary system is clearly favored.

The weighed scores indicate that both catenary and taut mooring systems can be viable options for the temporary wet storage of floating offshore wind foundations. The catenary system excels in dynamic behavior and hook-up efficiency, while the taut system offers improved spatial utilization and accessibility. However, the catenary system's overall performance, especially in dynamic behavior, makes it the preferable option in this analysis. The final decision should be based on specific project requirements, site conditions, and operational priorities.

6

Conclusions

This chapter presents the key findings derived from this research, addressing the main research questions, and concluding the investigation into the development of mooring systems for the temporary wet storage of floating offshore wind foundations.

6.1. Design objectives and criteria

The mooring systems for wet storage of floating offshore wind turbine foundations must ensure safe, reliable, and efficient storage. These foundations are originally designed for operational offshore conditions, not for extended storage, which places different requirements on the mooring system. The design objectives and criteria for a wet storage mooring system are identified as:

- The primary criterion for mooring system feasibility is identified as the dynamic behavior. A mooring system is considered feasible if it prevents excessive motions, including displacements, which could result in collisions between floaters, and maintains mooring line tensions below the breaking strength to avoid failure. The physical parameters used to assess this are floater motions and mooring line tensions, which must remain within defined limits under the influence of environmental forces like waves, wind, and currents.
- Spatial utilization is important in congested waters near fabrication harbors, where space is limited. This criterion assesses how many floaters can be accommodated within a given area, measured in floaters per square meter. The goal is to achieve a compact mooring arrangement that optimizes the use of available space without compromising safety. In scenarios where dynamic behavior is adequate, spatial utilization becomes a significant factor in determining the favorability of the mooring system.
- Accessibility refers to the ease of maneuvering tugs and vessels between moored floaters. This is assessed by the horizontal distance between floaters, with a minimum of 45 meters required to accommodate the typical size of harbor tugs. Adequate accessibility is essential for facilitating efficient operations such as hook-up and retrieval.
- Hook-up efficiency measures the complexity and time required to connect and disconnect the mooring lines. Systems with simpler, faster hook-up processes are preferred as they help reduce operational time and labor costs. Efficient hook-up operations are particularly important in temporary storage scenarios, where minimizing cycle times is an objective.
- The cost of the mooring system is determined by the amount of material used and the type of anchor selected. Catenary systems generally require more material due to their reliance on heavy chains, whereas taut systems use more expensive vertical load-bearing anchors.

6.2. Environmental conditions

It is found that the environmental factors most relevant to mooring system design for wet storage are waves, water depth, tidal ranges, wind, and currents. Wet storage sites are typically located in ar-

eas outside breakwaters, which present different environmental conditions compared to the offshore environments where floaters are originally designed to operate.

- Waves in nearshore areas undergo transformations like refraction, shoaling, and breaking due to shallower depths. In this study, waves were modeled using a JONSWAP spectrum based on extreme wave heights recorded at the case study location. While wave transformations occur, the JONSWAP spectrum adequately represents wave effects for mooring system design.
- Water depth and tidal ranges present challenges specific to nearshore areas. Shallow waters combined with high tidal ranges create large variations between high and low tide, significantly impacting mooring line tensions and system performance. Offshore locations, with deeper waters, experience less impact from tidal changes.
- Wind loads are less intense nearshore compared to offshore but still influence floater dynamics. In this study, wind forces were modeled consistently across all configurations, and though they varied little between cases, wind forces must be considered to ensure system integrity.
- Potentially stronger currents nearshore exert lateral forces on floaters. It is found that mooring systems must be designed to withstand these forces to maintain the floater's position and system stability.

6.3. Viable mooring concepts

As mentioned in section 6.2, the environmental conditions in nearshore wet storage locations differ from offshore sites, presenting both challenges and opportunities for mooring system design. The shallower water depths, reduced wave energy, shorter wave periods, and larger tidal ranges in these locations allow for different mooring concepts compared to those typically used offshore. For example, reduced depth makes pile fields feasible, which are impractical in deeper waters.

Based on literature and engineering knowledge, several mooring system concepts for wet storage have been identified:

- Catenary mooring, commonly used offshore, is expected to perform well in nearshore storage. It relies on heavy chains lying on the seabed, providing restoring forces through the weight of the lines. However, it may have lower spatial efficiency due to the long anchor distances required. Add-ons, such as clump weights, may improve spatial efficiency by reducing anchor distances and preventing uplift.
- Taut mooring offers better spatial utilization than catenary systems because of its smaller footprint. It uses tensioned lines rather than horizontal extensions. However, higher tensions, especially during tidal variations, may challenge system integrity. Taut mooring remains a potential option for nearshore storage based on its ability to maximize space.
- Pile field mooring is hypothesized to be a suitable solution for shallow waters, where piles can be installed as stable connection points. This concept offers reusability across multiple projects. However, its implementation may be limited by water depth and the willingness of port authorities to allocate space. Future studies and further analysis is needed to confirm its feasibility and dynamic performance.
- Shared buoy systems, such as Honeymooring, have been proposed in the literature for their potential to reduce material usage and enhance spatial utilization. This concept involves multiple floaters sharing common buoyancy points, but it may introduce risks such as cascading line failure. While promising, shared buoy systems require further investigation to assess their practicality and dynamic behavior in nearshore wet storage scenarios.

In summary, catenary and taut mooring systems are the most mature concepts, with strong literature support, making them the most viable for nearshore wet storage. Pile field mooring and shared buoy systems present potential advantages but require further research and validation before they can be applied confidently.

6.4. Modeling approach

It is found that different mooring configurations can be efficiently modeled and quantitatively verified using frequency domain (FD) analysis. This method enables rapid assessment of dynamic behavior under various environmental conditions, making it well-suited for early-stage development of wet storage solutions. The modeling process involves defining the floater, mooring lines, and the hydrodynamic properties of the system.

First-order loading, captured by FD analysis, provides a reliable estimate of the system's response to wave and environmental forces. Key parameters, such as Load Response Amplitude Operators (RAOs), added mass, stiffness, and damping coefficients, are calculated using potential flow-based diffraction tools like OrcaWave. These parameters are critical for evaluating the system's dynamic response, particularly for different water depths and floater drafts.

Verification of the model is achieved by comparing calculated RAOs and natural frequencies with reference data from the VoltturnUS 15 MW semi-submersible floater, using the same mooring system. The results closely match the reference data, confirming the model's accuracy in predicting mooring behavior.

Further modeling using OrcaFlex evaluates different mooring configurations under varying water depths and floater drafts. These configurations are analyzed within specific design constraints, such as fairlead tension, uplift limits, mooring line angles, and horizontal separation. Ensuring these parameters remain within operational limits is essential for system performance.

6.5. Quantitative comparison of mooring system designs

It is found that catenary mooring systems provide robust performance for the VoltturnUS 15 MW semi-submersible floater studied in this thesis. The catenary configuration, which relies on gravity to form its characteristic free-hanging shape with mooring lines resting on the seabed, effectively uses line weight to generate restoring forces. For all tested line diameters (LD), acceptable maximum tensions and displacements were observed. The highest tension, 1800 kN, occurred at a water depth of 45 meters (WD45) with LD300, while the highest displacement, 9.8 m, was recorded for WD35 LD300. These values were calculated using the Most Probable Maximum (MPM) for a 3-hour storm.

It is found that anchor distance and line length correlate with line diameter. As line diameter increases, weight per meter increases with the square of the diameter, improving spatial efficiency. However, this comes at the cost of higher tensions. For example, increasing the line diameter from LD100 to LD200 raises static tensions from 880 kN to 1100 kN on average, while reducing anchor distances from 247 m to 155 m. This highlights a trade-off between minimizing tension and shortening anchor distance and line length. Additionally, deeper water leads to increased tensions across all line diameters, as more of the mooring line is suspended from the fairlead, reducing seabed contact and increasing load on the fairlead.

The hook-up and retrieval procedures for catenary systems were also found to be feasible in calm waters and at low tide, provided that the procedure time is short compared to the tidal period. The required pretension in the mooring lines increases with line diameter, from 40 kN for LD50 to 500 kN for LD300. These values remain within the capacity of harbor tugs, which typically have a maximum bollard pull of 500 kN.

Taut mooring systems, in combination with the VoltturnUS floater, face challenges due to tidal variations. A tidal range of 10 meters over 40 meters water depth creates significant tension differences between high and low tide. To avoid slack lines at low tide, the system is designed to maintain tension at WD35. However, at high tide, tensions often exceed the mooring line's breaking strength. Both polyester and nylon lines showed limitations under these conditions.

For polyester, tensions exceeded the breaking strength for all diameters once deeper waters were simulated. The material was unable to balance taut line requirements at low tide without leading to excessive tension at high tide. Nylon exhibited similar issues, with maximum tensions surpassing the breaking strength in the WD45 LD100 and WD45 LD150 cases, reaching as high as 5100 kN for WD45 LD200. Only the largest diameter (LD200) remained within safe limits, making it the sole feasible option in the simulations. However, the pretension required for hook-up at low tide was 2800 kN, which would

demand specialized equipment. While this high pretension reduced displacements to 4.5 m for WD45 LD200, the complexity of the hook-up operation remains a significant challenge.

6.6. Applicability to other foundation types

The FD analysis methodology developed in this thesis provides a framework for evaluating mooring systems for various floating offshore wind foundations. Its strength lies in its ability to rapidly assess dynamic behavior across different mooring configurations and environmental conditions. This methodology has been applied to the VolturnUS 15 MW semi-submersible, and its general principles can be extended to other foundation types.

For example, catenary mooring systems can exhibit similar trade-offs between tension reduction and increased anchor distance across different floater types, although specific details will depend on the hydrodynamic properties of each foundation. Spar-buoys, which can potentially be wet-stored vertically or horizontally, face fewer space constraints in harbors due to their simpler shape, but may still require wet storage if logistically required.

In contrast, tension-leg platforms (TLPs) are less likely to be wet-stored due to their higher tension requirements and complex installation process. The significant tension involved with TLPs makes temporary storage solutions like wet storage impractical from a cost and operational perspective. Therefore, the framework developed in this thesis is more applicable to semi-submersibles and spar-buoys, where spatial utilization and dynamic behavior are critical factors for storage.

6.7. Designing mooring systems for wet storage

This research provides a framework for designing mooring systems that ensure technical feasibility and efficient spatial utilization for the temporary wet storage of floating offshore wind foundations. By identifying key design objectives such as managing dynamic behavior to prevent excessive motions and tensions, maximizing spatial use for congested nearshore areas, ensuring accessibility for vessels, improving hook-up efficiency, and considering costs, the study outlines criteria for mooring system design. Understanding environmental conditions such as waves, water depth, tidal ranges, wind, and currents at potential wet storage sites allows for customized mooring concepts. The analysis shows that catenary mooring systems perform effectively for semi-submersible platforms like the VolturnUS 15 MW, balancing tensions and displacements while optimizing spatial requirements. While taut mooring systems face challenges due to tidal variations, they may still be viable in locations with smaller tidal ranges.

Using frequency domain modeling enables efficient evaluation of different mooring configurations under various environmental conditions, facilitating rapid assessment during early design stages. The quantitative comparison of mooring designs and the applicability of the developed approach to other floating foundation types demonstrate the versatility of the framework. By integrating design criteria, environmental considerations, viable mooring concepts, modeling techniques, and quantitative analyses, this research offers a foundation for designing mooring systems suitable for wet storage.

7

Recommendations

Based on the findings and limitations identified in this study, several areas for further research are recommended to advance the understanding and design of mooring systems for temporary wet storage of floating offshore wind foundations. The recommendations are divided into two categories: exploration of alternative mooring concepts and improvements to modeling and validation.

7.1. Expanding the problem definition

Several alternative mooring concepts and broader research avenues could enhance the understanding of mooring systems for wet storage:

- Investigating alternative mooring concepts, such as Honeymooring and pile field concepts, which could offer more efficient configurations. Honeymooring is more compact and reduces material usage, though it may experience higher tensions in taut lines. Pile fields show promise in shallow waters for reusability, but their connection mechanisms require further investigation.
- Explore alternative mooring line materials and add-ons, such as clump weights and in-line load reduction devices, which may reduce tensions and improve load distribution. These options were not covered in this thesis but could enhance both catenary and taut systems.
- Expand the study to include different locations, environmental conditions, and floater types. This research focused on the VolturnUS 15 MW semi-submersible at a single location. Investigating the scalability of the framework across various floater designs and site conditions will provide a broader understanding of mooring performance. Notably, the tidal range in the Severn Estuary is one of the highest in the world, so concepts that face challenges here may work better in areas with lower tidal ranges.
- Evaluate the economic and logistical implications of wet storage for FOWTs through cost-benefit analyses. This should include assessing supply chain impacts and the feasibility of wet-storing integrated turbines, considering additional load and stability requirements.
- Integrate wet storage load cases into design standards such as DNV-ST-0119 [29] to ensure mooring systems are assessed against real-world conditions. Future design codes should account for multiple environmental forces specific to wet storage.
- Assess the environmental impact and sustainability of mooring systems, focusing on their effects on marine ecosystems and hydrodynamics. Long-term studies on material fatigue and degradation are also needed to ensure sustainable mooring solutions.

7.2. Modeling improvements

Enhancements to the modeling approach can improve the accuracy and reliability of mooring system assessments under more complex scenarios:

- While the use of FD analysis in this study was efficient in assessing various mooring options, it is recommended that the most promising configurations be further validated using TD analysis. TD analysis captures nonlinear behaviors such as slow drift and mooring line stiffness, which can influence mooring performance under real-world conditions. However, in locations where wet storage is expected, first-order loading, as captured by FD analysis, provides a reliable indication of mooring behavior. The rapid nature of FD calculations allows for the exploration of multiple design variations, making it a valuable tool for early-stage design. For safety and compliance with design codes, it is recommended that the final configuration be validated through TD analysis to ensure that the FD results are sufficient for real-world application. This step would ultimately confirm the reliability of the FD-based methodology developed in this thesis.
- Assess mooring system performance under Accidental Limit States (ALS), where anchor lines break. Testing these load cases is critical for verifying system stability and avoiding cascading failures under extreme conditions.
- Refine drag coefficients for wind and current load estimations using more detailed methods such as CFD simulations or experimental data. The current analysis used an empirical drag coefficient of 0.5, based on Reynolds numbers higher than 10^4 , but the complex geometry of the floater and environmental conditions suggest that more precise values would enhance the accuracy of the mooring system performance predictions, particularly under extreme conditions.

References

- [1] Mohammad Saud Afzal and Lalit Kumar. "Propagation of waves over a rugged topography". In: *Journal of Ocean Engineering and Science* 7.1 (2022), pp. 14–28. ISSN: 2468-0133. DOI: <https://doi.org/10.1016/j.joes.2021.04.004>. URL: <https://www.sciencedirect.com/science/article/pii/S2468013321000395>.
- [2] Adem Akpınar et al. "Evaluation of the numerical wave model (SWAN) for wave simulation in the Black Sea". In: *Continental Shelf Research* 50-51 (2012), pp. 80–99. ISSN: 0278-4343. DOI: <https://doi.org/10.1016/j.csr.2012.09.012>. URL: <https://www.sciencedirect.com/science/article/pii/S0278434312002671>.
- [3] ALE. *Transverse Load-Out for 1st Semi-Sub OWF*. Accessed: 2024-06-21. 2019. URL: <https://www.heavyliftnews.com/transverse-load-out-for-1st-semi-sub-owf/>.
- [4] Christopher Allen et al. "Definition of the UMaine VoltturnUS-S Reference Platform Developed for the IEA Wind 15-Megawatt Offshore Reference Wind Turbine". In: (July 2020). DOI: 10.2172/1660012. URL: <https://www.osti.gov/biblio/1660012>.
- [5] Elsayed Aziz, Sven Esche, and C. Chassapis. "Online Wind Tunnel Laboratory". In: (June 2008). DOI: 10.18260/1-2--3402.
- [6] Magnus Thorsen Bach-Gansmo et al. "Parametric Study of a Taut Compliant Mooring System for a FOWT Compared to a Catenary Mooring". In: *Journal of Marine Science and Engineering* 8.6 (2020). ISSN: 2077-1312. DOI: 10.3390/jmse8060431. URL: <https://www.mdpi.com/2077-1312/8/6/431>.
- [7] Balmoral Offshore. *In-Line Mooring Buoyancy*. Accessed: 2024-07-07. 2024. URL: <https://www.balmoraloffshore.com/solutions/offshore-wind/floating-wind-turbine-solutions/in-line-mooring-buoyancy>.
- [8] Nigel Barltrop. *Floating structures: a guide for design and analysis*. June 1998. ISBN: 1870553357.
- [9] Srikanth Bashetty and Selahattin Ozcelik. "Review on Dynamics of Offshore Floating Wind Turbine Platforms". In: *Energies* 14.19 (2021). ISSN: 1996-1073. DOI: 10.3390/en14196026. URL: <https://www.mdpi.com/1996-1073/14/19/6026>.
- [10] I. Bayati, S. Gueydon, and M. Belloli. "Study of the Effect of Water Depth on Potential Flow Solution of the OC4 Semisubmersible Floating Offshore Wind Turbine". In: *Energy Procedia* 80 (Jan. 2015), pp. 168–176. ISSN: 1876-6102. DOI: 10.1016/J.EGYPRO.2015.11.419.
- [11] Guido Benassai et al. "Optimization of Mooring Systems for Floating Offshore Wind Turbines". In: *Coastal Engineering Journal* 57.04 (2015), p. 1550021. DOI: 10.1142/S0578563415500217. eprint: <https://doi.org/10.1142/S0578563415500217>. URL: <https://doi.org/10.1142/S0578563415500217>.
- [12] Guido Benassai et al. "Ultimate and accidental limit state design for mooring systems of floating offshore wind turbines". In: *Ocean Engineering* 92 (Sept. 2014), pp. 64–74. DOI: 10.1016/j.oceaneng.2014.09.036.
- [13] Chris Binnie. "Tidal energy from the Severn estuary, UK". In: *Proceedings of the Institution of Civil Engineers - Energy* 169.1 (2016), pp. 3–17. DOI: 10.1680/jener.14.00025. eprint: <https://doi.org/10.1680/jener.14.00025>. URL: <https://doi.org/10.1680/jener.14.00025>.
- [14] M. Böhm et al. "Optimization-based calibration of hydrodynamic drag coefficients for a semisubmersible platform using experimental data of an irregular sea state". In: *Journal of Physics: Conference Series* 1669 (2020), p. 012023. DOI: 10.1088/1742-6596/1669/1/012023. URL: [https://iopscience-iop-org.tudelft.idm.oclc.org/article/10.1088/1742-6596/1669/1/012023](https://iopscience.iop.org/tudelft.idm.oclc.org/article/10.1088/1742-6596/1669/1/012023).

- [15] Antonio Bonaduce et al. "Wave Climate Change in the North Sea and Baltic Sea". In: *Journal of Marine Science and Engineering* 7.6 (2019). ISSN: 2077-1312. DOI: 10.3390/jmse7060166. URL: <https://www.mdpi.com/2077-1312/7/6/166>.
- [16] L.M.M. Bos and Benjamin Sanderse. "Uncertainty quantification for wind energy applications - Literature review". In: *Technical Report SC-170* (2017).
- [17] Boskalis. *Bollard Pull Data for Anchor Handling Tugs*. Accessed: 2024-06-21. 2024. URL: <https://boskalis.com/about-us/fleet-and-equipment/offshore-vessels/anchor-handling-tugs>.
- [18] Matthias Brommundt et al. "Mooring System Optimization for Floating Wind Turbines using Frequency Domain Analysis". In: *Energy Procedia* 24 (2012). Selected papers from Deep Sea Offshore Wind R&D Conference, Trondheim, Norway, 19-20 January 2012, pp. 289–296. ISSN: 1876-6102. DOI: <https://doi.org/10.1016/j.egypro.2012.06.111>. URL: <https://www.sciencedirect.com/science/article/pii/S1876610212011514>.
- [19] BVG Associates. *Guide to a floating offshore wind farm*. Tech. rep. 2023.
- [20] Laura Castro-Santos and Vicente Diaz-Casas. *Floating offshore wind farms*. Springer, 2016.
- [21] Rahul Chitteth Ramachandran et al. "Floating wind turbines: marine operations challenges and opportunities". In: *Wind Energy Science* 7.2 (2022), pp. 903–924.
- [22] Alan Crowle. "Floating offshore wind turbines - installation methods". In: *International Journal of Research -GRANTHAALAYAH* 12.2 (Feb. 2024), pp. 1–18. DOI: 10.29121/granthaalayah.v12.i2.2024.5459. URL: <https://www.granthaalayahpublication.org/journals/granthaalayah/article/view/5459>.
- [23] Brian D. Diaz et al. "Multiline anchors for floating offshore wind towers". In: (July 2016), pp. 1–9. DOI: 10.1109/OCEANS.2016.7761374.
- [24] DNV-OS-E302. *Offshore mooring chain*. Standard. Oslo, NO: DNV, July 2022.
- [25] DNV-RP-C205. *Environmental conditions and environmental loads*. Standard. Oslo, NO: DNV, Sept. 2021.
- [26] DNV-RP-E301. *Design and installation of fluke anchors*. Standard. Oslo, NO: DNV, Oct. 2021.
- [27] DNV-RP-E302. *Design and installation of plate anchors in clay*. Standard. Oslo, NO: DNV, Oct. 2021.
- [28] DNV-RP-E303. *Geotechnical design and installation of suction anchors in clay*. Standard. Oslo, NO: DNV, Oct. 2021.
- [29] DNV-ST-0119. *Floating wind turbine structures*. Standard. Oslo, NO: DNV, June 2021.
- [30] DNV-ST-N001. *Marine operations and marine warranty*. Standard. Oslo, NO: DNV, Sept. 2021.
- [31] Dublin Offshore. *Load Reduction Device Overview*. Accessed: 2024-07-07. 2024. URL: https://www.dublinoffshore.ie/media/pages/technology/55ca8e6c33-1719217061/dublin-offshore_lrd-overview.pdf.
- [32] Mads Røge Eldrup and Thomas Lykke Andersen. "Numerical Study on Regular Wave Shoaling, De-Shoaling and Decomposition of Free/Bound Waves on Gentle and Steep Foreshores". In: *Journal of Marine Science and Engineering* 8.5 (2020). ISSN: 2077-1312. DOI: 10.3390/jmse8050334. URL: <https://www.mdpi.com/2077-1312/8/5/334>.
- [33] NS-EN-1537:2013. *Execution of special geotechnical works — Ground anchors*. Standard. Oslo, No: Standard Norge, 2013.
- [34] Engineers Edge. *Viscosity of Air, Dynamic and Kinematic*. https://www.engineersedge.com/physics/viscosity_of_air_dynamic_and_kinematic_14483.htm. Accessed: 2024-08-02.
- [35] Equinor. *Hywind Tampen: the world's first renewable power for offshore oil and gas*. Accessed 10 May 2024. 2024. URL: <https://www.equinor.com/energy/hywind-tampen>.
- [36] Erik Falkenberg, Vidar Åhjem, and Limin Yang. "Best Practice for Analysis of Polyester Rope Mooring Systems". In: OTC Offshore Technology Conference Day 3 Wed, May 03, 2017 (May 2017), D031S034R006. DOI: 10.4043/27761-MS.

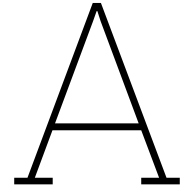
- [37] O.M. Faltinsen. *Sea Loads on Ships and Offshore Structures*. Cambridge University Press, 1990.
- [38] Farinia Group. *Windfloat Clump Weights*. Accessed: 2024-07-07. 2024. URL: <https://www.farinia.com/news/windfloat-clump-weights>.
- [39] Casey Fontana. "A multiline anchor concept for floating offshore wind turbines". In: (2019). DOI: <https://doi.org/10.7275/13483708>.
- [40] Casey Fontana et al. "Efficient Multiline Anchor Systems for Floating Offshore Wind Turbines". In: (June 2016). DOI: 10.1115/OMAE2016-54476.
- [41] J Fredsøe. *Hydrodynamics*. Den private Ingeniørfond, 2013.
- [42] Evan Gaertner et al. *IEA wind TCP task 37: definition of the IEA 15-megawatt offshore reference wind turbine*. Tech. rep. National Renewable Energy Lab.(NREL), Golden, CO (United States), 2020.
- [43] Alberto Ghigo et al. "Mooring System Design and Analysis for a Floating Offshore Wind Turbine in Pantelleria". In: Turbo Expo: Power for Land, Sea, and Air Volume 11: Wind Energy (June 2022), V011T38A021. DOI: 10.1115/GT2022-83219. eprint: <https://asmedigitalcollection.asme.org/GT/proceedings-pdf/GT2022/86137/V011T38A021/6937401/v011t38a021-gt2022-83219.pdf>. URL: <https://doi.org/10.1115/GT2022-83219>.
- [44] Global Wind Energy Council. "Global offshore wind report 2024". In: *GWEC: Brussels, Belgium 19* (2024), pp. 10–12.
- [45] Chris Golightly. "Anchoring & Mooring for Floating Offshore Wind Brussels 8th November 2017". In: Nov. 2017. URL: https://www.researchgate.net/publication/321011241_Anchoring_Mooring_for_Floating_Offshore_Wind_Brussels_8th_November_2017.
- [46] Sara Ferreño González and Vicente Diaz-Casas. "Present and Future of Floating Offshore Wind". In: *Floating Offshore Wind Farms*. Ed. by Laura Castro-Santos and Vicente Diaz-Casas. Cham: Springer International Publishing, 2016, pp. 1–22. ISBN: 978-3-319-27972-5. DOI: 10.1007/978-3-319-27972-5_1. URL: https://doi.org/10.1007/978-3-319-27972-5_1.
- [47] Michael R. Gourlay. "Wave Shoaling and Refraction". In: *Encyclopedia of Modern Coral Reefs: Structure, Form and Process*. Ed. by David Hopley. Dordrecht: Springer Netherlands, 2011, pp. 1149–1154. ISBN: 978-90-481-2639-2. DOI: 10.1007/978-90-481-2639-2_164. URL: https://doi.org/10.1007/978-90-481-2639-2_164.
- [48] Matthew Hall and Andrew Goupee. "Validation of a lumped-mass mooring line model with DeepCwind semisubmersible model test data". In: *Ocean Engineering* 104 (2015), pp. 590–603. ISSN: 0029-8018. DOI: <https://doi.org/10.1016/j.oceaneng.2015.05.035>. URL: <https://www.sciencedirect.com/science/article/pii/S0029801815002279>.
- [49] Finn-Christian Wickmann Hanssen, Niklas Norman, and Per Sørum. *A quick guide to Honey-mooring*. Tech. rep. Semar, 2018.
- [50] Heerema Engineering Solutions. *Logistical Process of Installing a Floating Offshore Wind Turbine*. Image courtesy of Heerema Engineering Solutions. 2024.
- [51] Heerema Marine Contractors. *Forces in catenary mooring line*. Accessed via internal intranet. 2024.
- [52] Hans Hersbach et al. "The ERA5 global reanalysis". In: *Quarterly Journal of the Royal Meteorological Society* 146.730 (2020), pp. 1999–2049. DOI: <https://doi.org/10.1002/qj.3803>. eprint: <https://rmets.onlinelibrary.wiley.com/doi/pdf/10.1002/qj.3803>. URL: <https://rmets.onlinelibrary.wiley.com/doi/abs/10.1002/qj.3803>.
- [53] Rob Holman. "Nearshore processes". In: *Reviews of Geophysics* 33.S2 (1995), pp. 1237–1247.
- [54] Sunghun Hong et al. "Floating offshore wind farm installation, challenges and opportunities: A comprehensive survey". In: *Ocean Engineering* 304 (2024), p. 117793. ISSN: 0029-8018. DOI: <https://doi.org/10.1016/j.oceaneng.2024.117793>. URL: <https://www.sciencedirect.com/science/article/pii/S0029801824011314>.
- [55] ABSG Consulting Inc. "Floating Offshore Wind Turbine Development Assessment". In: *Final Report and Technical Summary to BOEM-Office of Renewable Energy Programs* (2021).

- [56] Oleksii Ishchuk. *Problems of Floating Offshore Wind Farms Verification in Industry*. <https://www.linkedin.com/pulse/problems-floating-offshore-wind-farms-verification-industry-ishchuk/>. Accessed: 2024-09-25. 2023.
- [57] Takeshi Ishihara and Yuliang Liu. "Dynamic Response Analysis of a Semi-Submersible Floating Wind Turbine in Combined Wave and Current Conditions Using Advanced Hydrodynamic Models". In: *Energies* 13.21 (2020). ISSN: 1996-1073. DOI: 10.3390/en13215820. URL: <https://www.mdpi.com/1996-1073/13/21/5820>.
- [58] R. James and M. C. Ros. *Floating offshore wind: Market and technology review*. Carbon Trust 2015, 1, 439. 2015. URL: <https://www.carbontrust.com/our-work-and-impact/guides-reports-and-tools/floating-offshore-wind-market-technology-review>.
- [59] Chun-yan Ji, Zhi-Ming Yuan, and Ming-lu Chen. "Study on a new mooring system integrating catenary with taut mooring". In: *China Ocean Engineering* 25 (Sept. 2011), pp. 427–440. DOI: 10.1007/s13344-011-0035-4.
- [60] Zhiyu Jiang. "Installation of offshore wind turbines: A technical review". In: *Renewable and Sustainable Energy Reviews* 139 (2021), p. 110576. ISSN: 1364-0321. DOI: <https://doi.org/10.1016/j.rser.2020.110576>. URL: <https://www.sciencedirect.com/science/article/pii/S1364032120308601>.
- [61] Jason Mark Jonkman. *Dynamics modeling and loads analysis of an offshore floating wind turbine*. University of Colorado at Boulder, 2007.
- [62] M. Karimi, B. Buckham, and C. Crawford. "A fully coupled frequency domain model for floating offshore wind turbines". In: *Journal of Ocean Engineering and Marine Energy* (2019), pp. 1–24. DOI: 10.1007/S40722-019-00134-X.
- [63] Mareike Leimeister, A Kolios, and Maurizio Collu. "Critical review of floating support structures for offshore wind farm deployment". In: *Journal of Physics: Conference Series* 1104 (Oct. 2018), p. 012007. DOI: 10.1088/1742-6596/1104/1/012007.
- [64] Guodong Liang et al. "Numerical analysis of a tethered buoy mooring system for a prototype floating wind farm". In: *Wind Energy* (Feb. 2024). DOI: 10.1002/we.2898.
- [65] Estelle Limon. *The start of the race for floating wind in the Celtic Sea*. Aug. 2022. URL: <https://www.regen.co.uk/the-start-of-the-race-for-floating-wind-in-the-celtic-sea/>.
- [66] Yichao Liu et al. "Developments in semi-submersible floating foundations supporting wind turbines: A comprehensive review". In: *Renewable and Sustainable Energy Reviews* 60 (2016), pp. 433–449. ISSN: 1364-0321. DOI: <https://doi.org/10.1016/j.rser.2016.01.109>. URL: <https://www.sciencedirect.com/science/article/pii/S1364032116001398>.
- [67] Orcina Ltd. *OrcaWave Documentation*. Accessed: 2024-07-24. 2024. URL: <https://www.orcina.com/webhelp/OrcaWave/>.
- [68] Kai-Tung Ma et al. *Mooring System Engineering for Offshore Structures*. Ed. by Kai-Tung Ma et al. Gulf Professional Publishing, 2019. ISBN: 978-0-12-818551-3. DOI: <https://doi.org/10.1016/B978-0-12-818551-3.00002-8>. URL: <https://www.sciencedirect.com/science/article/pii/B9780128185513000028>.
- [69] Gerhard Masselink. *Waves*. Ed. by Charles W. Finkl and Christopher Makowski. Cham: Springer International Publishing, 2018, pp. 1–11. ISBN: 978-3-319-48657-4. DOI: 10.1007/978-3-319-48657-4_350-2. URL: https://doi.org/10.1007/978-3-319-48657-4_350-2.
- [70] J.R. Morison, J.W. Johnson, and S.A. Schaaf. "The Force Exerted by Surface Waves on Piles". In: *Journal of Petroleum Technology* 2.05 (May 1950), pp. 149–154. ISSN: 0149-2136. DOI: 10.2118/950149-G. eprint: <https://onepetro.org/JPT/article-pdf/2/05/149/2238818/spe-950149-g.pdf>. URL: <https://doi.org/10.2118/950149-G>.
- [71] Walter Musial et al. *Offshore Wind Market Report: 2023 Edition*. Tech. rep. US Department of Energy, 2023.
- [72] J.N. Newman. "Efficient hydrodynamic analysis of very large floating structures". In: *Marine Structures* 18.2 (2005). Very Large Floating Structures, pp. 169–180. ISSN: 0951-8339. DOI: <https://doi.org/10.1016/j.marstruc.2005.07.003>. URL: <https://www.sciencedirect.com/science/article/pii/S0951833905000432>.

- [73] John Nicholas Newman. "The drift force and moment on ships in waves". In: *Journal of ship research* 11.01 (1967), pp. 51–60.
- [74] Daniel Nilsson and Anders Westin. "Floating Wind Power in Norway: Analysis of Future Opportunities and Challenges". Master's Thesis. Lund, Sweden: Division of Industrial Electrical Engineering and Automation, Faculty of Engineering, Lund University, 2014. URL: https://www.iea.lth.se/publications/MS-Theses/Full%20document/5331_full_document_Floating%20wind%20power%20in%20Norway.pdf.
- [75] Norwegian Petroleum Directorate. *Regulations relating to loadbearing structures in the petroleum activities*. NPD, 1995. Norwegian Petroleum Directorate, 1995.
- [76] Oil Companies International Marine Forum. *Prediction of Wind and Current Loads on VLCCs*. 2nd. London: Witherby & Co., 1994.
- [77] Orcina. *K03 15MW semi-sub FOWT*. Jan. 2024. URL: <https://www.orcina.com/wp-content/uploads/examples/k/k03/K03%2015MW%20semi-sub%20FOWT.pdf>.
- [78] Orcina. *Line Breaking Strengths for mooring lines*. Values generated using the Orcina line type wizard. 2024.
- [79] Orcina. *OrcaFlex Documentation: Frequency Domain Solution*. <https://www.orcina.com/webhelp/OrcaFlex/Content/html/Dynamicanalysis,Frequencydomainsolution.htm>. 2024. URL: <https://www.orcina.com/webhelp/OrcaFlex/Content/html/Dynamicanalysis,Frequencydomainsolution.htm> (visited on 07/23/2024).
- [80] Orcina. *OrcaFlex Documentation: Line Theory Overview*. 2024. URL: <https://www.orcina.com/webhelp/OrcaFlex/Content/html/Linetheory,Overview.htm> (visited on 07/22/2024).
- [81] Hong-Duc Pham et al. "Dynamic modeling of nylon mooring lines for a floating wind turbine". In: *Applied Ocean Research* 87 (2019), pp. 1–8. ISSN: 0141-1187. DOI: <https://doi.org/10.1016/j.apor.2019.03.013>. URL: <https://www.sciencedirect.com/science/article/pii/S0141118718307296>.
- [82] JA Pinkster. "Low-frequency phenomena associated with vessels moored at sea". In: *Society of Petroleum Engineers Journal* 15.06 (1975), pp. 487–494.
- [83] Principle Power. *The WindFloat Advantage: Fabrication*. <https://www.principlepower.com/windfloat/advantage/fabrication>. Accessed: 2024-06-21. 2024.
- [84] Amir R. Nejad, Erin Bachynski-Polić, and Torgeir Moan. "Effect of Axial Acceleration on Drive-train Responses in a Spar-Type Floating Wind Turbine". In: *Journal of Offshore Mechanics and Arctic Engineering* 141 (Nov. 2018). DOI: 10.1115/1.4041996.
- [85] National Network of Regional Coastal Monitoring Programmes of England. *Coastal Wave Network Annual Report*. Annual Report. NNRCMP, May 2023.
- [86] I. Rivera-Arreba et al. "Modeling of a Semisubmersible Floating Wind Platform in Severe Waves". In: *International Conference on Offshore Mechanics and Arctic Engineering Volume 9: Offshore Geotechnics; Honoring Symposium for Professor Bernard Molin on Marine and Offshore Hydrodynamics* (June 2018), V009T13A002. DOI: 10.1115/0MAE2018-77680. eprint: <https://asmedigitalcollection.asme.org/OMAE/proceedings-pdf/OMAE2018/51302/V009T13A002/2536554/v009t13a002-omae2018-77680.pdf>. URL: <https://doi.org/10.1115/0MAE2018-77680>.
- [87] Line Roald et al. "The Effect of Second-Order Hydrodynamics on Floating Offshore Wind Turbines". In: *Energy Procedia* 35 (Dec. 2013). DOI: 10.1016/j.egypro.2013.07.178.
- [88] A N Robertson et al. "OC6 Phase I: Investigating the underprediction of low-frequency hydrodynamic loads and responses of a floating wind turbine". In: *Journal of Physics: Conference Series* 1618.3 (July 2020), p. 032033. DOI: 10.1088/1742-6596/1618/3/032033. URL: <https://dx.doi.org/10.1088/1742-6596/1618/3/032033>.
- [89] Patryk Sapięga, Tamara Zalewska, and Piotr Struzik. "Application of SWAN model for wave forecasting in the southern Baltic Sea supplemented with measurement and satellite data". In: *Environmental Modelling & Software* 163 (2023), p. 105624. ISSN: 1364-8152. DOI: <https://doi.org/10.1016/j.envsoft.2023.105624>. URL: <https://www.sciencedirect.com/science/article/pii/S1364815223000105>.

- [90] Michael J. Scott and Erik K. Antonsson. "Compensation and Weights for Trade-offs in Engineering Design: Beyond the Weighted Sum". In: *Journal of Mechanical Design* 127.6 (Jan. 2005), pp. 1045–1055. DOI: 10.1115/1.1909204.
- [91] Severn Estuary Partnership. *Oceanography of the Severn Estuary*. Accessed: 2024-06-21. 2024. URL: <https://severnestuarypartnership.org.uk/the-estuary/environmental-quality/oceanography/>.
- [92] W. Sheng and Hui Li. "A Method for Energy and Resource Assessment of Waves in Finite Water Depths". In: *Energies* 10 (Apr. 2017), p. 460. DOI: 10.3390/en10040460.
- [93] Matt Shields et al. *The Impacts of Developing a Port Network for Floating Offshore Wind Energy on the West Coast of the United States*. Tech. rep. National Renewable Energy Laboratory (NREL), Golden, CO (United States), 2023.
- [94] Alexandre N. Simos et al. "Slow-drift of a floating wind turbine: An assessment of frequency-domain methods based on model tests". In: *Renewable Energy* 116 (2018), pp. 133–154. ISSN: 0960-1481. DOI: <https://doi.org/10.1016/j.renene.2017.09.059>. URL: <https://www.sciencedirect.com/science/article/pii/S0960148117309229>.
- [95] TFI Marine. *Load reduction spring*. Accessed: 2024-07-07. 2024. URL: <https://www.tfimarine.com/>.
- [96] SW Thakare, Aparna H Chavan, and AI Dhattrak. "Performance of suction pile anchor for floating offshore structures". In: *Construction in Geotechnical Engineering: Proceedings of IGC 2018*. Springer. 2020, pp. 271–284.
- [97] T. Tran and Dong-Hyun Kim. "The coupled dynamic response computation for a semi-submersible platform of floating offshore wind turbine". In: *Journal of Wind Engineering and Industrial Aerodynamics* 147 (2015), pp. 104–119. DOI: 10.1016/J.JWEIA.2015.09.016.
- [98] Vryhof Anchors. "Anchor Manual 2015: The Guide to Anchoring". In: *AC Capelle a/d Yssel* (2015).
- [99] Kunpeng Wang et al. "Frequency domain approach for the coupled analysis of floating wind turbine system". In: *Ships and Offshore Structures* 12.6 (2017), pp. 767–774.
- [100] Johan Wichers. *Guide to single point moorings*. WMooring, 2013.
- [101] Matijs Wiegel. "Mapping port operability indicators across the world: Screening the suitability of port locations related to metocean conditions". In: (2020). URL: <https://repository.tudelft.nl/record/uuid:bae26c8b-5800-45d8-8aec-7dac18658653>.
- [102] Wind Europe. *Wind Energy in Europe*. Apr. 2022. URL: <https://windeurope.org/intelligence-platform/product/wind-energy-in-europe-2023-statistics-and-the-outlook-for-2024-2030/>.
- [103] Windplus. *World's first semi-submersible floating offshore wind farm*. Accessed 16 May 2024. 2024. URL: <https://www.windfloat-atlantic.com/>.
- [104] Yongyan Wu et al. "A New Mooring System for Floating Offshore Wind Turbines: Theory, Design and Industrialization". In: OTC Offshore Technology Conference Day 1 Mon, May 01, 2023 (May 2023), D011S012R004. DOI: 10.4043/32646-MS. eprint: <https://onepetro.org/OTCONF/proceedings-pdf/230TC/1-230TC/D011S012R004/3104879/otc-32646-ms.pdf>. URL: <https://doi.org/10.4043/32646-MS>.
- [105] Kun Xu, Zhen Gao, and Torgeir Moan. "Effect of hydrodynamic load modelling on the response of floating wind turbines and its mooring system in small water depths". In: *Journal of Physics: Conference Series*. Vol. 1104. 1. IOP Publishing. 2018, p. 012006.
- [106] Kun Xu et al. "Design and comparative analysis of alternative mooring systems for floating wind turbines in shallow water with emphasis on ultimate limit state design". In: *Ocean Engineering* 219 (2021), p. 108377. ISSN: 0029-8018. DOI: <https://doi.org/10.1016/j.oceaneng.2020.108377>. URL: <https://www.sciencedirect.com/science/article/pii/S0029801820312841>.
- [107] Ray-Yeng Yang et al. "Dynamic Response of an Offshore Floating Wind Turbine at Accidental Limit States—Mooring Failure Event". In: *Applied Sciences* 12 (Jan. 2022), p. 1525. DOI: 10.3390/app12031525.

- [108] Frederik Zahle et al. *Definition of the IEA Wind 22-Megawatt Offshore Reference Wind Turbine: IEA Wind TCP Task 55*. American English. Tech. rep. 2024. DOI: 10.11581/DTU.00000317.
- [109] Lixian Zhang et al. "Second-order hydrodynamic effects on the response of three semisubmersible floating offshore wind turbines". In: *Ocean Engineering* 207 (2020), p. 107371. ISSN: 0029-8018. DOI: <https://doi.org/10.1016/j.oceaneng.2020.107371>. URL: <https://www.sciencedirect.com/science/article/pii/S0029801820304029>.
- [110] Zhixin Zhao et al. "Effects of second-order hydrodynamics on an ultra-large semi-submersible floating offshore wind turbine". In: *Structures* 28 (2020), pp. 2260–2275. ISSN: 2352-0124. DOI: <https://doi.org/10.1016/j.istruc.2020.10.058>. URL: <https://www.sciencedirect.com/science/article/pii/S2352012420306135>.



Anchor distance and line lengths algorithm

This section explains the algorithm for calculating the shortest valid anchor distance and line length. It ensures compliance with constraints and computational efficiency.

The process starts with `catenary.py` or `taut.py`, which define the mooring concept, water depths, and line diameters. They specify a `base_waterdepth` for determining the shortest anchor distance and line length, applied uniformly across all depths of the tidal range. These nearly identical scripts are the entry point for the algorithm. They set parameters like mooring concept (catenary or taut), water depths, and line diameters, and establish initial conditions with the `base_waterdepth`.

These scripts call two primary functions: `initial_creator.py` and `analyse_catenary_and_taut.py`.

A.1. File creation

The `initial_creator.py` script is responsible for generating the OrcaFlex files necessary for the dynamic analysis. It does so by first creating a file for a single floater using `single_floater.py`. This floater is configured with its respective mooring lines, floater type, draft, and environmental conditions, as specified in the `Vessel_types.dat` input file.

Once the single floater file is prepared, `check_Uplift.py` is called to evaluate various combinations of anchor distances and line lengths. The goal is to find the smallest combination that satisfies all constraints (as outlined in Section 4.3.3). This is achieved through a nested loop structure, where the outer loop iterates over anchor distances and the inner loop over line lengths.

To optimize computational efficiency, the algorithm begins with a coarse search using a step size of 50 meters. Upon finding an initial valid combination, the algorithm refines the search using a finer step size of 2 meters.

A.1.1. Constraint handling

Within `check_Uplift.py`, several helper functions are employed:

- `calculate_uplift_and_tensions.py`: Calculates the uplift forces, declinations, and tensions in the mooring lines.
- `check_anchor_angles.py`, `check_angle_range.py`, `check_fairlead_angles.py`, `check_relative_fairlead_anchor.py`: These functions verify that the mooring system adheres to the constraints regarding angles and relative positions.

After determining the appropriate anchor distance and line length for the `base_waterdepth`, these values are applied to files corresponding to other water depths.

A.1.2. Expanding to multiple floaters

The next step in `initial_creator.py` involves expanding the model from a single floater to a configuration with multiple floaters. This is accomplished by first calling `hexagon_definer.py`, which generates a hexagonal pattern of nodes representing the positions of floaters and anchors. This pattern is based on the shortest anchor distance identified earlier.

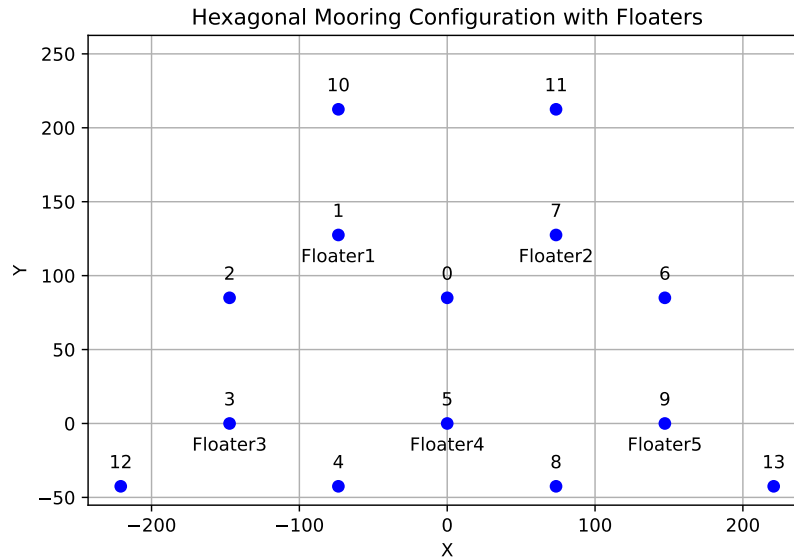


Figure A.1: Node locations for an anchor distance of 85 m

Figure A.1 shows an example hexagonal mooring configuration, which is created based on the anchor distance. The layout utilizes nodal points to create an efficient arrangement for the floaters while maintaining compliance with design constraints.

The `create_layout.py` script is then used to create files for dynamic analysis, with and without environmental conditions. Within this function, `clone_and_reposition.py` is employed to clone the floater and position it according to the node locations.

A.2. Post-processing

Finally, after the layout files are prepared, `catenary.py` or `taut.py` calls `analyse_catenary_and_taut.py` for post-processing. This script generates Excel files containing all the results and creates the plots used for the analysis presented in this report.

The anchor distance and line length algorithm ensures the mooring system meets constraints efficiently. Coarse-to-fine search methods, constraint application, and expanding from single to multiple floaters are used to generate the analysed results.

B

Load RAOs

This appendix presents the Load Response Amplitude Operators (RAOs) for the surge, heave, and pitch load RAOs under various categories. These RAOs are used to assess the behavior of the modeled system under different loading conditions. The categories analyzed in this appendix are as follows:

- Comparison with NREL reference data
- Effect of draft
- Effect of moored draft
- Comparison of water depths
- Effect of tidal range

Each figure below shows the load RAO for surge, heave, or pitch under these specific categories, offering insights into how the system responds to changes in these parameters.

B.1. Comparison with available literature

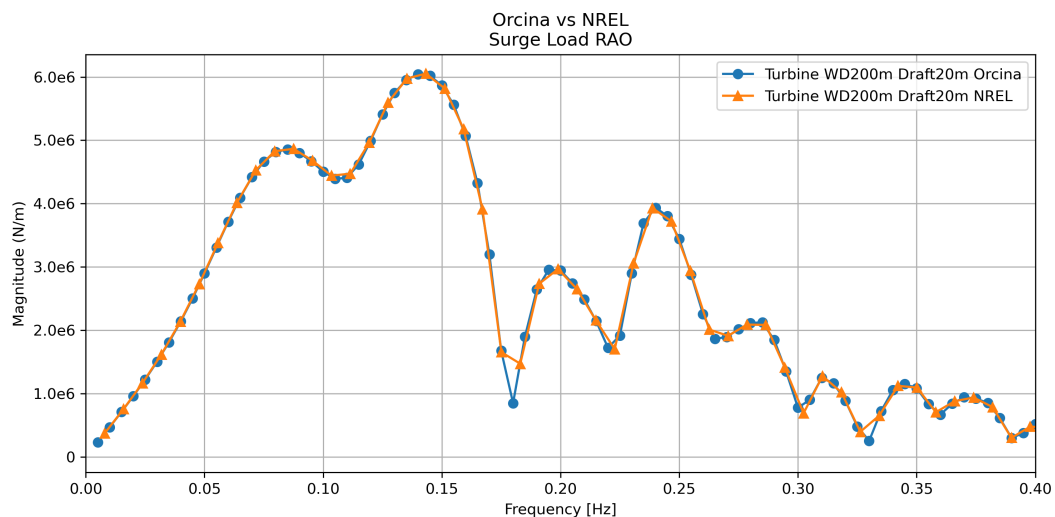


Figure B.1: Comparison of NREL and Orcina results for surge load RAO

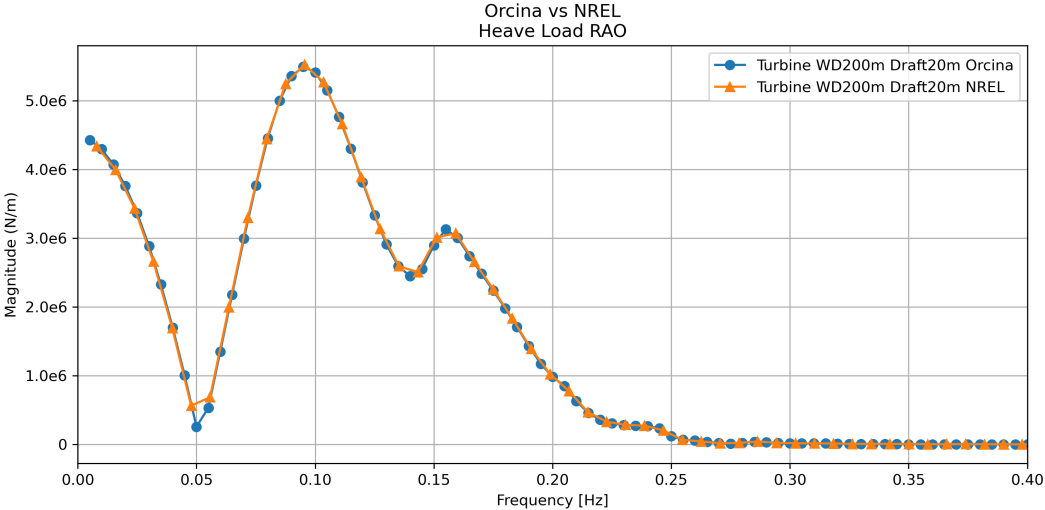


Figure B.2: Comparison of NREL and Orcina results for heave load RAO

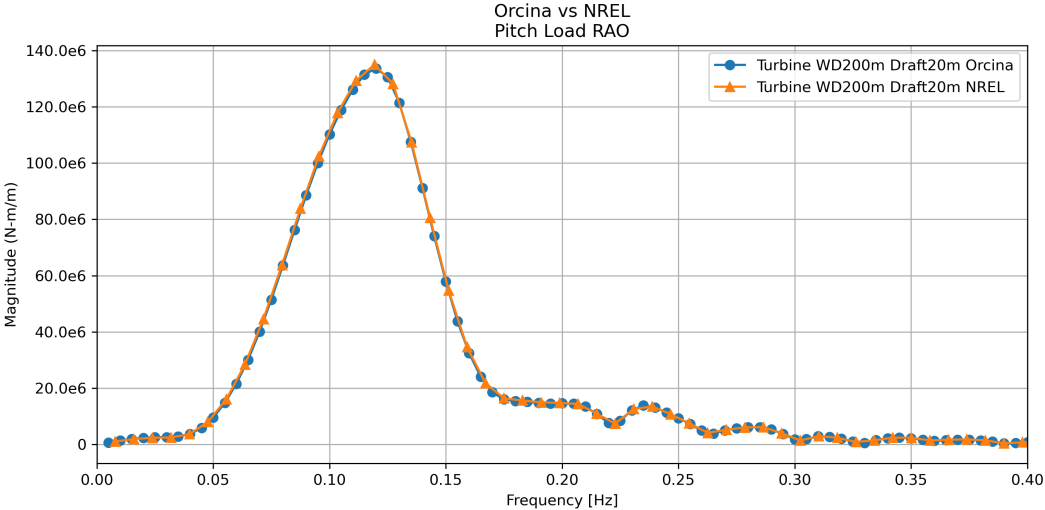


Figure B.3: Comparison of NREL and Orcina results for pitch load RAO

B.2. Effect of draft

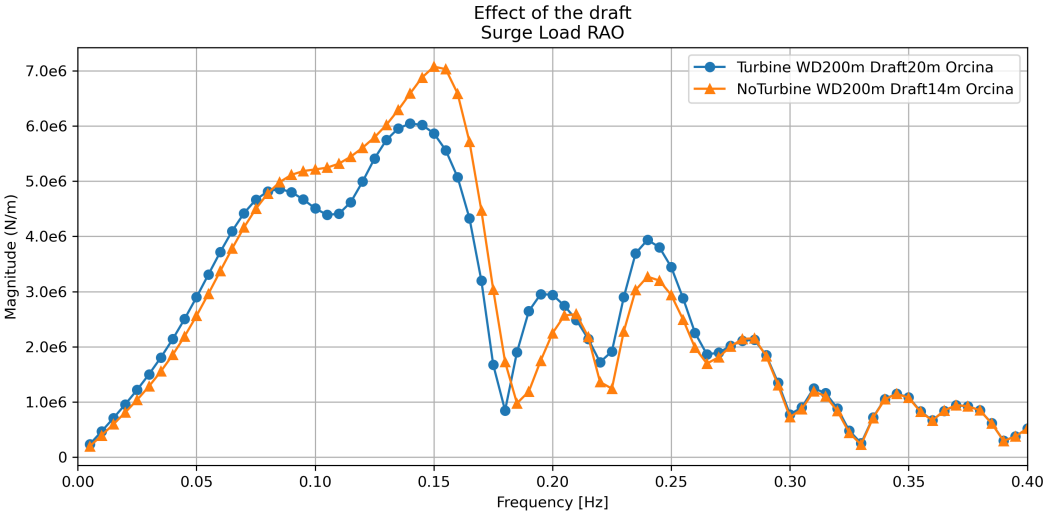


Figure B.4: Effect of draft on surge load RAO

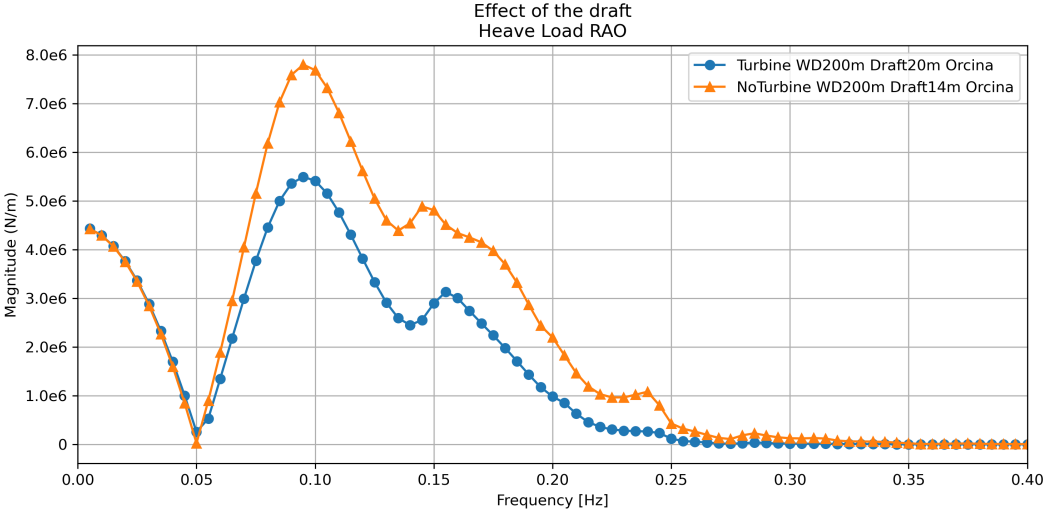


Figure B.5: Effect of draft on heave load RAO

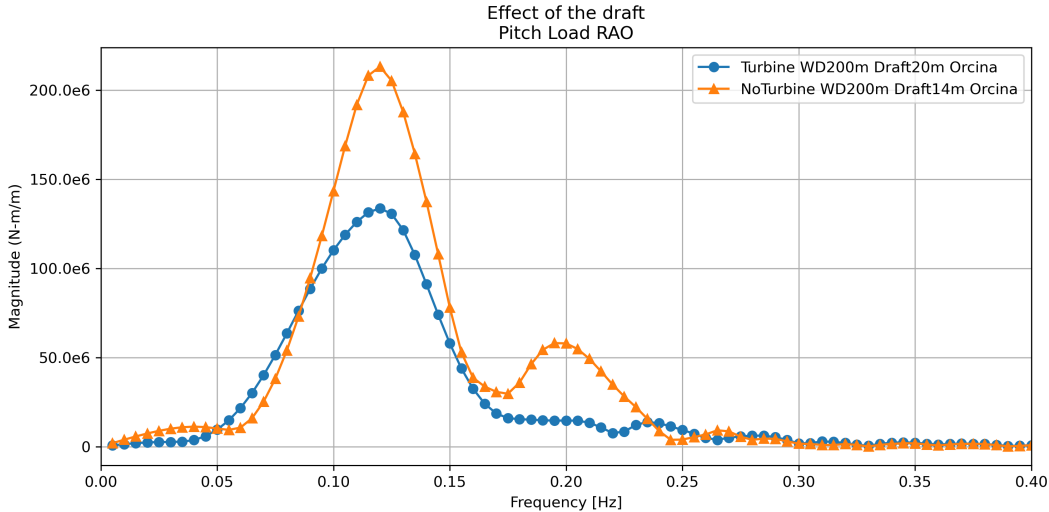


Figure B.6: Effect of draft on pitch load RAO

B.3. Effect of moored draft

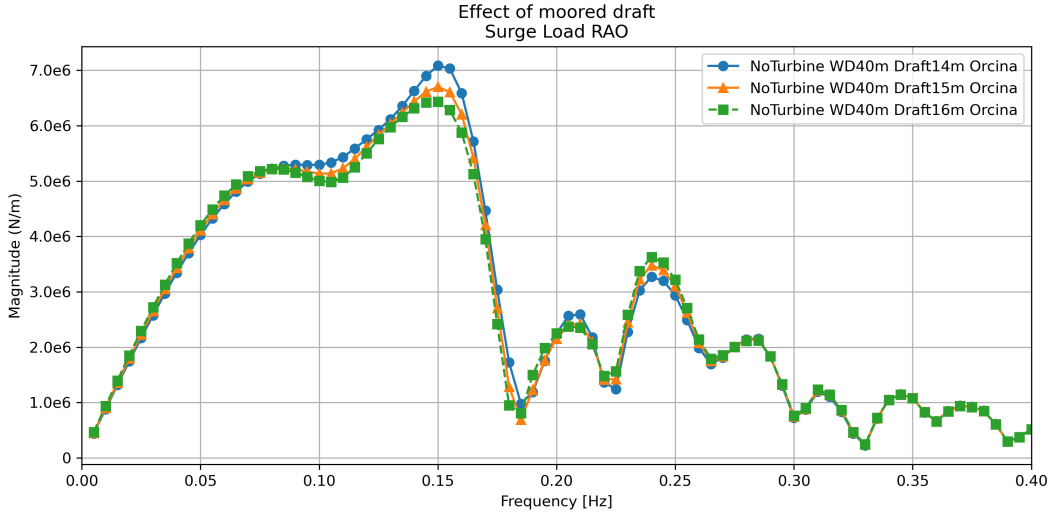


Figure B.7: Effect of mooring draft on surge load RAO

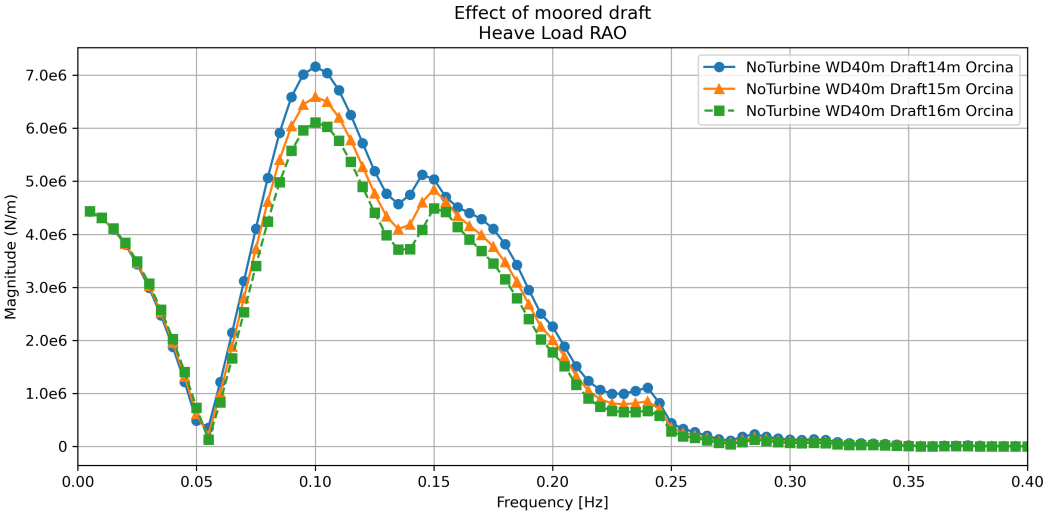


Figure B.8: Effect of mooring draft on heave load RAO

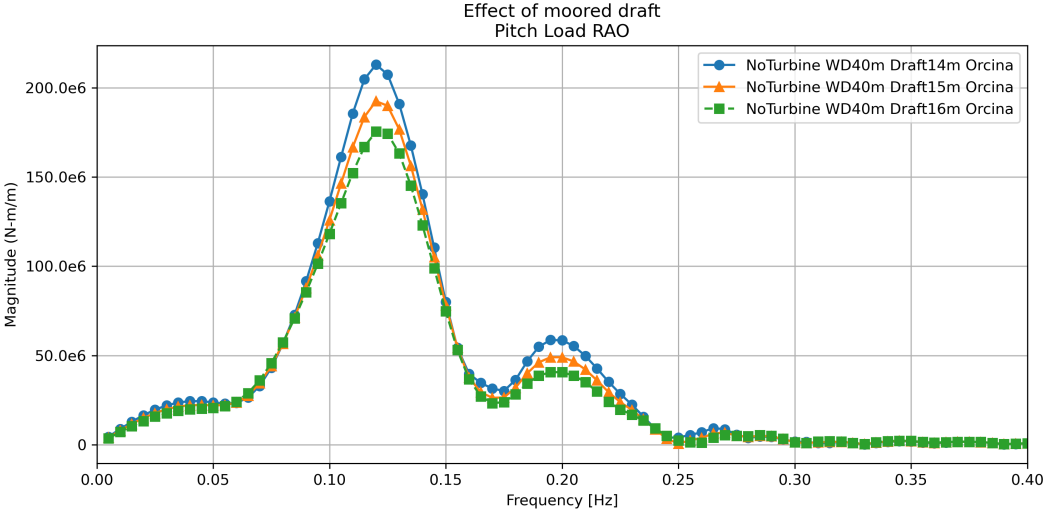


Figure B.9: Effect of mooring draft on pitch load RAO

B.4. Comparison of water depths

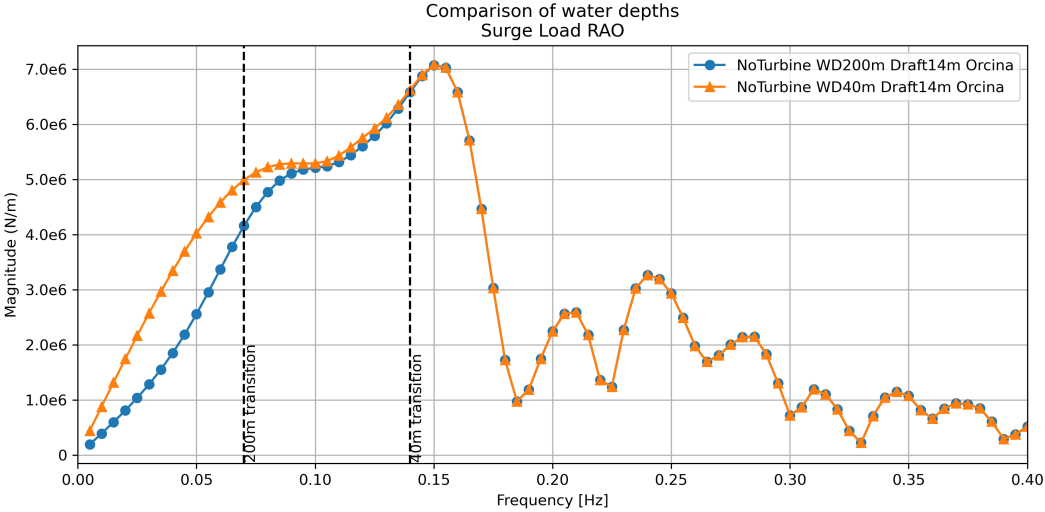


Figure B.10: Comparison of water depths on surge load RAO

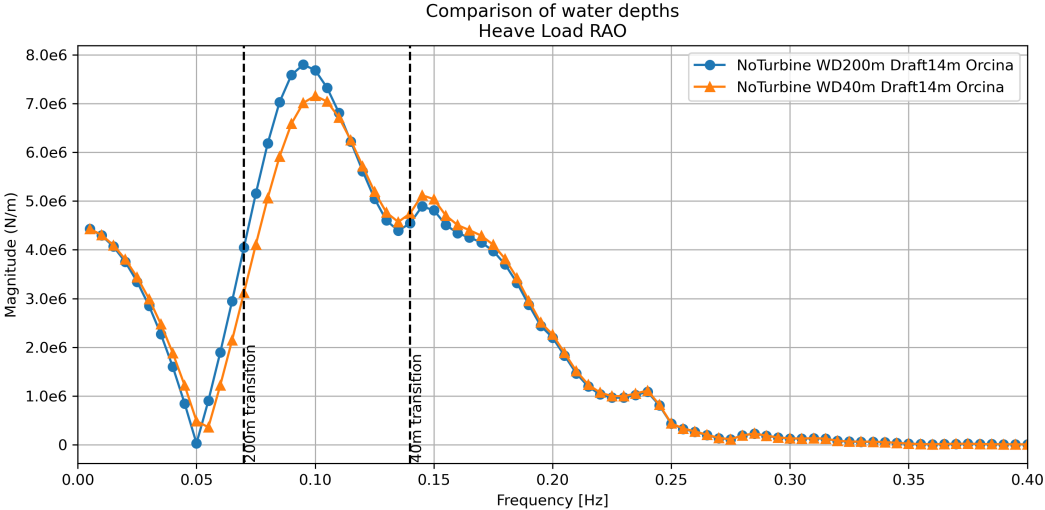


Figure B.11: Comparison of water depths on heave load RAO

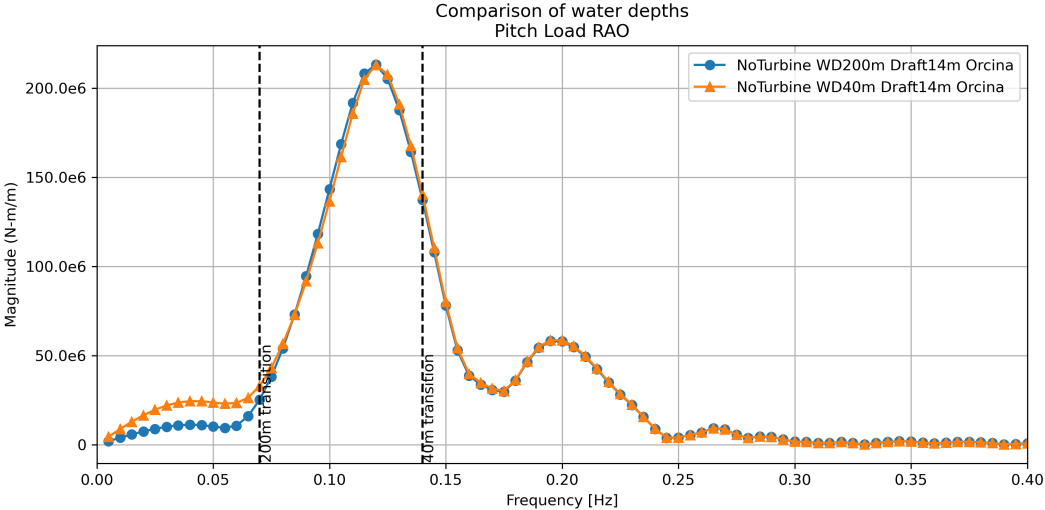


Figure B.12: Comparison of water depths on pitch load RAO

B.5. Effect of tidal range

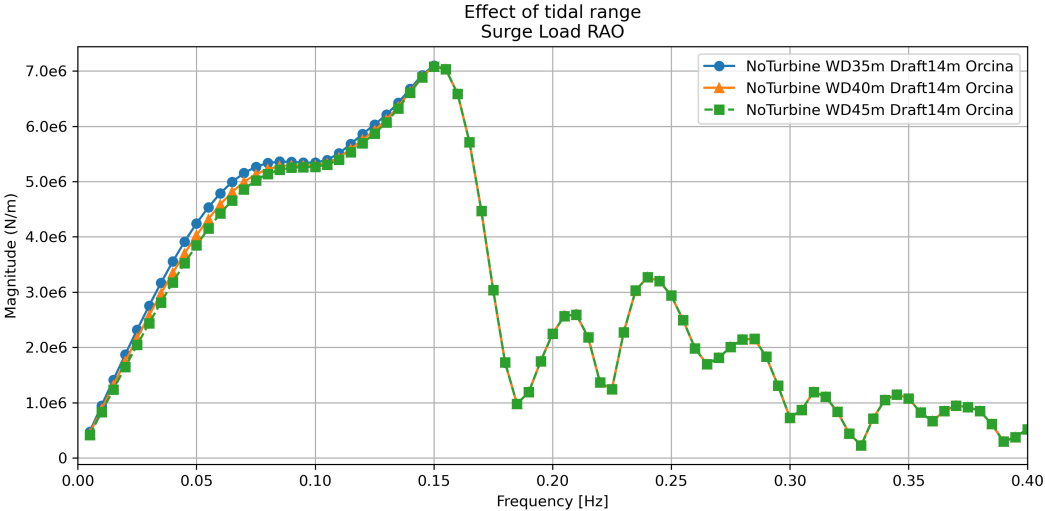


Figure B.13: Effect of tidal range on surge load RAO

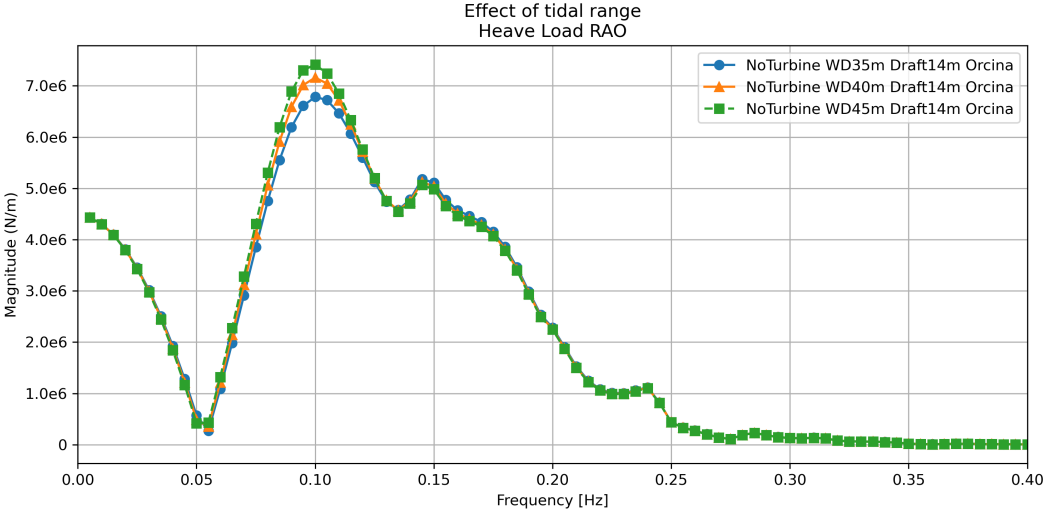


Figure B.14: Effect of tidal range on heave load RAO

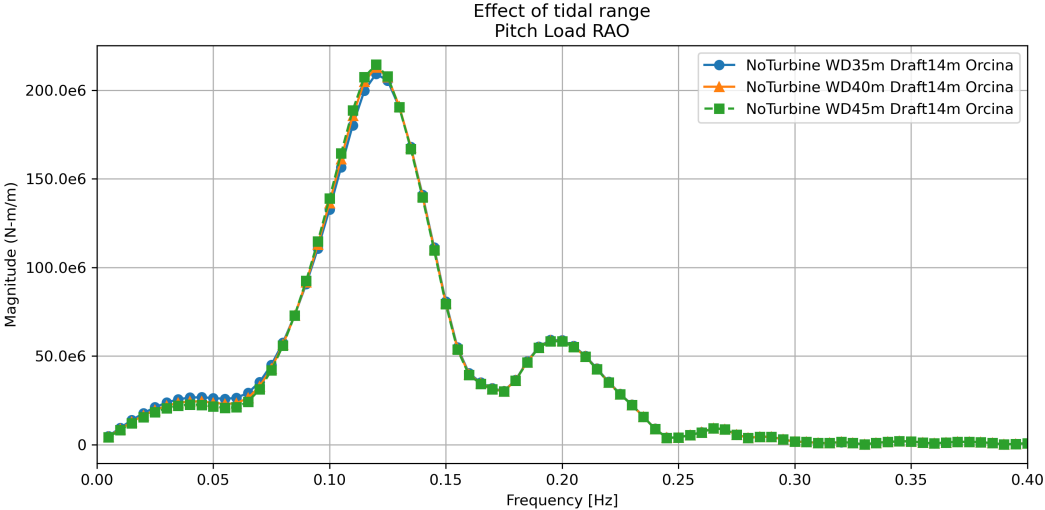


Figure B.15: Effect of tidal range on pitch load RAO

C

Free-decay plots

This appendix presents the free-decay time histories for the six degrees of freedom (DOFs) of the floating structure under consideration: surge, sway, heave, roll, pitch, and yaw. These plots are derived from dynamic simulations that analyze how the structure responds to perturbations over time. Each figure below illustrates the decay behavior of one of the six DOFs, capturing the system's natural damping characteristics and oscillatory motion after an initial displacement.

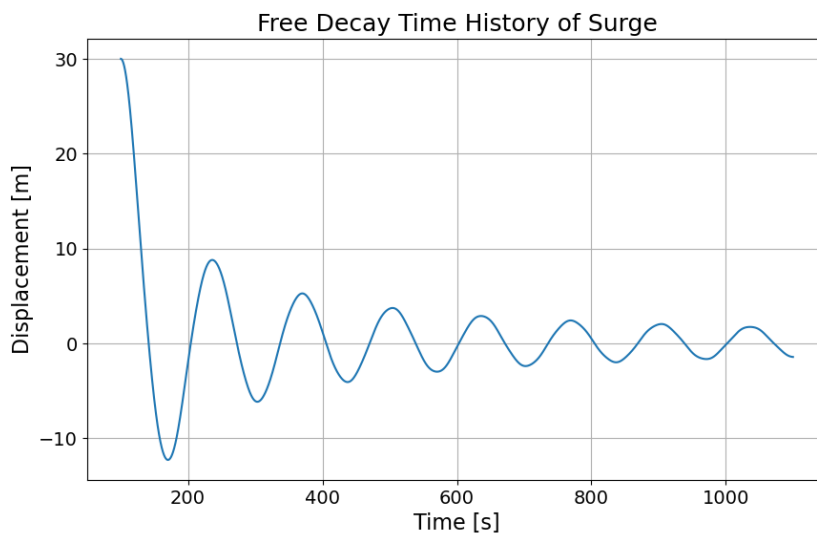


Figure C.1: Decay time history for surge

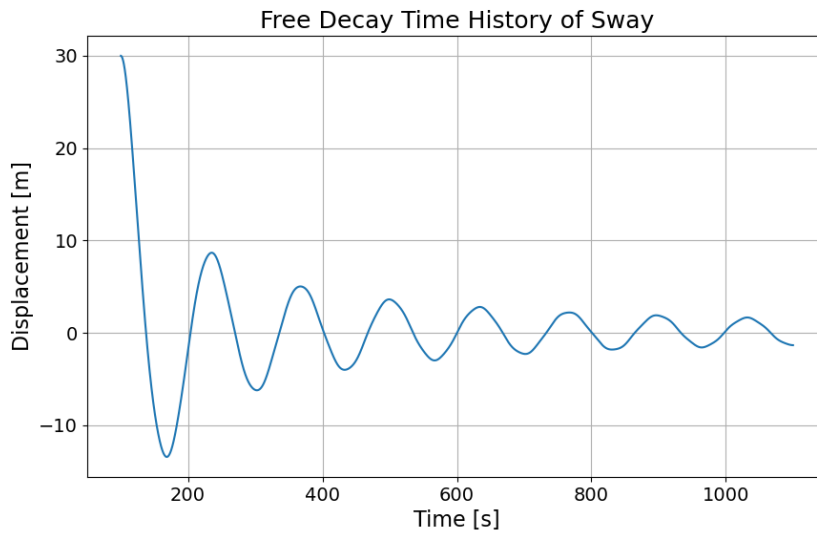


Figure C.2: Decay time history for sway

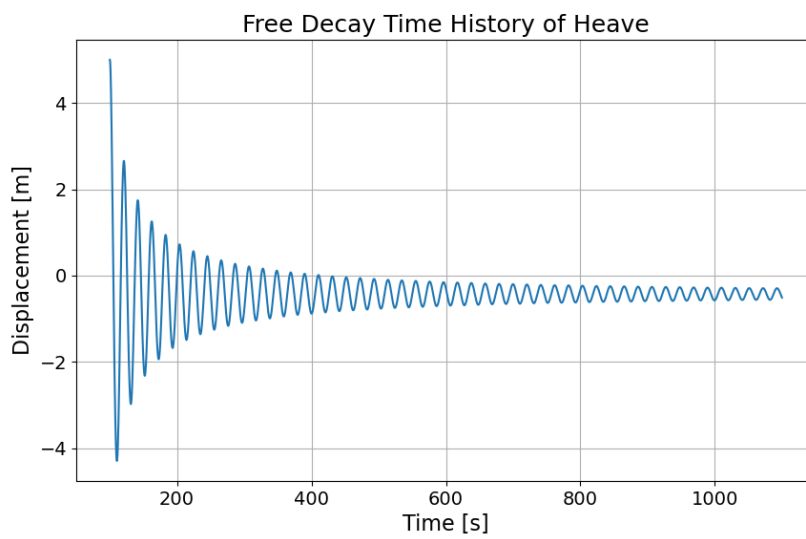


Figure C.3: Decay time history for heave

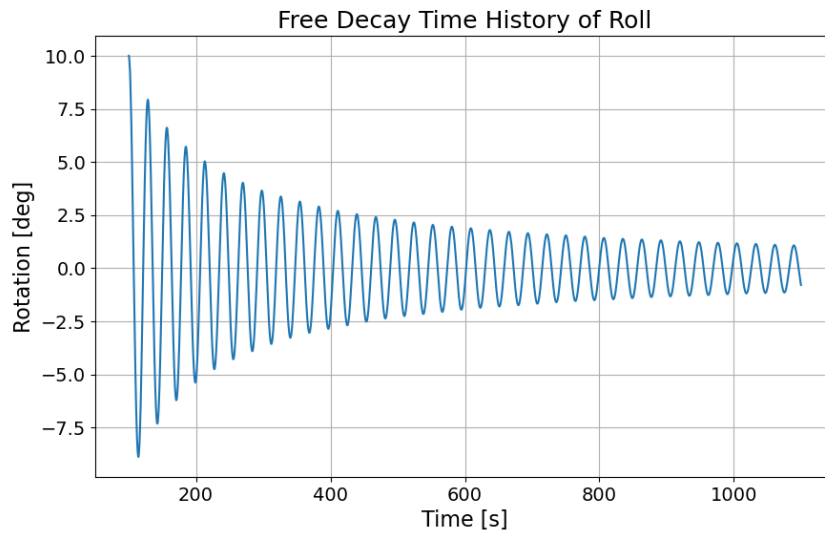


Figure C.4: Decay time history for roll

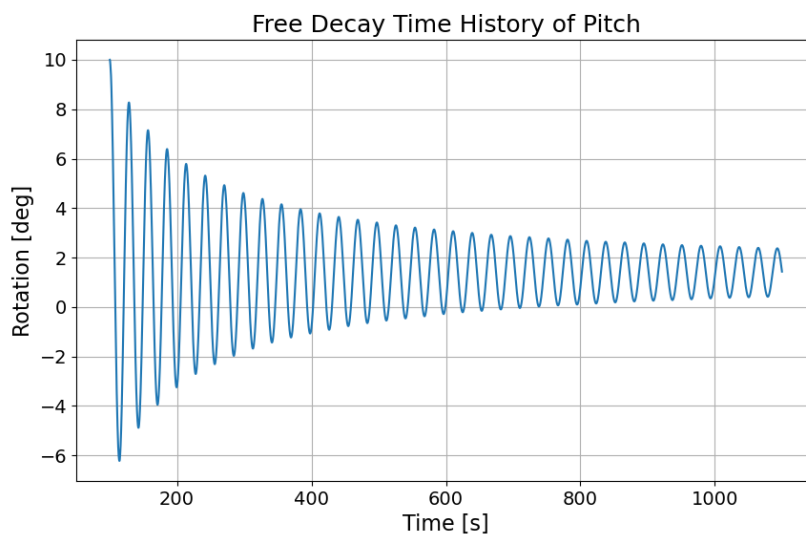


Figure C.5: Decay time history for pitch

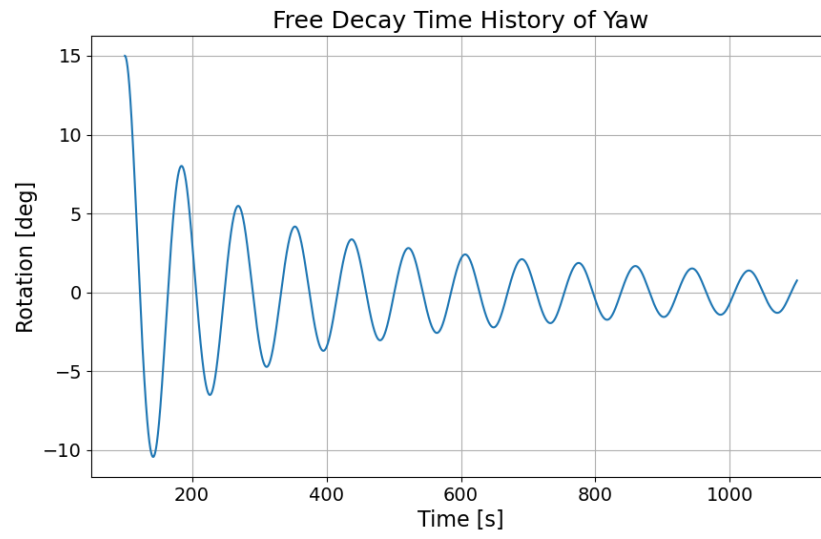


Figure C.6: Decay time history for yaw

D

Added mass over frequency for all DOFs

This appendix provides detailed graphs showing the added mass as a function of frequency for the six degrees of freedom (DOFs) of the floating offshore wind platform. These DOFs include surge-surge, sway-sway, heave-heave, roll-roll, pitch-pitch, and yaw-yaw.

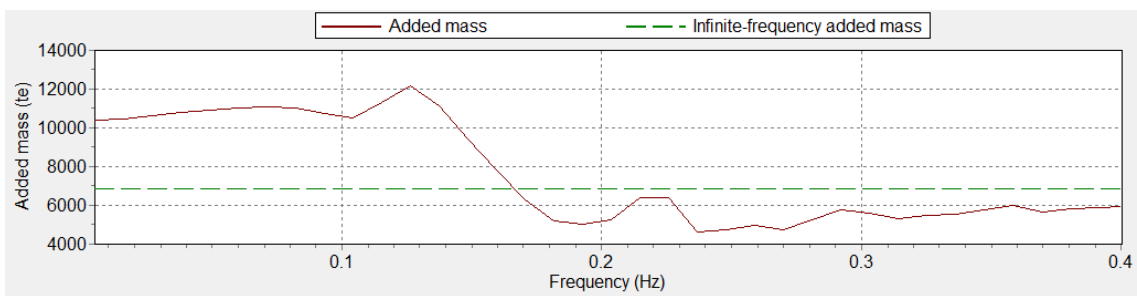


Figure D.1: Added mass as a function of frequency for surge-surge DOF

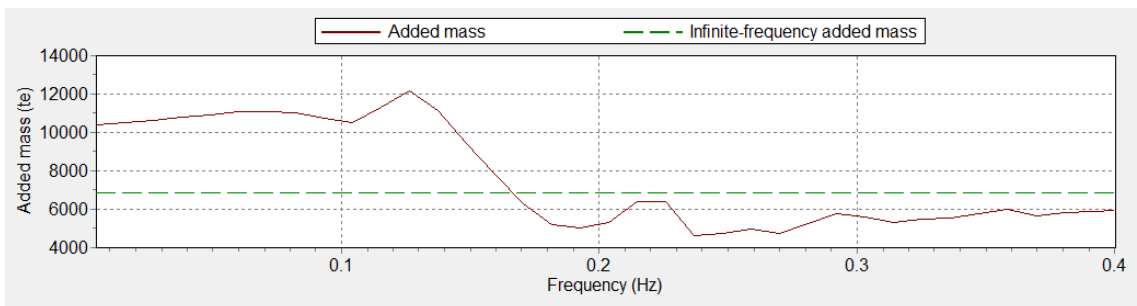


Figure D.2: Added mass as a function of frequency for sway-sway DOF

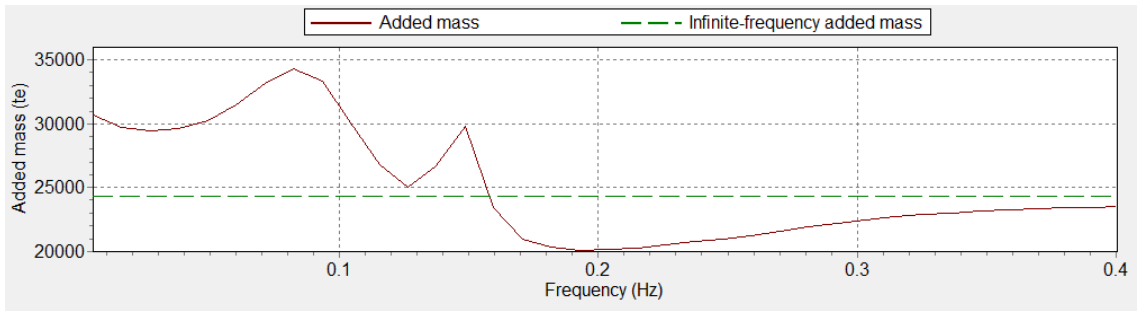


Figure D.3: Added mass as a function of frequency for heave-heave DOF

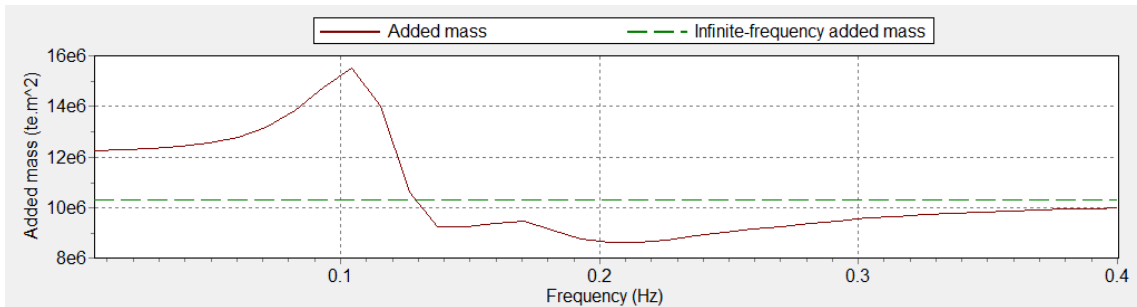


Figure D.4: Added mass as a function of frequency for roll-roll DOF

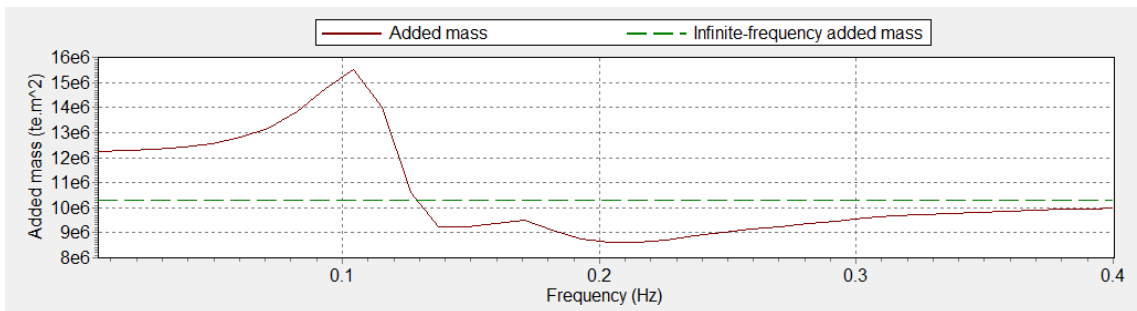


Figure D.5: Added mass as a function of frequency for pitch-pitch DOF

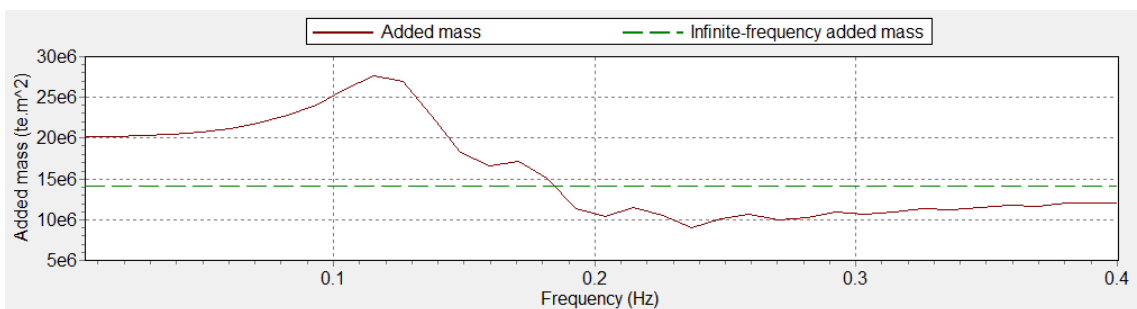


Figure D.6: Added mass as a function of frequency for yaw-yaw DOF

These graphs illustrate the behavior of the added mass for each degree of freedom over a range of frequencies, providing a view of how the added mass varies with frequency. This information is required to understand the dynamic characteristics of the floating offshore wind platform and validating the use of a constant added mass in the frequency domain analysis.